CHARACTERIZATION OF THE UNMYELINATED TYPE II AFFERENTS AS COCHLEAR NOCICEPTORS

by
Chang Liu

A dissertation submitted to Johns Hopkins University in conformity with the requirements for the degree of Doctor of Philosophy

Baltimore, Maryland

March, 2016

Abstract

In the mammalian cochlea, acoustic information is carried to the brain by the predominant (95%) large diameter, myelinated type I afferents, each of which is postsynaptic to a single inner hair cell. The remaining thin, unmyelinated type II afferents extend hundreds of microns along the cochlear duct to contact many outer hair cells. Despite this extensive arbor, type II afferents are weakly activated by outer hair cell transmitter release, and are insensitive to sound. Their function has been mysterious for decades due to their scarcity and lack of specific genetic markers. Intriguingly, type II afferents remain intact in damaged regions of the cochlea while outer hair cells and type I afferents are damaged by noise exposure. In this thesis, using whole-cell patch clamp recordings directly from the dendrites of type II afferents, we found that the weak synaptic transmission is mediated by GluA2 containing AMPA receptors. In contrast, ATP released from the damaged cochlea more potently activates type II afferents. We show that type II afferents are strongly depolarized when outer hair cells are damaged. This response depends on both ionotropic (P2X) and metabotropic (P2Y) purinergic receptors, binding ATP released from nearby supporting cells in response to hair cell damage. Selective activation of P2Y receptors increased type II afferent excitability by the closure of KCNQ-type potassium channels, a potential mechanism for the painful hypersensitivity that can accompany hearing loss. Exposure to the KCNQ channel activator retigabine suppressed the type II fiber's response to hair cell damage.

Type II afferents may be the cochlea's nociceptors, prompting avoidance of further damage to the irreparable inner ear.

Thesis advisors: Paul A. Fuchs, Ph.D. and Elisabeth Glowatzki, Ph.D.

Thesis readers: Paul A. Fuchs, Ph.D. and Michael J. Caterina, Ph.D.

Thesis Committee:

Michael J. Caterina, Ph.D. (Chair)

Richard L. Huganir, Ph.D.

King-Wai Yau, Ph.D.

Acknowledgement

First and foremost, I would like to thank my thesis advisors Paul and Elisabeth, for making my PhD training such a great experience. I was fortunate to be able to work with them and received their tremendous support, guidance and encouragement over the years. This project tackles an important question in the auditory field, but requires a lot of persistence and patience due to the difficulty in the recording technique. Paul and Elisabeth were always there to help and prioritize the training of their students. I still remember in the early days, Elisabeth showed me how to pull a patch electrode; Paul sit next to me to teach me the fundamentals of the experiments, and cheered with me upon my first successful recording on type II afferent. As the project moved forward, I was given a lot of freedom to become an independent researcher, explore different directions and design the experiments, while Paul and Elisabeth were always available to give advice, from the interpretation of the data to big picture of my thesis. Their enthusiasm and devotion to science have influenced me in many ways and were indispensable for my scientific development.

I would like to thank my thesis committee members – Michael Caterina, Richard Huganir and King-Wai Yau for giving me invaluable advice both through thesis committee meetings and personal communications. My experience in King's lab gave me great influence and I was very fortunate to get King's advice, both scientifically and about personal life. Mike had been my pre-thesis advisor and the conversation with him was always exciting and inspiring. I am also very lucky to be among a collaborative and supportive environment of Fuchs and Glowatzki lab. I would like to thank all the present

Table of Contents

List of Tables

List of Figures

by AMPA receptors.

Results

x

cochlea.

List of Abbreviations

ABR   auditory brainstem response

ACh   Acetylcholine

AMPA   α-amino-3-hydroxy-5-methyl-4-isoxazole propionic acid

cAMP   cyclic adenosine monophosphate

CtBP2   C-terminal binding protein 2

DAG   Diacylglycerol

DFNA2   deafness autosomal dominant autosomal locus 2

DPOAE   distortion product otoacoustic emission

DREADDs   designer receptors exclusively activated by designer drugs

DRG   dorsal root ganglion

EM   electron microscopy

E-NPP   ecto-nucleotide pyrophosphatase/phosphodiesterase

E-NTPDase   ecto-nucleoside triphosphate diphosphohydrolase

EP   endolymphatic potential

EPSC   Excitatory postsynaptic current

EPSP   Excitatory postsynaptic potential

GABA   γ-aminobutyric acid

GIRK   G protein-coupled inward rectifiers K^+ channels

GPCR   G protein coupled receptor

HRP   horseradish peroxidase

IHC   inner hair cell

IP3	inositol triphosphate
KCNQ	potassium voltage-gated channel subfamily Q
MOC efferent	medial olivocochlear efferent
NF200	200 kDa neurofilament protein
NMDA	N-methyl-D-aspartate
OHC	outer hair cell
OSF	outer spiral fiber
PIP2	phosphatidylinositol 4,5-bisphosphate
PLC	phospholipase C
PPADS	pyridoxalphosphate-6-azophenyl-2′,4′-disulfonic acid
SGN	spiral ganglion neuron
TMEM16A	transmembrane protein 16A
TMR	transmembrane spanning region

Background

1. Morphology of type II cochlear afferents

1.1 Basic structure of the auditory end organ

The sense of hearing starts in the ear. Sound consists of compression and rarefaction of air, and travels in the form of pressure waves through the external ear canal. The resulting vibration of the tympanic membrane is transferred to the motion of fluids in the snail-shaped cochlea through the three middle ear bones. This fluid movement vibrates the basilar membrane in the inner ear, where the auditory sensory epithelium – the organ of Corti - is situated.

The organ of Corti is the site of sound transduction in the cochlea, a beautiful and highly organized structure consisting of sensory cells and supporting cells. The organ of Corti contains one row of inner hair cells (IHCs) and three rows of outer hair cells (OHCs), serving as the receptors of the auditory system. These receptor cells are covered by a cantilevered gelatinous structure called the tectorial membrane. When sound strikes the eardrum and causes a traveling wave along the basilar membrane, a shearing force is created between the tectorial membrane and hair cells, bending hair cell bundles and gating the cation permeable mechanotransduction channels for sound transduction. Postsynaptic to the hair cells are the cochlear afferents that carry information from the auditory periphery to the brain. The mammalian cochlea is innervated by two classes of cochlear afferents – the majority population (~90 – 95 %) consists of type I afferents that contact IHCs and the minority population includes type II afferents that innervate the OHC region (Figure B1). Depolarization of IHCs triggers Ca^{2+}-dependent release of

glutamate from a ribbon synapse, which in turn activates the postsynaptic type I afferents (Glowatzki and Fuchs, 2002; Goutman and Glowatzki, 2007; Grant et al., 2010), Each type I afferent projects to a single IHC, whereas each IHC contacts on average 20-30 type I afferents. The IHC – type I synapse encodes the timing, intensity and frequency selectivity of sound information. Sound timing and intensity are encoded by the firing rates of type I afferents as a result of a related pattern of synaptic transmission from inner hair cells (Fuchs, 2005; Fuchs and Glowatzki, 2015; Moser et al., 2006). Frequency representation is determined by the position of the sensory neurons, as a consequence of 'tonotopy' – that sound vibrates the basilar membrane in a frequency – specific manner. High frequency sound activates the sensory neurons at the base of the cochlea and low frequency sound activates the apical neurons. Type I afferents project directly to the hair cells corresponding to their characteristic frequency – a frequency to which they are most sensitive, thereby forming a tonotopic array along the cochlea (Liberman, 1982).

The remaining 5 – 10 % of cochlear afferents are small-caliber, unmyelinated type II afferents. Each of them sends a long peripheral process and contacts multiple hair cells, receiving weak synaptic transmission. Current understanding about their morphology, synaptic transfer and functions is described in the following text.
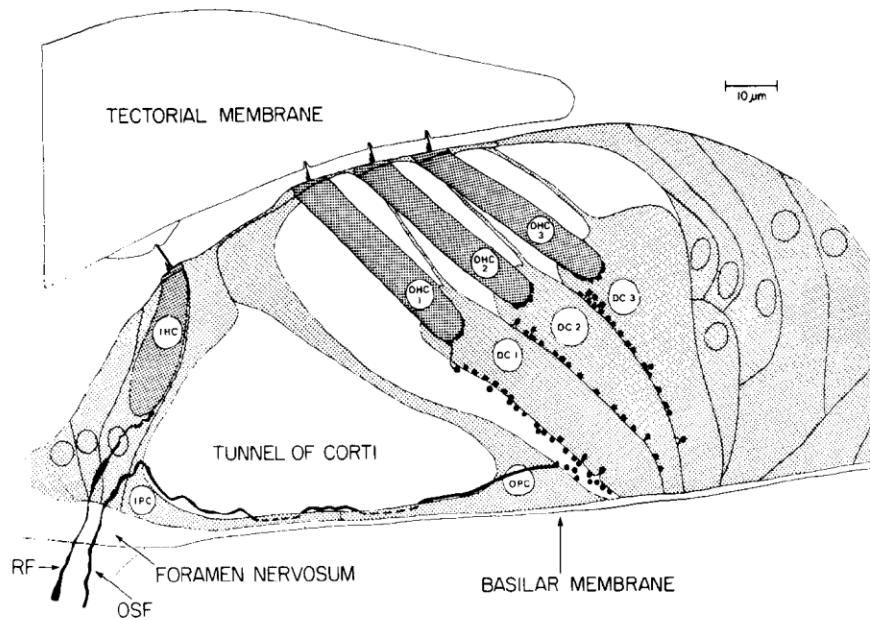
Figure B1. Schematic illustration of afferent innervation in a cross section of the organ of Corti. RF: a radial fiber as an example of a type I afferent contacts a single IHC. OSF: an outer spiral fiber (type II afferent) travel on the floor of the tunnel of Corti, and then rise to contact OHCs. Efferents were not illustrated in this scheme (Simmons and Liberman, 1988a).

1.2 Type II neurons in the spiral ganglion

The somata of type I and type II cochlear afferents are named type I and type II spiral ganglion neurons (SGNs). They both reside in Rosenthal's canal (also called the spiral canal) of the cochlea, a section of the bony labyrinth. Compared to type I neurons, type II neurons are smaller in diameter and make up 5-10% of SGNs. Their somata were found in the more peripheral regions of the spiral ganglion (Berglund and Ryugo, 1987; Brown, 1987b). The cytoplasm of type II neurons was found to be more filamentous, showing fewer cytoplasmic organelles. This is reflected by basic stains and immunohistochemistry. With Nissl staining which primarily labels endoplasmic reticulum and the nucleus, type I neurons demonstrate denser intracellular Nissl bodies

than do type II afferents. On the other hand, when cytoskeletal elements were examined, type II afferents were more intensely stained, revealed by silver stains as well as antibodies against neurofilament 200 kDa (NF200) (Berglund and Ryugo, 1986; Berglund and Ryugo, 1991) and the intermediate filament protein peripherin (Hafidi, 1998; Hafidi et al., 1993). Type II neurons are bipolar or pseudomonopolar, branched to send one peripheral process toward the organ of Corti and one central process to the cochlear nucleus in the brainstem. The peripheral and central processes of type II neurons are roughly equal in diameter, in contrast to the type I neurons where a thinner caliber peripheral branch is found in many species (Berglund and Ryugo, 1986; Kiang et al., 1982).
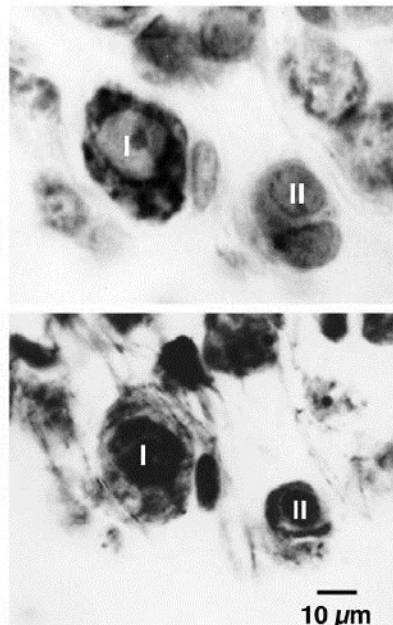
Figure B2. Somata of type I and type II neurons under light microscopy. Top: Cresyl violet staining showed more prominent Nissl substance in the slightly larger, type I neurons. Bottom: Protargol staining on the same cells after cresyl violet washed out. The cytosol of type II neurons was more heavily stained by neurofilaments. (Berglund and Ryugo, 1986)

4

1.3. Peripheral process of type II neurons

Type II afferents are unmyelinated and have a smaller diameter than type I afferents (Bernard and Spoendlin, 1973; Perkins and Morest, 1975; Romand and Romand, 1987; Romand and Romand, 1984; Spoendlin, 1971a). The radial processes of type II afferents project together with those of type I afferents toward the organ of Corti. Each type I projection terminates at the inner hair cell region, forming a synapse with a single inner hair cell. Type II afferents project past the inner hair cells, cross the tunnel of Corti and travel radially on its floor. After reaching the outer hair cell region, the fibers make a right angle turn towards the base of the cochlea, which represents higher frequencies. These are the spiral processes of type II afferents, also called outer spiral fibers (OSFs) according to their position in the cochlea. The spiral processes almost always turn toward the base and travel for hundreds of microns along the outer hair cell region (Berglund and Ryugo, 1987; Brown, 1987b; Ginzberg and Morest, 1983; Ginzberg and Morest, 1984; Perkins and Morest, 1975; Simmons and Liberman, 1988b), with the exception of the very apical fibers near the helicotrema which were identified as bi-directional and can project both apicalward and basalward (Perkins and Morest, 1975). The initial part of the spiral process usually stays far below the outer hair cells, and runs under the supporting cells (Deiters' cells) for distances up to 0.5 mm. Then the process gradually risees to the base of the outer hair cells, extending a terminal portion commonly around 100 – 200 μm, which is characterized by 10 – 20 synaptic branches contacting the sides and bases of OHCs. Angular enlargements of the spiral fibers were also observed, possibly serving as *en passant* synapses (Brown, 1987a; Ginzberg and Morest, 1983; Perkins and Morest, 1975; Simmons and Liberman, 1988b). The length of the entire spiral process reaches

670 μm in rat (Perkins and Morest, 1975) and up to 1200 μm in cat (Simmons and Liberman, 1988a; Spoendlin, 1969). Electron microscopic analysis revealed about 28 afferent terminals innervating apical OHCs and about 7.75 terminals per OHC at the base in guinea pig (Hashimoto and Kimura, 1988). In cats, an average of 6-8 afferent terminals were found on each OHC base (Ginzberg and Morest, 1984). In some cases, the major shaft of the process could branch and contact multiple rows of outer hair cells. Only 3 out of 34 type II afferents in adult guinea pig were found to contact multiple rows (Brown, 1987a), whereas 23 of 51 fibers contacted two rows and 8 of 51 fibers contacted three rows in young cats (Perkins and Morest, 1975), and 15 of 85 fibers contacted multiple rows in adult cats (Simmons and Liberman, 1988a). It is unknown if such differences arise from the age or species of the animals. Among the multiple-row type II afferents in adult cats, more than 50% of their synaptic branches innervate only to a single row of OHCs. It was also reported that basal type II afferents tend to innervate only one row of OHCs (Simmons and Liberman, 1988a).

AFFERENT INNERVATION OF HAIR CELLS

OHCs

Tunnel of Corti

IHCs

Spiral ganglion
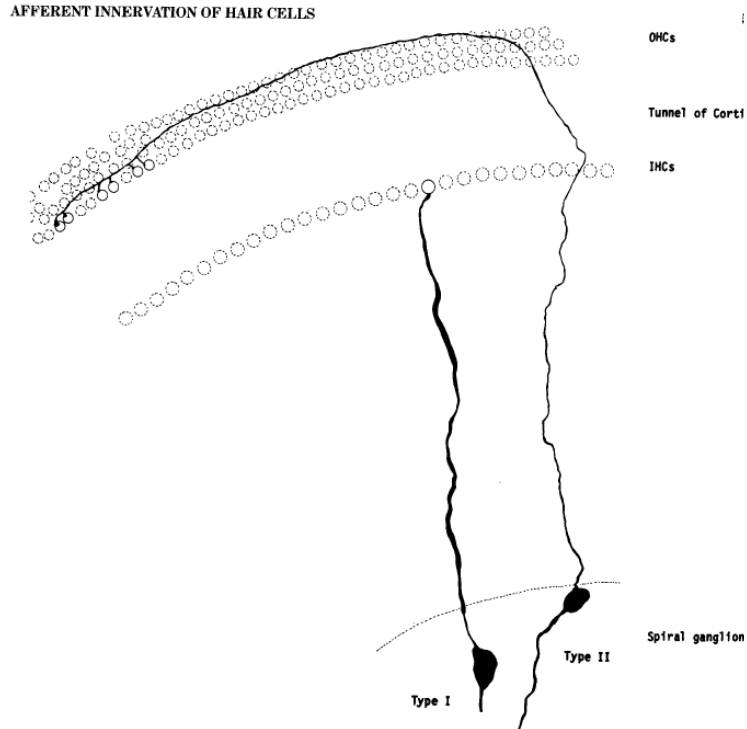
Type II

Type I

Figure B3. Drawing of type I and type II afferents innervation in a whole-mount cochlea preparation. Showing the spiral ganglion, one row of IHCs and three row of OHCs.(Berglund and Ryugo, 1987)

Certain morphological features of type II afferents might be related to the specific row of OHCs contacted. In cat cochlea, more type II afferents seem to contact the first row of OHCs (44% to 48% of reconstructed fibers examined in two samples), and similar numbers of afferents contact row-2 and row-3 (24% - 31%). Row-3 type II afferents have more synaptic branches and longer terminal regions (Simmons and Liberman, 1988a). Similar observations in guinea pig cochlea showed that row-3 type II afferents are longer in length, with larger terminal regions and more synaptic branches. The number of OHCs contacted by row-3 type II afferents could be 2 – 3 times more than that of row-1 type II

afferents, according to 34 fibers reconstructed from horseradish peroxidase (HRP) staining (Brown, 1987a).
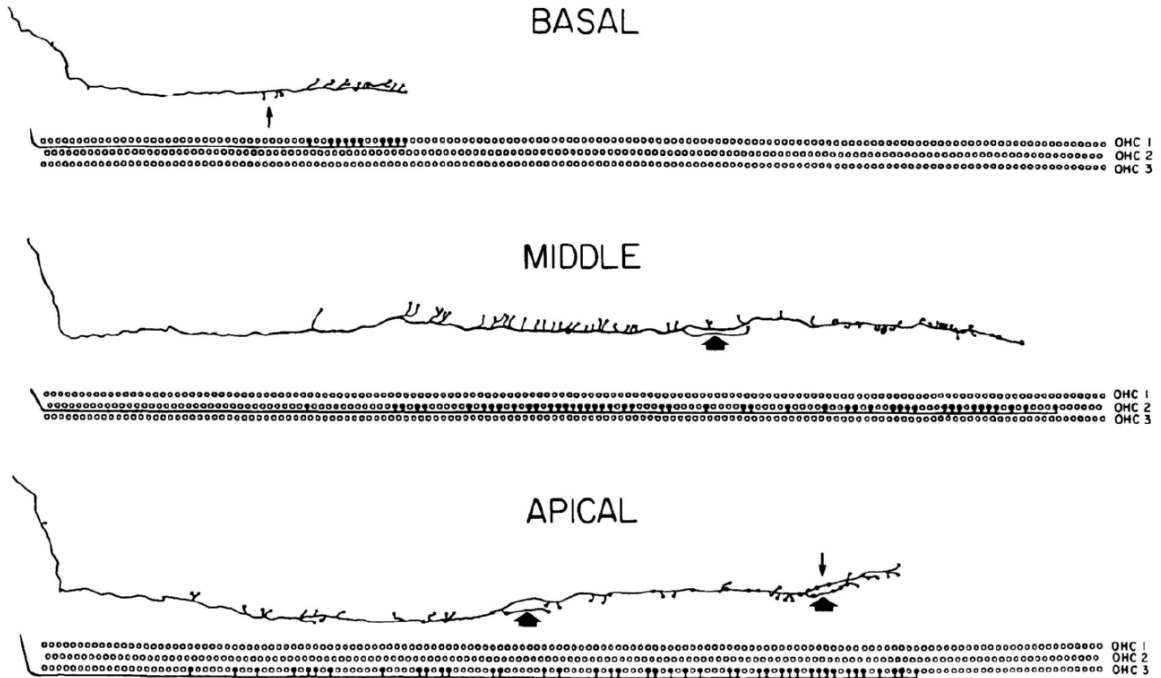
Figure B4. Difference of type II afferents' morphology in the apical, middle, and basal turn of the cochlea. Schematic innervation of the three rows of OHCs were illustrated under the fibers, with the blackened dots representing OHC contacts. (Simmons and Liberman, 1988a)

An apical-basal difference of type II afferents' morphology was also reported (Figure B3). The length of type II afferents as well as the length of their terminal regions were found to be maximum in the apical portion of the middle turn, with decreasing length of both when moving to either apical or basal portions of cat cochlea. Apical type II afferents have larger diameters, about 0.8 μm, while those of basal type II afferents averaged about 0.2 μm. The apical type II afferents seem to have both *en passant* and

8

terminal synapses whereas the basal type II afferents have more terminal branches and few *en passant* synapses (Simmons and Liberman, 1988a). Up to all three rows of OHCs can be innervated by a single apical type II afferent, which is rarely seen at the basal part of the cochlea. More elaborate patterns of innervation were observed in the apical but not the basal type II afferents (Brown, 1987a; Fechner et al., 2001; Simmons and Liberman, 1988a).

Besides outer hair cells, several morphological studies suggest that type II afferents may contact other cell types. Collaterals occasionally appeared in the portion of type II afferents that passes inner hair cells (Perkins and Morest, 1975). But it was not certain if these are definite and functional synaptic structures. Supporting cells in the outer hair cell region, including Deiters' and Hensen's cells, are proposed to form synapses with type II afferents. This is only observed in the apical half of the cochlea but not the basal half (Burgess et al., 1997; Fechner et al., 2001). Electron microscopic analysis showed synaptic specializations between these supporting cells and adjacent fibers presumed to be type II afferents, because these fibers were negative for acetylcholinesterase and densely stained for neurofilaments (Burgess et al., 1997). In the apical part of the guinea pig cochlea, type II afferents were found to send branches onto Deiters' and Hensen's cells (Fechner et al., 1998; Fechner et al., 2001). These putative supporting cell – type II synapses have not been functionally characterized. Additional ultrastructural studies also revealed efferent to type II afferent synapses (Nadol, 1983; Thiers et al., 2002) and reciprocal synapses between OHC and type II afferents (Francis and Nadol, 1993; Nadol, 1981; Thiers et al., 2002; Thiers et al., 2008). These synapses were identified through the observation of small numbers of vesicles accumulating close

to the afferent's cell membrane, as well as some asymmetric membrane thickenings and a synaptic cistern in the hair cell. Whether these are functional synapses and what role they play is unknown.

1.4. Central projections of type II neurons

The central processes of cochlear afferents, including those of both type I and type II afferents, are bundled together to form the auditory nerve. They enter the cochlear nucleus as the root branch, and then the axons of both type I and type II afferents bifurcate (Figure B5) (Brown et al., 1988a; Fekete et al., 1984; Pillsbury, 1996). The position of the bifurcation is arranged in a tonotopic manner, which reflects the fiber's position in the cochlea (Liberman, 1982). After bifurcation, the ascending branch of the axon projects to the anteroventral cochlear nucleus (AVCN), and the descending branch passes through the posteroventral cochlear nucleus (PVCN) and terminates in the dorsal cochlear nucleus (DCN). Similar to the position of bifurcation, the ascending and descending branches are also arranged tonotopically, with higher frequency fibers positioned more dorsally (Nayagam et al., 2011). A variety of postsynaptic targets of type I afferents have been identified in the magnocellular core of the cochlear nucleus which contains large neurons that project in turn to the higher centers of the auditory pathway (Brawer and Morest, 1975; Rouiller et al., 1986). Collaterals from these axons form *en passant* swellings (which may or may not be synapses) and terminal branches which are characterized to be the sites of synapses (Fekete et al., 1984; Ryugo and Sento, 1991). These type I axon terminals were found to be restricted to the core of the cochlear

nucleus (Berglund and Brown, 1994; Brown et al., 1988a; Brown and Ledwith, 1990). In contrast, the ellipsoidal swellings present on type II afferents within the magnocellular regions do not seem to form synapses (Berglund et al., 1996; Ryugo and Sento, 1991). However, type II afferents extend their axon beyond the core regions of cochlear nucleus, with addition termination at a bordering region called the granule-cell lamina (Figure B5) (Benson and Brown, 2004; Berglund and Brown, 1994; Hurd et al., 1999). Postsynaptic targets of type II afferents were identified by serial-section electron microscopy with type II afferent terminals labeled by HRP. Most of the targets were small dendrites from the "small cells" at the edge of granule cell layer. Axosomatic synaptic contacts on large cells were also observed. These large cells were presumed to be multipolar or globular bushy cells, but their identity was not confirmed anatomically (Benson and Brown, 2004). Another study suggests that type II afferents contact local interneurons in the granule cell layer, including small stellate and mitt cells but perhaps not granule cells (Hurd et al., 1999). In addition to the type II afferent innervation, the granule cell layer also receives a wide variety of auditory descending inputs and non-auditory projections, such as somatosensory input (Paloff and Usunoff, 1992; Shore and Zhou, 2006; Wright and Ryugo, 1996; Zhan and Ryugo, 2007) and collaterals from olivocochlear efferents that innervate OHCs (Benson and Brown, 1990; Brown et al., 1988b; Brown et al., 1991). Therefore, the granule cell layer is considered an integrative zone, where convergence of information from different sources including type II afferents might occur. The higher-order targets of type II afferent following this "non-canonical" pathway remains to be determined.
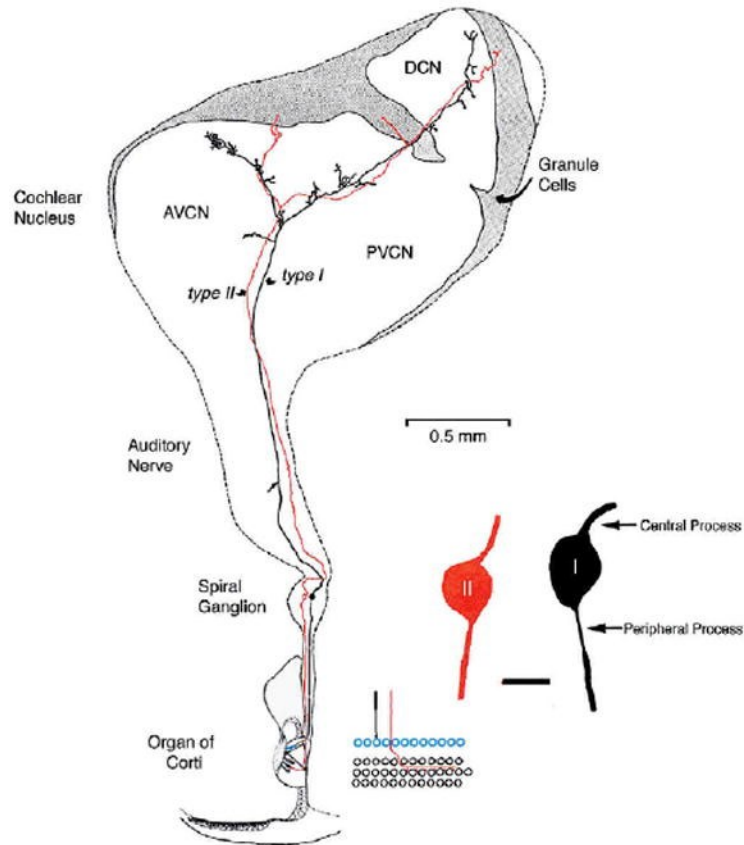
Figure B5. Schematic drawing of central innervation patterns of type I and type II afferents. Modified from Brown et al., 1988.

1.5 Labeling of type II afferents

Besides their small population size and difficulty in recording type II afferents, the lack of specific genetic marker for type II afferents has also hindered progress to isolate the function of these neurons. Neurofilament proteins are present in both type I and type II afferents, proposed to have a role in maintaining the structural integrity and axon growth during development (Barclay et al., 2010; Barclay et al., 2011). These proteins have been examined for their potential as specific markers. An antibody (RT-97)

12

against the heavy (200 kDa) chain of neurofilament – NF-200 - seems to label type II neurons. Such labeling was found to be highly dependent on the phosphorylation state of the heavy neurofilament in type II neurons, and only the somata were labeled, without confirmation by dendritic projection pattern (Berglund and Ryugo, 1986; Berglund and Ryugo, 1991). Another study reported that a more general neurofilament antibody (polyclonal anti-NF200) could label both type I and type II afferents (McLean et al., 2009). The same study showed that antibody against a sodium-potassium ATPase NKAα3 labels the type I afferents under the IHCs and medial olivocochlear efferents in the outer hair cell regions, but not type II afferents. So far the most recognized type II 'marker' protein is the type III intermediate filament protein peripherin. However, peripherin is expressed in both type I and type II afferents in early development. During the embryonic days, peripherin expression was found throughout the spiral ganglion. After P3, peripherin immunoreactivity was reduced in most of the spiral ganglion neurons. In adulthood, only a small population (roughly 8% of total SGNs) of peripherin positive neurons was seen that correspond numerically to the type II afferents (Hafidi et al., 1993), and such labeling was also observed in their peripheral and central processes (Hafidi, 1998). Another study suggests that as early as P6, peripherin expression is restricted to type II afferents, whereas TMRD (tetramethylrhodamine-conjugated dextran) labels a separate population of neurons representing type I afferents (Huang et al., 2007a). The innervation pattern of type II afferents has been examined in a peripherin knockout mouse line (Lariviere et al., 2002). In neonatal ages (P1 and P7), type II afferent innervation in the outer hair cell regions was found to be normal, as revealed by the immunofluorescence of β-tubulin in the cochlea of peripherin null mouse

13

(Barclay et al., 2010). In the adult cochlea though, type II afferents were found missing when the same mouse line was examined, reflected by the loss of NF200 positive fibers in the outer hair cell regions and the loss of type II afferents terminals by EM analysis of 3 OHCs (Froud et al., 2015). Peripherin might therefore be a good candidate for type II specific labeling. However, a conditional peripherin-CreER mouse line is more desirable, in order to eliminate the possible developmental influence on type I afferents due to its transient expression on all SGNs in embryonic and early postnatal days.

2. Synaptic transfer at OHC – type II afferent synapses

Each type II afferent is postsynaptic to multiple OHCs. However, limited numbers of *in vivo* single unit recordings revealed that these fibers are mostly likely insensitive to sound. Among the 11 recorded type II neurons reported by three papers, only one of them responded to intense broad band sound and even it was not anatomically confirmed (Brown, 1994; Robertson, 1984; Robertson et al., 1999). A breakthrough on this question has been made by whole-cell patch clamp recording from spiral processes of type II afferents, showing that type II afferents are excitable and receive synaptic inputs from multiple outer hair cells (Weisz et al., 2009; Weisz et al., 2012). The synaptic transfer is rather weak (Weisz et al., 2012), consistent with the hypothesis that type II afferents may only respond to loudest or even traumatic levels of sound that activate large numbers of presynaptic OHCs.

Hair cell synaptic transmission is mediated by the ribbon synapse. This highly specialized synaptic structure contains a pre-synaptic electron dense body – ribbon, a

halo of vesicles tethered to the ribbon and voltage-gated calcium channels clustered and forming patches under it. Ribbon synapses were found in mammalian cochlear and vestibular hair cells as well as retinal photoreceptors and bipolar cells, although there are differences in the size and the organization of vesicles. Similar to inner hair cells, outer hair cells also contain ribbons, but with a smaller number (2-5 ribbons per OHC versus 20-30 ribbons per IHC). More ribbons were found in immature OHCs in young animals, and there appears to be a developmental change in the expression of synaptic proteins (Beurg et al., 2008; Fujikawa et al., 2014; Siegel and Brownell, 1981). Electron microscopy studies identified ribbons associated with type II afferents terminals in guinea pig and chinchilla OHCs (Siegel and Brownell, 1981; Smith and Sjostrand, 1961). Anatomical differences among ribbons were found when the OHC ribbons were compared with IHC ribbons by ultrastructural studies (Figure B6). OHC ribbons have a slightly higher height to width ratio so that they are taller and narrower. A big cloud of vesicles was observed in young IHCs that extended several micrometers away from the ribbon, but not in OHCs. Close to the synaptic site, IHC ribbons have 2-3 times more nearby, tethered, and docked vesicles than do OHC ribbons (Weisz et al., 2012). Expression of the Cav1.3 L-type calcium channels has also been demonstrated in OHCs, responsible for the release of vesicles. They are found to co-localize with immunolabel for C-terminal binding protein 2 (CtBP2) – Ribeye, a protein component of the ribbon (Hafidi and Dulon, 2004; Knirsch et al., 2007; Michna et al., 2003). Although the calcium current in OHCs is smaller, the calcium current per ribbon is similar for OHC and IHC synapses (Knirsch et al., 2007). Calcium currents have been related to capacitance measurement of OHCs, providing evidence for synaptic vesicle exocytosis from likely

two distinctive vesicle pools (a readily releasable pool and a slowly releasable pool) in immature OHCs (Beurg et al., 2008).
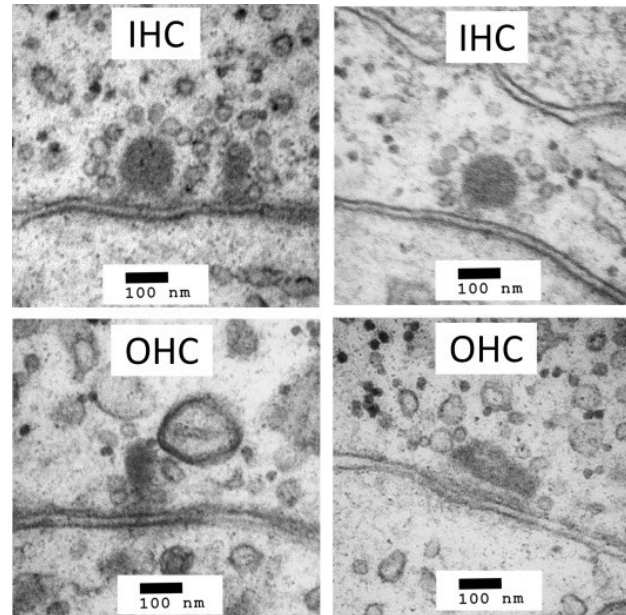
Figure B6. Ultrastructural image of ribbon synapses of IHC and OHC, from apical turn cochlea of P9 rats.(Fuchs and Glowatzki, 2015)

These minor distinctions in ribbon structure and channel-coupling seem insufficient to explain the major differences in release efficiency between OHCs and IHCs. In young rats, each action potential in IHCs causes the release of 40-50 vesicles at a single synaptic contact (Beutner et al., 2001; Glowatzki and Fuchs, 2002). In sharp contrast, each action potential in OHCs has only one fourth probability to trigger single vesicular release at OHC synapses. Maybe the better organization of the IHC ribbon structure could account for more their effective transmission (Wittig and Parsons, 2008). Another possible explanation might be the smaller aggregation of calcium channels under outer hair cell ribbons – the patches thought to include voltage-gated calcium channels

are four times smaller in OHCs than in IHCs (Saito, 1990). Immunohistochemistry studies also found a lack of the vesicular glutamate transporter VGlut3 in OHC. VGlut3 is used in IHC vesicles and is required for IHC synaptic transmission (Seal et al., 2008). It is unknown whether other vesicular glutamate transporter isoforms underlie OHC synaptic transmission.

Like the IHC-type I synapse, synaptic transmission at the OHC – type II afferents synapse is also likely to be mediated by AMPA(α-amino-3-hydroxy-5-methyl-4-isoxazole propionic acid)-type glutamate receptors. Whole-cell patch clamp recordings made directly from type II afferent spiral dendrites revealed typical fast excitatory postsynaptic currents (EPSCs) when OHCs were depolarized by high potassium solution. These EPSCs can be reversibly blocked by the AMPA receptor antagonist NBQX (Figure B7) (Weisz et al., 2009). However, this physiological evidence was not supported by the previous immunohistochemistry studies that examined the postsynaptic glutamate receptors expressed in the cochlea. Many studies have demonstrated puncta of GluA2/3 antibody staining at the type I afferent terminals, but failed to label the postsynaptic receptor in type II afferents (Flores-Otero and Davis, 2011; Khimich et al., 2005; Liberman et al., 2011; Matsubara et al., 1999; Thiers et al., 2008). A recent study using antibody against only the GluA2 subunit revealed puncta of GluA2 receptors juxtaposed to Ribeye – a protein component of the ribbon. However the staining was observed in P8 but not adult rat cochlea (Huang et al., 2012). This immunohistochemistry study on mouse cochlea proposed development changes in synaptic markers expression, showing a synaptic refinement process. Excess CtBP2 and GluA2/3 puncta were found in the outer hair cell regions in newborn mice, from P0 to around P3/P6. After that, great reduction of

these immunostaining puncta was seen until the onset of hearing (P12). Although the

study claimed the presence of GluA2/3 in adult mouse outer hair cell region, the labeling

was rather weak and was found not associated with the presynaptic marker CtBP2,

therefore it is still unclear if AMPARs participate in the OHC-type II synapse.
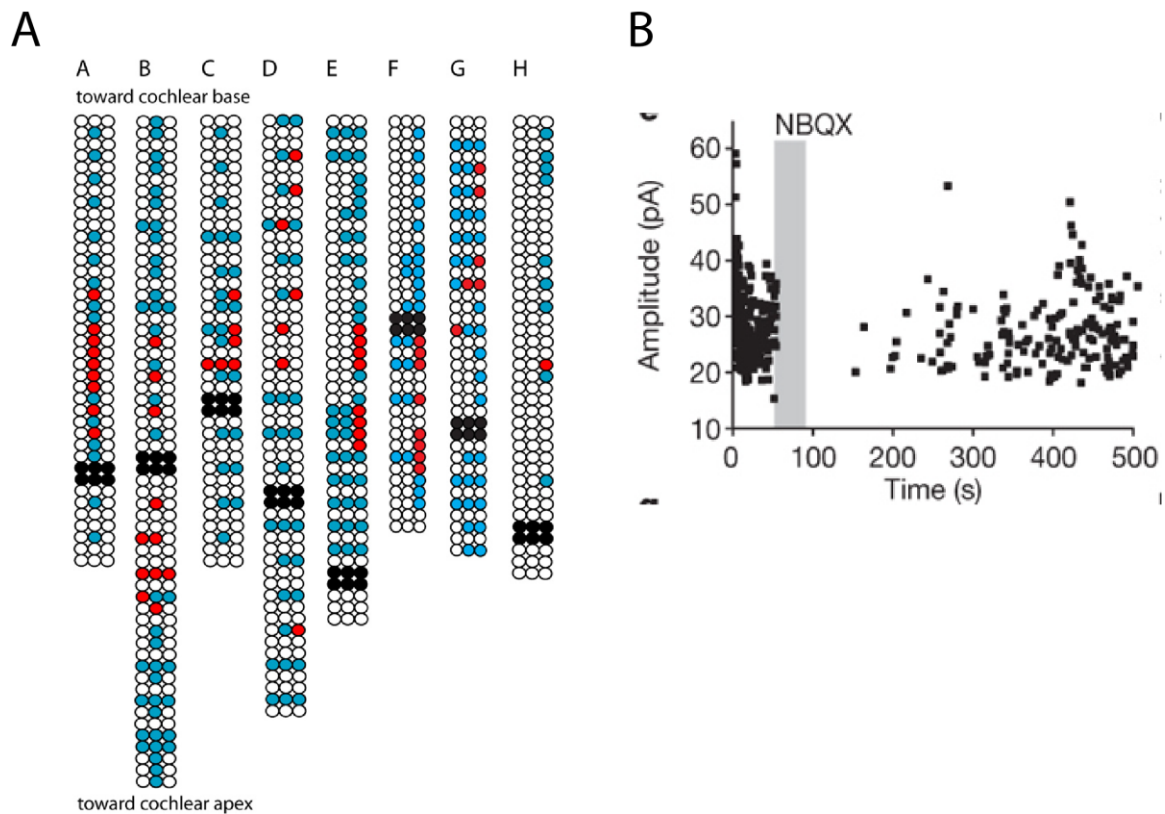
Figure B7. Synaptic transmission from OHC to type II afferents is likely mediated by AMPA receptors. A. Receptive field map of OHC inputs onto eight different type II afferents. Red: functionally connected OHCs. Blue: OHCs showed no synaptic inputs to recorded type II afferents. White: OHCs have not been tested. Black: OHCs removed for type II afferents recordings. (Weisz et al., 2012). B. EPSCs triggered by OHC depolarization can be blocked by the AMPAR antagonist NBQX. (Weisz et al., 2009)

On the other hand, two subtypes of kainate receptors – GluK2 and GluK5 have

been shown to be consistently expressed in the OHC region in both young and adult rat

cochlea (Fujikawa et al., 2014). GluK2 was found juxtaposed to CtBP2 (the marker for presynaptic ribbon), whereas GluK5 was found associated with every puncta of the PSD-93 (a postsynaptic density protein) that extends in a string – named "C-shape" in this work (Figure B8). Both GluK2 and GluK5 antibody labeling were also found in the medial efferent terminals and in the center of the OHC base (Fujikawa et al., 2014). Kainate receptor is another class of ionotropic glutamate receptor, less understood than AMPA and NMDA (N-methyl-D-aspartate) receptors. Current understandings about their function include that they could mediate some synaptic current at certain synapses; they potentially modulate synaptic transmission; and they support maturation of neural circuitry via an unconventional metabotropic pathway (Lerma and Marques, 2013). In native neurons, kainate receptor-mediated EPSCs are prominently slower in kinetics than AMPA receptor-mediated EPSCs (Castillo et al., 1997; Frerking et al., 1998; Vignes et al., 1998), due to the action of the auxiliary subunit Neto (Straub et al., 2011). The AMPA receptor antagonist NBQX used in the physiological study may also serve as competitive antagonist for kainate receptors (Kew and Kemp, 2005), leaving open the possibility for kainate receptor-mediated EPSCs in type II cochlear afferents. To resolve this discrepancy, a more optimized characterization of synaptic proteins by immunostaining, as well as pharmacological studies with more specific kainate or AMPA receptor antagonists are needed.
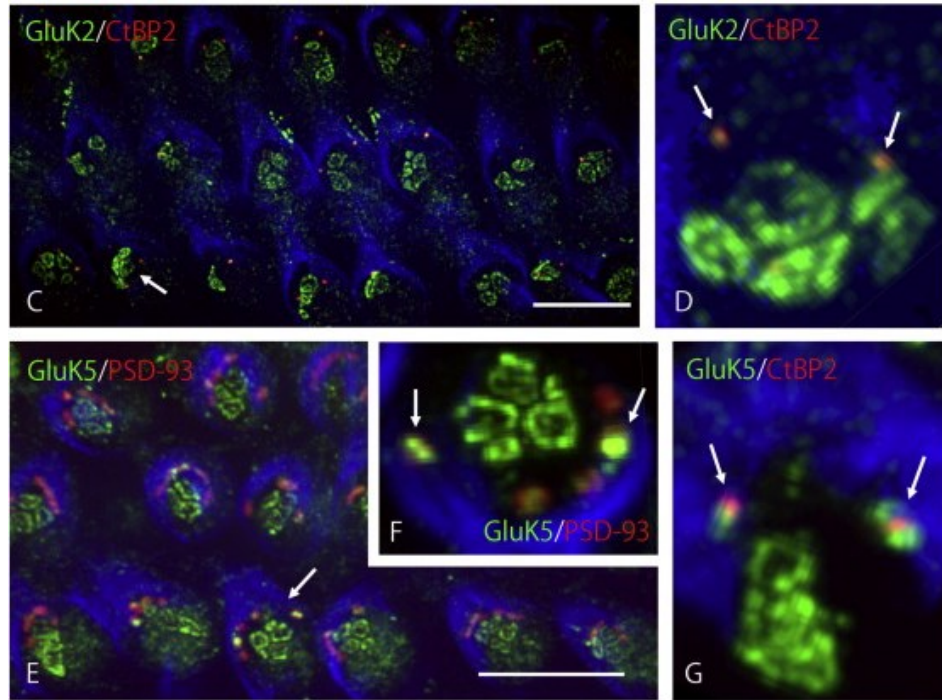
Figure B8. Kainate receptors GluK2 and GluK5 expression in OHC region of adult rat cochleae. Arrows in D and G point to postsynaptic densities thought to be on type II terminals, whereas the more bulky GluK2 or GluK5 labeled terminal are likely belong to the medial efferents. (Fujikawa et al., 2014)

Intracellular recordings from type II afferents revealed weak synaptic activation of type II afferents by OHCs. Excitatory postsynaptic potentials (EPSPs) recorded from type II afferents were small (3.8±2.0 mV) compared with the depolarization needed to reach action potential threshold (~25 mV) (Weisz et al., 2009). Functional connections between OHC and type II afferents were mapped by recording from type II afferents while puffing high potassium solution to activate each individual OHC (Weisz et al., 2012). Mapping of presynaptic OHCs yields an estimation of at least ten OHCs providing synaptic inputs to type II afferents. Taking into account the low release probability of OHC (average ~ 0.25) also measured in this set of experiments, it suggests that type II

afferents may fire action potentials only when the entire pool of presynaptic OHCs are activated and the EPSPs are able to summate. Dual electrode recordings from type II afferents demonstrated a length contact longer than the extent of their spiral process, therefore summation of EPSPs over the long synaptic input regions is possible (Weisz et al., 2014). In addition to the weak synaptic inputs onto type II afferents, large responses to ATP were recorded in type II afferents. ATP-induced responses include a synaptic component through activation of OHCs by ATP (Nakagawa et al., 1990), and a more prominent, slow current that seems to be a direct effect of ATP on type II afferents (Weisz et al., 2009). Therefore, ATP seems to be a more potent way to activate type II afferents than the weak synaptic transmission from OHCs. The types of ATP receptors and their functional implication remained to be determined.

3. Purinergic signaling and function in the cochlea

3.1 General properties of purinergic receptors

Purinergic receptors are one of the most abundant receptors in the living organism. They are widely expressed in neurons and non-neural tissues, mediating cell-to-cell communication through synaptic transmission (as neurotransmitter or co-transmitter) or paracrine mechanisms (Abbracchio et al., 2009; Burnstock, 2009; Burnstock, 2013). They further divided in two families according to their endogenous agonists. A P1 receptor family activated by adenosine is subdivided into four classes (A_1, A_{2A}, A_{2B} and A_3) and are all G-protein coupled receptors. A P2 receptor family (primarily sensing adenine and uracil tri- and dinucleotides) includes two classes of receptors – P2X and

P2Y receptors with distinctive molecular properties and agonist selectivity. All of these

receptor subtypes were identified in the cochlea (Housley et al., 2009).

The ionotropic P2X receptors are non-selective cation channels that open in

response to extracellular ATP. Upon ATP binding the pore allows passage of Na^+ and K^+

(equal permeability), with significant permeability to Ca^{2+} (Egan and Khakh, 2004). They

include seven subtypes (designated as $P2X_1 - P2X_7$, according to historical order of

cloning) forming homomeric ($P2X_1$-$P2X_5$, and $P2X_7$) or heteromeric ($P2X_{1/2}$, $P2X_{1/4}$,

$P2X_{1/5}$, $P2X_{2/3}$, $P2X_{2/6}$, $P2X_{4/6}$ and $P2X_{4/7}$) trimers (Guo et al., 2007; Nicke et al., 1998;

North, 2002; Roberts et al., 2006). Hydropathy analysis and crystallography studies

revealed that each subunit possesses two hydrophobic transmembrane spanning regions

(TMRs), a large extracellular loop and intracellular NH_2 and COOH termini (Figure B9)

(Gonzales et al., 2009; Hattori and Gouaux, 2012; Kawate et al., 2009). The subunit

stoichiometry determines their differential ligand affinity and ligand-induced receptor

desensitization kinetics. In general, most P2X receptors have an EC50 of 1-10μM ATP

activation, except for the homomeric P2X7 which is less sensitive and activated at 100-

1000μM ATP concentrations (Junger, 2011). Once opened by ATP, P2X receptors could

serve as a significant source of Ca^{2+} entry, being able to regulate neurotransmitter release

(Sperlagh et al., 2007) and interact with many channels through Ca^{2+} signaling, including

nicotinic acetylcholine receptors, $GABA_A$ receptors and NMDA receptors (Khakh et al.,

2000; Pankratov et al., 2009).
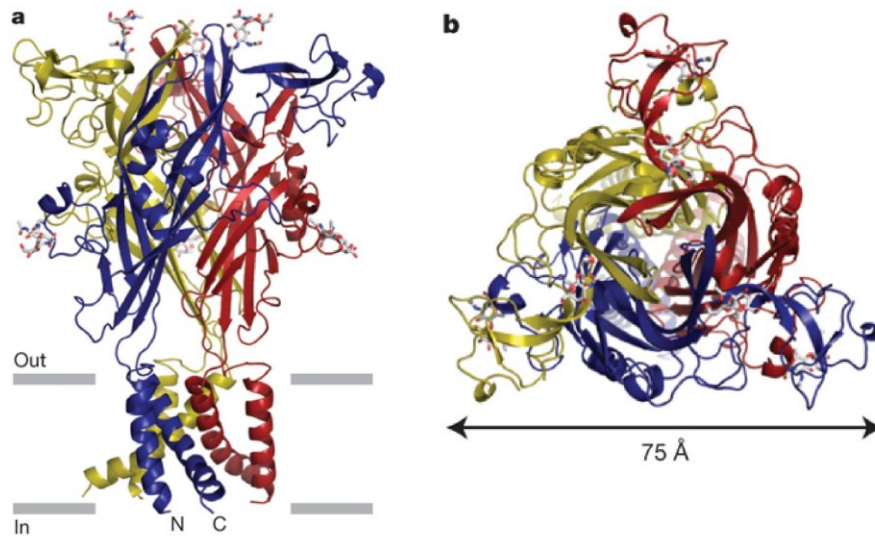
Figure B9. Stereoview of the homotrimeric P2X4 receptor structure. Modified from (Kawate et al., 2009).

The other class of P2 receptors includes P2Y receptors that are seven-transmembrane-spanning G-protein coupled receptors (GPCRs), forming homodimers or heterodimers (Figure B10). Among the eight P2Y receptors, P2Y1, P2Y2, P2Y4, P2Y6 and P2Y11 use G_q/G_{11} to activate phospholipase C (PLC), and therefore robustly trigger inositol lipid signaling responses, including the production of diacylglycerol (DAG) and inositol triphosphate (IP3) which could trigger IP3-mediated mobilization of internal Ca^{2+} stores and increased activity of protein kinase C. Activated Gαq may also promote Rho signaling through a guanine nucleotide exchange factor (p64 RhoGEF) (Lutz et al., 2005). The other subgroup of P2Y receptors, including P2Y12, P2Y13 and P2Y14, activate Gi and lead to Gαi-dependent inhibition of adenylyl cyclase and decreased levels of cyclic adenosine monophosphate (cAMP), regulating channels and protein kinases (Abbracchio et al., 2006). Because of their difference in amino acid sequence and molecular properties,

23

each P2Y receptor has a distinct pharmacological profile and is activated by different sets of adenine and uracil tri- and dinucleotides (Table B1) (von Kugelgen and Harden, 2011). UTP was found to activate P2Y2, P2Y4 and P2Y6 receptors. ATP could activate P2Y2, P2Y11, P2Y13 as well as rodent P2Y4 receptors. The EC50 for ATP activation is in the nano-molar range for P2Y2 and P2Y13 receptors, and is higher for rodent P2Y4 receptors (around 2 μM) and is highest for P2Y 11 receptors (around 17 μM) (Junger, 2011).
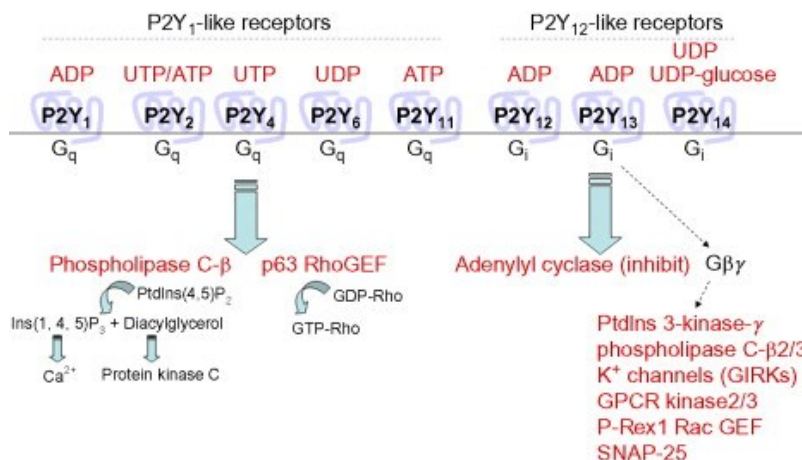
Figure B10. P2Y receptor subtypes and second messenger – mediated signaling pathways. (von Kugelgen and Harden, 2011).

Selected compounds acting as agonists at functionally defined mammalian P2Y receptor subtypes.

Type	Principle agonists	Selected references
P2Y$_1$	MRS2365>2-MeSADP > ADP = ADPβS	Henderson et al., 1995; Tokuyama et al., 1995; Ayyanthan et al., 1996; Janssens et al., 1996; Léon et al., 1996, 1997; Chhatriwala et al., 2004; Waldo and Harden, 2004
P2Y$_2$	PSB1114 > UTP = MRS2698 ≥ ATP > INS37217 > Ap4A > ATPγS	Lustig et al., 1993; Parr et al., 1994; Lazarowski et al., 1995; Rice et al., 1995; Chen et al., 1996; Nicholas et al., 1996; Ivanov et al., 2007; El-Tayeb et al., 2011
P2Y$_4$	UTP > UTPγS (human)	Communi et al., 1995, 1996a,b; Nguyen et al., 1995; Nicholas et al., 1996;
	UTP = ATP (rat, mouse)	Kennedy et al., 2000; Suarez-Huerta et al., 2001; Herold et al., 2004
P2Y$_6$	5-OMe-UDP(a-B) > MRS2693 > PSB0474 > UDP > UTP >> ATP	Chang et al., 1995; Communi et al., 1996b; Nicholas et al., 1996; Besada et al., 2006; El-Tayeb et al., 2006; Ginsburg-Shmuel et al., 2012
P2Y$_{11}$	ATPγS = BzATP > NF546 > ARC67085 > ATP (human)	Communi et al., 1997, 1999; Qi et al., 2001b; Zambon et al., 2001; White et al., 2003;
	ADPβS = 2-MeSADP > ATP (canine)	Meis et al., 2010
P2Y$_{12}$	2-methylthio-ADP > ADP > ATP	Foster et al., 2001; Hollopeter et al., 2001; Takasaki et al., 2001; Zhang et al., 2001; Chhatriwala et al., 2004
P2Y$_{13}$	ADP = 2-methylthio-ADP > ADPβS	Communi et al., 2001; Zhang et al., 2002; Marteau et al., 2003; Fumagalli et al., 2004
P2Y$_{14}$	α,β-methylene-2-thio-UDP > MRS2690 > UDP = UDP-glucose	Charlton et al., 1997; Chambers et al., 2000; Freeman et al., 2001; Ko et al., 2007; Fricks et al., 2009; Das et al., 2010; Gao et al., 2010

ARC67085, 2-propylthio-β,γ-difluoromethylene-D-ATP; Ap4A, diadenosine-tetraphosphate; ATPγS, adenosine-(O-3-thiotriphosphate); BzATP, benzoyl-benzoyl-ATP; INS37217, P^1-(uridine 5′)-P^4-(2′-deoxycytidine-5′)tetraphosphate; 2-MeSADP, 2-methylthio-ADP; MRS2365, (N)-methanocarba-2-methylthio-ADP; 2-MeSATP, 2-methylthio-ATP; MRS2690, diphosphoric acid 1-a-D-glucopyranosyl ester 2-[(4′-methylthio)uridin-5″-yl] ester; MRS2693, 5-iodo-UdP; MRS2698, 2′-amino-2′-deoxy-2-thio-UTP; NF546, 4,4′-(carbonylbis(imino-3,1-phenylene-carbonylimino-3,1-(4-methyl-phenylene)carbonylimino))-bis(1,3-xylene-α,α′-diphosphonic acid); PSB0474, 3-phenacyl-UDP; UTPγS, uridine-(O-3-thiotriphosphate).

Table B1. Compounds acting as gonists for P2Y receptor subtypes. Modified from (von Kugelgen and Harden, 2011).

ATP can be released from neurons and glia through multiple mechanisms. ATP was found to accumulate in secretory and synaptic vesicles, can be co-released with other neurotransmitters (e.g. GABA, glutamate and noradrenaline), and some evidence suggests the existence of ATP-only vesicles in the cortex and medial habenula (Pankratov et al., 2006; Pankratov et al., 2007). Despite the compelling evidence of vesicular release of ATP, it had been assumed that ATP could be released only from damaged or dying cells. But more evidence suggests that ATP can be released even from healthy cells under stress conditions, including mechanical stress, osmotic changes as well as hypoxia and stimulation of certain agents. Such mechanisms involve ATP exit through large-pore channels – connexin or pannexin hemichannels, plasmalemmal voltage-dependent anion channels and P2X7 receptors (Bodin and Burnstock, 2001; Lazarowski, 2012). It is not clear though whether other nucleotides (e.g. UTP, ADP and UDP) are released by similar mechanisms under physiological or pathological conditions. Once released, ATP undergoes rapid enzymatic degradation by ectonucleosidases (Yegutkin, 2008). In this way the lifetime of ATP is controlled and the action of ATP sensitive receptors is decreased. The products of enzymatic reaction could serve as ligands for additional purinergic receptors. For example, ATP can be degraded to ADP and AMP, through the action of E-NTPDases (ecto-nucleoside triphosphate diphosphohydrolases) and E-NPPs (ecto-nucleotide pyrophosphatase/phosphodiesterases), and further to adenosine by ecto-5'-nucleotidases. Indeed, enzymatic breakdown generates the most recognized source of adenosine acting on the P1 receptors, although some subpopulations of neurons or astrocytes may directly release adenosine (Wall and Dale, 2007).

3.2 Purinergic receptor expression and function in the cochlea

Purinergic components are widely expressed in the neural and non-neural structures in the young and adult cochlea. P2X receptor mediated currents have been recorded from isolated inner and outer hair cells of the adult guinea pig (Housley et al., 1999; Sugasawa et al., 1996). P2X2 receptors are expressed in hair cells and its expression pattern has been both anatomically and functionally localized to the apical surface and stereocilia (Housley et al., 1992; Housley et al., 1999; Housley et al., 1998; Jarlebark et al., 2000; Mockett et al., 1994; Yan et al., 2013). P2X receptor-mediated currents were recorded in isolated OHCs (Glowatzki et al., 1997). The current only appeared upon puffing ATP onto the apical surface but not upon local application of ATP to the basolateral sides of OHCs (Housley et al., 1992). This is further supported by calcium imaging studies. Focal application of ATP triggers Ca^{2+} entry first from the apical surface of the OHCs, and then a second surge of Ca^{2+} signal was observed at the base which is proposed to be mediated by IP3 receptors on a specialized ER structure (known as Hensen's body) in the hair cell (Mammano et al., 1999b). The role for these ATP-induced currents in OHCs is not clear. It has been reported that direct application ATP affected the electromotility of OHCs and reduced the gain of the cochlear amplifier (Zhao et al., 2005). However, another study found that ATP responses did not interfere with the electromotility of OHCs (Mammano et al., 1999b). Another proposal is that the nonselective conductance of P2X receptors may shunt K^+ out of the endolymphatic compartment, being a protective mechanism against acoustic stress (see discussion in part 3.3 of this Introduction). P2X7 receptors are expressed transiently in hair cells before postnatal day 6 but their function is unknown (Nikolic et al., 2003). Expression of P2Y1,

P2Y2 and P2Y4 receptors was found in the outer hair cells of guinea pig by immunolabeling (Mammano et al., 1999a; Szucs et al., 2004). However, these findings are confounded by the lack of UTP induced current in guinea pig outer hair cells (Housley et al., 1999).

In spiral ganglion neurons, immunohistochemistry and in situ RT-PCR experiments have identified a variety of P2 receptors, including P2X3 receptors in early postnatal days and P2X2 and P2X7 as sustained expression throughout life (Huang et al., 2005; Huang et al., 2007b; Nikolic et al., 2003; Salih et al., 1998). It has been proposed that the transient expression of P2X2/P2X3 receptors regulates neurite outgrowth during development. In early postnatal days, type I and type II afferents form excess innervation on both inner and outer hair cells followed by pruning and refinement of the mis-matched fibers to reach specific synaptic innervation patterns. The expression of P2X2/P2X3 receptors was detected by quantitative singe cell RT-PCR. Activation of these receptors was proposed to inhibit neurite extension elicited by the neurotrophin BDNF and to contribute to the withdrawal phase of pruning (Greenwood et al., 2007). P2X2 has been localized to the postsynaptic specialization of the afferents under inner and outer hair cells by immunogold labeling (Housley et al., 1999), and was found to be expressed in the somata of spiral ganglion neurons (Salih et al., 1998). P2X7 receptor expression has been detected in the embryonic (E14–E18 days) and postnatal (P0–adult) rat cochlea using immunohistochemistry. Immunolabeling for P2X7 was detected in the spiral ganglion, efferent and afferent bundle that cross the tunnel of Corti, and synaptic regions beneath inner and outer hair cells (Nikolic et al., 2003). The metabotropic P2Y receptors have also been found to express in the spiral ganglion by immunolabeling, although type

I and type II neurons were not distinguished (Huang et al., 2010). Despite the findings of various P2 receptor expression in SGNs of which 95% are type I neurons, their response to ATP is rather small, according to direct recording from type I afferent boutons in an *ex vivo* preparation of young rat cochlea (Tritsch et al., 2007). A contradictory result comes from recordings on the soma of isolated SGN in neonatal rats (Ito and Dulon, 2002). The response of SGNs to 100μM ATP is big but variable (760 ± 530 pA, Vhold = -50 mV, n = 135) and ~77% of the cells displayed two components – a faster P2X-like conductance with a response latency of less than 50 ms, and a slower response (occurred over 1 s) that was attributed to P2Y receptors and with a reversal potential at 0 mV. Such discrepancy could have arisen from the differential distribution of receptors in dendrites versus somata, or the effect of mechanical and enzymatic treatment on the receptors during the cell isolation process.

On the other hand, it is clear that type II afferents respond to ATP robustly at least in early postnatal days. Direct recording from type II afferents' dendrites revealed large depolarizations induced by ATP, and action potentials were elicited in extracellular recordings during ATP application. These action potentials could be blocked by pyridoxalphosphate-6-azophenyl-2′,4′-disulfonic acid (PPADS), a P2X receptor antagonist that also partially blocks P2Y4 and P2Y6 receptors. After the onset of hearing, ATP responses of type II afferents persist but apparently become smaller (Weisz et al., 2009). It is unknown whether both P2X and P2Y receptors mediate such responses and what might be the functional significance of P2 receptor mediated signaling in type II afferents. Only one study localized the P2X2 immunogold labeling at type II afferent terminals (Housley et al., 1999), providing a candidate receptor mediating the PPADS

sensitive response. P2Y2 receptors are expressed in a small subset of SGNs, labeling around 5% -10% of the total population and so consistent with type II afferents, but this study did not provide further evidence for the identity of these SGNs (Huang et al., 2010).

Purinergic signaling is important for the development of synaptic connections in the auditory system. Before the onset of hearing, a transient pseudo-stratified epithelium, known as Kölliker's organ is formed medial to the inner hair cells. The inner supporting cells of the Kölliker's organ spontaneously release ATP and play a crucial role in generating periodic, high-frequency bursts of activity in the developing auditory pathway (Tritsch et al., 2010; Tritsch et al., 2007). This phenomenon involves ATP-induced ATP release, which activates the autoreceptor (P2Y receptor) on the inner supporting cells, thus triggering an increase in intracellular Ca^{2+}. This in turn activates TMEM16A (transmembrane protein 16A), a Ca^{2+}-activated Cl^- channel, which not only expels Cl^-, but also triggers efflux of K^+ (as counter ions) and water (Figure B11) (Wang et al., 2015). The rise in extracellular K^+ depolarizes IHCs to trigger glutamate release, generating repetitive firing of type I afferents. ATP is indispensable for this process, because such effects can be blocked by the application of apyrase, an enzyme that hydrolyzes ATP (Tritsch et al., 2007). The repetitive firing of type I afferents stopped around the onset of hearing (~ postnatal day 12) and at time when the Kölliker's organ is degenerated. This neural activity in early development mediated by ATP is considered to promote targeting and refinement of neuronal projections and maturation of the auditory system.
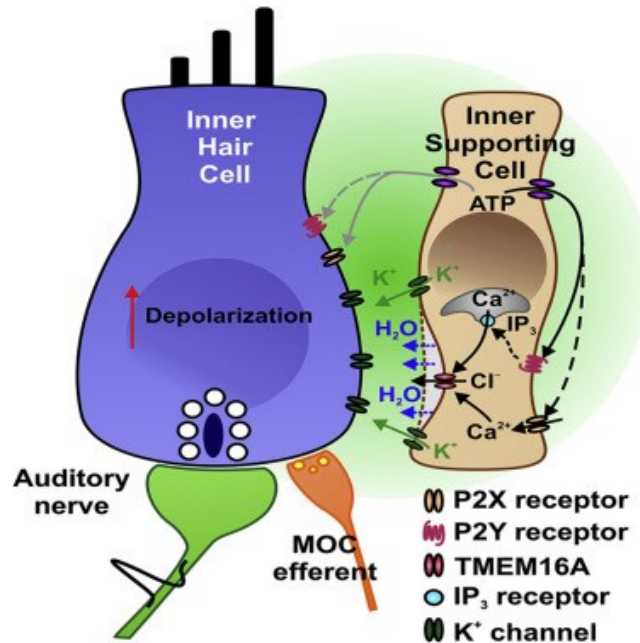
Figure B11. Mechanism underlies spontaneous activity in developing cochlea before hearing onset. (Wang et al., 2015)

3.3 Purinergic signaling involved in acoustic damage

Acoustic overexposure damages structures and cells in the middle and inner ear and can cause permanent hearing deficits. At very high sound pressure levels (e.g. blasts), the eardrum and the cochlea can be ruptured immediately, leading to permanent deafness (Hamernik et al., 1984; Kerr and Byrne, 1975). At lesser sound pressure levels (usually below 140 decibels), such as a loud concert, noise progressively damages sensory neurons in the inner ear, resulting in the death of outer hair cells (Figure B12), as well as swelling and retraction of type I afferent terminals which carry sound information to the brain (Kujawa and Liberman, 2009; Liberman and Kiang, 1978; Wong and Ryan, 2015). The effect of noise exposure can be long-lasting, with degeneration of SGNs over months

after noise exposure (Kujawa and Liberman, 2009). Unlike non-mammalian vertebrates, the sensory neurons in mammalian cochlea do not regenerate. The resulting loss of sensory components and the hearing deficits are thus irreversible. The acoustic stapedius reflex in the middle ear (Brask, 1979) and efferent inhibition of hair cells (Guinan, 2006) can attenuate acoustic damage to some extent. However, a more effective way is to warn the animal of the damaging level of sound and trigger avoidance behavior by means of nociception.
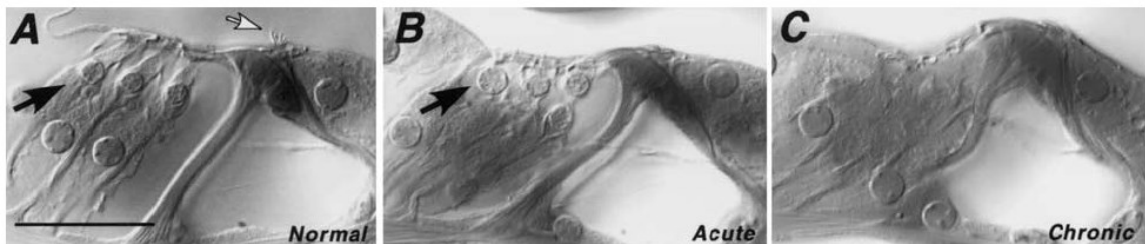
Figure B12. Noise exposure damages OHCs. A. control. B. OHC swells after 24 hours exposure to noise band at 116 dB (arrow). C. Selective loss of outer hair cells after over one week exposure to 116 dB noise. (Wang et al., 2002)

Interestingly, the concentration of ATP is increased in the cochlea during stress conditions *in vitro* and acoustic damage *in vivo*, serving as a potential nociceptive signal as in the somatosensory system. ATP is kept at low concentrations (10 - 20 nM) in the endolymph and perilymph (Munoz et al., 1995), likely due to the basal activity of various types of ectonucleotidases in the cochlea (Vlajkovic et al., 1996). After noise exposure (15 min, 10 kHz, 110 dB SPL. broad band), ATP concentration in the cochlear fluid is increased 2-3 fold, measured by the luciferase – luciferin assay (Munoz et al., 2001). ATP release also can be induced in physiological conditions, such as hypotonic stress (275 mOsm external solutions) and mechanical stimulation (puffing micro glass beads),

tested by a whole-mount *in vitro* preparation of adult guinea pig cochlea (Zhao et al., 2005).
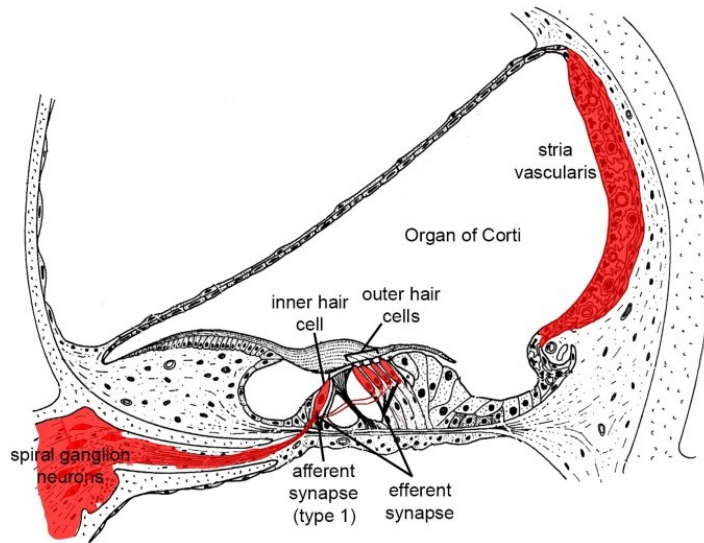
Figure B13. Cochlear structures that are prone to damage and death over acoustic overstimulation. Shown in red. (Wong and Ryan, 2015)

The source of ATP release includes multiple structures that are prone to acoustic damage, including the stria vascularis and the organ of Corti (Figure B13). Vesicular storage of ATP was found in the marginal cells of stria vascularis (Munoz et al., 2001; White et al., 1995), serving as a possible source of ATP after acoustic damage. ATP release from the organ of Corti is mediated by the connexin hemichannels in outer supporting cells, including Deiters' and Hensen's cells of the outer hair cell region. Mechanical or focal damage of a single outer hair cell is enough to trigger a Ca^{2+} rise in the surrounding supporting cells, causing ATP release through connexin hemichannels. ATP could further act on purinergic receptors of the adjacent cells, activating the inositol lipid signaling and mobilizing internal Ca^{2+} stores (Piazza et al., 2007). With such

32

positive feedback, this process triggers a regenerative Ca^{2+} wave that spreads hundreds of microns along the cochlear spiral, releasing a great amount of ATP over tens of seconds upon each outer hair cell ablation (Figure B14). This process is highly dependent on ATP release through the connexin hemichannels, because the propagation of Ca^{2+} waves can be blocked by apyrase that hydrolyzes ATP (Gale et al., 2004) and by connexin hemichannel blockers (Anselmi et al., 2008). Lanthanum, a blocker for cell surface-expressed connexin hemichannels that does not affect gap junction between cells, was enough to limit the propagation of the calcium wave, suggesting that such process is dependent on extracellular release of ATP acting on the neighboring cells (Anselmi et al., 2008). This mechanism is highly sensitive to ATP. Application of nano-molar concentrations of ATP is enough to trigger the regenerative Ca^{2+} waves (Gale et al., 2004). In addition, a faster ATP-dependent Ca^{2+} wave in outer hair cell rows has been observed to be triggered by hair cell damage and might be mediated by P2X4 receptors (Lahne and Gale, 2010). The oscillatory Ca^{2+} wave in the outer supporting cell region reflects a characteristic damage signal in the cochlea, which could further contribute to the activation of extracellularly regulated kinases 1 and 2 (ERK1/2) and c-Jun N-terminal kinase (JNK) (Gale et al., 2004; Lahne and Gale, 2008), leading to protective effects such as hair-cell engulfment and scarring of the reticular lamina.
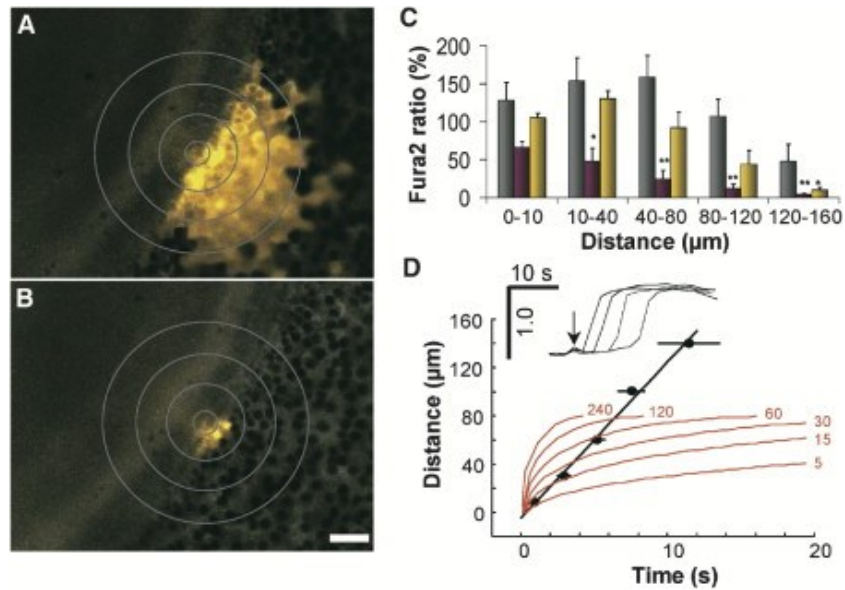
Figure B14. A regenerative calcium wave triggered by ablation of a single hair cell. The calcium wave in control (A) can be blocked by apyrase, an enzyme that hydrolyzes ATP (B). (C) Calcium signal spreading from the site of damage can travel over a hundred microns. Grey: control; purple: in apyrase; gold: wash. (D) Comparison between measured wave speed (grey closed circle) and a diffusion model with varying coefficients (red) suggest an active mechanism for wave propagation. (Gale et al., 2004)

Purinergic signaling has also been proposed as a protective mechanism against acoustic trauma by shunting K^+ in the endolymph to reduce the endolymphatic potential. In the intact cochlea, the apical surface of outer hair cells is bathed in endolymph and the basolateral surface bathed in perilymph. In addition to this unique ionic composition, an endolymphatic potential (EP) of ~80 mV contributes significantly to the driving force and is essential for mechanotransduction in hair cells (Wangemann, 2006). The integrity of the endolymphatic compartment is ensured by the tight junctions of cells lining the scala media. It has been found that P2X2 receptors are expressed on the cell surfaces facing the endolymphatic compartment (Figure B15), including Reissner's membrane, inner and outer sulcus cells and hair cells (Housley et al., 1999; Housley and Ryan, 1997; Jarlebark et al., 2000). It has been proposed that ATP released under stress conditions (e.g. acoustic

overstimulation) could activate P2X2 receptors. These non-selective cation channels surrounding the endolymphatic component allow ion flow and could shunt K^+ out of endolymph, resulting in a measurable reduction of the EP. This mechanism is considered as neuroprotective because it reduces the responsiveness of hair cells through decreasing EP under stress conditions in the cochlea. This hypothesis was further tested in P2X2-null mice. Under noise exposure, lack of P2X2 receptors leads to enhanced activity of outer hair cells and in the inner hair cell – type I afferent pathway, measured by distortion product otoacoustic emission (DPOAE) and auditory brainstem response (ABR), and the P2X2-null mice were more vulnerable to noise-induced permanent hearing loss (Housley et al., 2013; Yan et al., 2013). A P2X2 mutation was shown to be associated with a dominantly inherited, progressive sensorineural hearing loss DFNA41 in human (Yan et al., 2013). Noise exposure might also dynamically regulate the expression of purinergic components in the cochlea, causing up-regulation of P2 receptors (Wang et al., 2003) and ectonucleotidases that hydrolyze ATP (Vlajkovic et al., 2004; Vlajkovic et al., 2006).
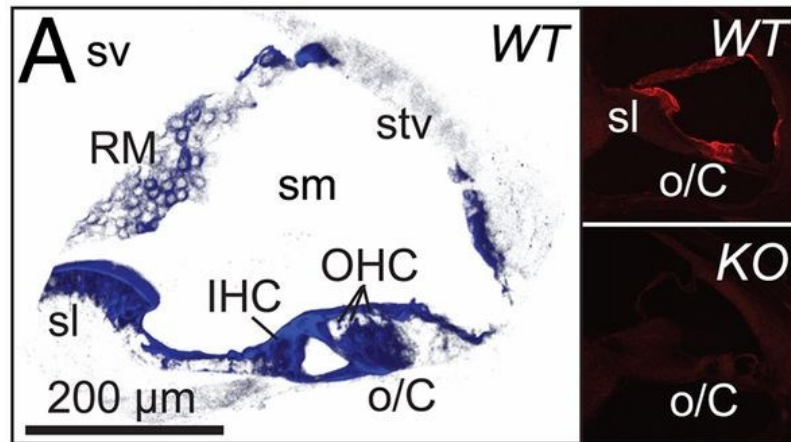
Figure B15. P2X2 receptors are expressed in the cells lining the endolymphatic compartment in the mouse cochlea. P2X2 are expressed in the Reissner's membrane

epithelial cells (RM), spiral limbus (sl), and organ of Corti (o/C), including IHCs and
OHCs. sm, scala media; stv, stria vascularis; sv, scala vestibuli. (Housley et al., 2013)

4. Hypersensitivity in pain and auditory pathologies

4.1 Purinergic signaling and pain

The hypothesis that ATP serves a nociceptive signal in the ear invites comparison

with the canonical pain mechanism in the somatosensory system. ATP has been

identified as an algogenic reagent through early studies demonstrating that injection of

ATP into human skin blisters induces the sensation of pain (Bleehen and Keele, 1977;

Collier et al., 1966). Animal models with sub- or intra-plantar injection of ATP could

also induce nocifensive behavior, such as hindpaw lifting and licking (Bland-Ward and

Humphrey, 1997; Hamilton et al., 1999). Homomeric P2X3 receptors and heteromeric

P2X2/3 receptors were localized predominantly to the non-peptidergic small nociceptive

sensory neurons in dorsal root ganglion (DRG). At L4/5 P2X3 positive neurons were

found to constitute ~35% of the DRG neurons (Bradbury et al., 1998; Chen et al., 1995;

Lewis et al., 1995). These pseudomonopolar neurons give off unmyelinated C-fibers,

with central projections terminating at the inner lamina II of the dorsal horn and

peripheral terminals targeting skin, oral cavity and visceral organs (Burnstock, 2009;

Burnstock, 2013). P2X receptor-expressing small diameter DRG neurons were found to

largely overlap with the subpopulation that is labeled by the isolectin IB4 (Bradbury et al.,

1998). ATP responses have been extensively characterized using whole cell gigaohm

recordings of dissociated DRG neurons. Most of the DRG neurons respond to ATP with a

transient current, whereas other subpopulations of DRG neurons developed persistent or

biphasic responses to ATP. This discrepancy has been attributed to the different subtypes of P2X receptors expressed – P2X3 receptors mediated the fast desensitizing transient responses; P2X2 receptors mediating the slowly desensitizing responses; coexpression of P2X2/3 receptors demonstrating both features and the responses becoming biphasic (Burgard et al., 1999; Rae et al., 1998). This has been further confirmed in knockout mice that P2X3$^{-/-}$ DRG has more sustained responses and P2X2$^{-/-}$ has more transient responses (Cockayne et al., 2005; Zhong et al., 2001). Double mutants for both receptors eliminate DRG neurons' responses to ATP and the animal had reduced pain-related behavior (Cockayne et al., 2005). As previously discussed, ATP can be released from many kinds of non-neuronal tissues during hypoxia or tissue stress, as well as from dying or damaged cells. In an *in vitro* preparation, it has been shown that nociceptive neurons could be activated when a nearby skin cell was damaged. The response was ATP and P2X receptor dependent and could trigger action potentials in these nociceptors (Cook and McCleskey, 2002). ATP is thought to be involved in acute pain. It has also been shown that during inflammation or in the presence of other algogenic compounds, ATP may contribute to increased sensitivity to mildly painful stimuli (hyperalgesia) or to painful sensations to previously innocuous stimuli (allodynia). In carrageenan – inflamed skin, there was an increased number of ATP responsive neurons in the DRG, and the C-fibers' responses were enhanced (Hamilton et al., 2001). Locally injected ATP could sensitize the mechanosensitive fibers, leading to elevated nociceptive responses to pressure or touch (Zhang et al., 2001).

The role of P2Y receptors in pain was less studied compared to P2X receptors. In DRG neurons, mRNA of various P2Y receptors has been detected, including P2Y1,

P2Y2, P2Y4 and P2Y6 (Kobayashi et al., 2006). Among them, P2Y2 receptors have been proposed as the major form of DRG expressing P2Y receptor (Malin et al., 2008), and P2Y receptors have been found to localize with P2X3 receptors as well as the capsaicin-sensitive transient receptor potential vanilloid 1(TRPV1) channels (Gerevich and Illes, 2004; Ruan and Burnstock, 2003). Signaling through P2Y receptors in DRG neurons has been shown to cause release of Ca^{2+} from intracellular stores (Sanada et al., 2002), affect thermal nociception (Malin et al., 2008), and seems to potentiate pain induced mechanically or chemically via TRPV1 channels (Moriyama et al., 2003).

4.2 KCNQ channels and neuronal excitability regulation

As mentioned above, chronic pain could involve a decreased threshold to painful stimuli - hyperalgesia. *Allodynia* refers to the pain that occurs in response to normally innocuous stimuli. Chronic pain is usually associated with enhanced or abnormal excitability of neurons, for example the nociceptors or central neurons demonstrating enhanced responsiveness or lowered threshold for stimulation and synaptic inputs (Sandkuhler, 2009). Potassium channels play an important role in regulating neuronal excitability. All of the four major groups of potassium channels (i.e. voltage-gated, two-pore, calcium-activated and inward rectifying potassium channels) have been examined in DRG neurons in pathologies related to pain. Opening of potassium channels was proposed to reduce excitability of the sensory neurons. This mechanism could counteract action potential generation at the peripheral terminals, decrease overall conduction

fidelity along the fibers and affect synaptic transmission onto the central neurons (Tsantoulas and McMahon, 2014).

Among the potassium channels, some are known to be regulated by G-protein coupled second messenger pathways, so could be modulated by nucleotides (e.g. ATP). P2Y receptor regulated potassium channels include GIRK (G protein-coupled inward rectifiers K^+ channels) and KCNQ (potassium voltage-gated channel subfamily Q) channels. GIRK channels can be activated by $Gi_{/o}$-coupled metabotropic receptors. Activation of $Gq_{/11}$ pathway may also modulate GIRK channels, leading to decreased activity through activation of protein kinase C or depletion of PIP2 (phosphatidylinositol 4,5-bisphosphate) (Luscher and Slesinger, 2010). A role for GIRK channels in hyperalgesia has been suggested in both peripheral and central neurons. Phosphorylation of GIRKs decreases channels activity and is thought to promote sensitization at dorsal horn of the spinal cord following neuropathy or inflammation (Ippolito et al., 2005). GIRKs are also found to be associated with the analgesic effect of opioids and endocannabinoids (Nockemann et al., 2013; Ocana et al., 2004).

On the other hand, current findings suggest that KCNQ channel modulation by G protein-coupled pathways is solely by inhibition. KCNQ channels belong to the Kv7 family voltage-gated potassium channels. They are also called 'M-channels' due to the first identification of these channels through muscarinic suppression (Brown and Adams, 1980). The 'M-currents' recorded in bullfrog sympathetic neurons were found to be inhibited by the application of ATP and UTP in the early days (Adams et al., 1982; Akasu et al., 1983). Later studies suggest that the mechanism of KCNQ channel

inhibition is due to the reduction of PIP2 as a result of $Gq_{/11}$ activation. It has been shown

that PIP2 is crucial for keeping the KCNQ channels open (Robbins et al., 2006; Suh and

Hille, 2002; Suh et al., 2006; Zhang et al., 2003) by binding to the C-terminus of the

channels (Hernandez et al., 2008). Activation of metabotropic receptors that link to $Gq_{/11}$

(for example muscarinic acetylcholine receptors, P2Y receptors, histamine H1, mGluR1

and mGluR5 glutamate receptors) leads to activation of phospholipase C that rapidly

hydrolyzes PIP2, causing a great reduction (up to 90%) of membrane PIP2 within a few

seconds (Suh et al., 2004; Winks et al., 2005). As a consequence, KCNQ channels are

closed upon receptor activation (Brown and Passmore, 2009).
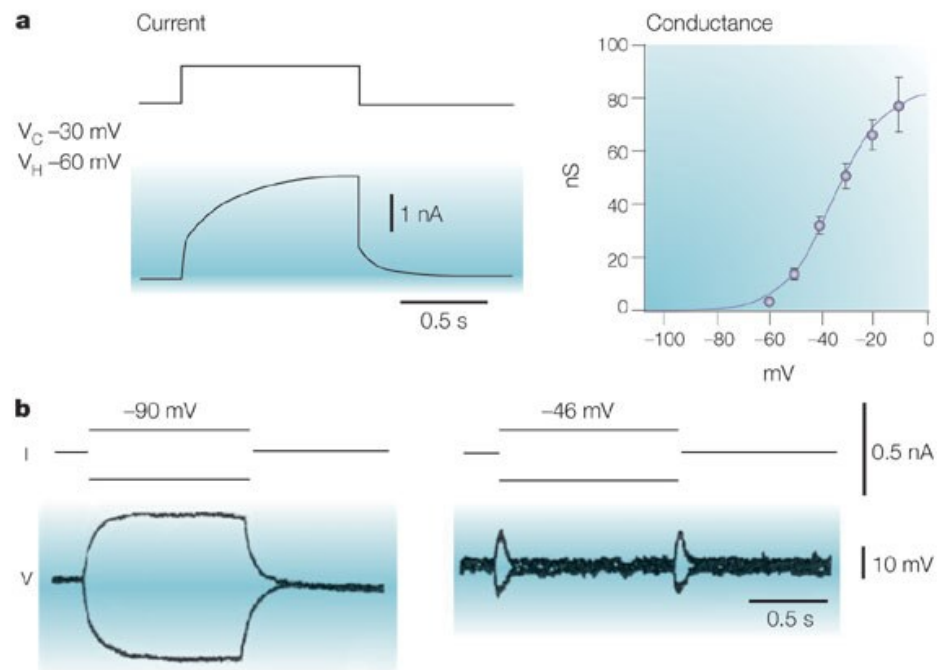
Figure B16. Physiological properties of KCNQ channels. A. KCNQ channels are slow activating and do not inactivate. Right: the increase in whole-cell conductance as a function of voltage changes. B. KCNQ currents 'clamps' the membrane potential. (Delmas and Brown, 2005)

40

The voltage-gated KCNQ channels have some unique properties. They are activated slowly by depolarization (usually tens of milliseconds) and therefore do not contribute to individual action potentials (for example the repolarization phase) which occurs on a much faster time scale. KCNQ channels start to activate around the normal resting membrane potential (~ -60mV) but do not inactivate, generating a steady outward current at depolarizing voltages (Figure B16 A). Therefore KCNQ channels are important for neuronal excitability and could serve as a 'brake' on repetitive firing (Figure B16 B) (Brown and Passmore, 2009; Delmas and Brown, 2005). At more depolarized voltages when many KCNQ channels are opened, the effect of further depolarization could be counteracted by the shunting effect of opened KCNQ channels. For example the same current injection step at -46 mV (~30% opened KCNQ channels) induced a much smaller depolarization than at -90 mV (all closed). In this way KCNQ channels have a profound dampening effect on repetitive firing and when cells are depolarized (Brown, 1988). Consequently, activation of GPCRs or pharmacological manipulations that close these channels would lead to elevated neuronal excitability and in some cases an altered tonic firing pattern. In rat sympathetic neurons, retigabine (a KCNQ channel opener) enhanced the M current that hyperpolarized the neuron and stopped firing. XE991 (a KCNQ channel blocker) reduced the M current and made the neuron more excitable, changing from a phasic to tonic firing pattern (Figure B17) (Brown and Passmore, 2009). Among DRG neurons, KCNQ channels were found co-expressed with TRPV1 channels in small neurons (Passmore et al., 2003). Opening of KCNQ channels by retigabine was found to decrease the activity of Aδ and C fibers, and could exert analgesic effects on

41

somatosensory pain (Blackburn-Munro and Jensen, 2003; Dost et al., 2004; Lang et al., 2008; Passmore et al., 2003; Rivera-Arconada and Lopez-Garcia, 2006)
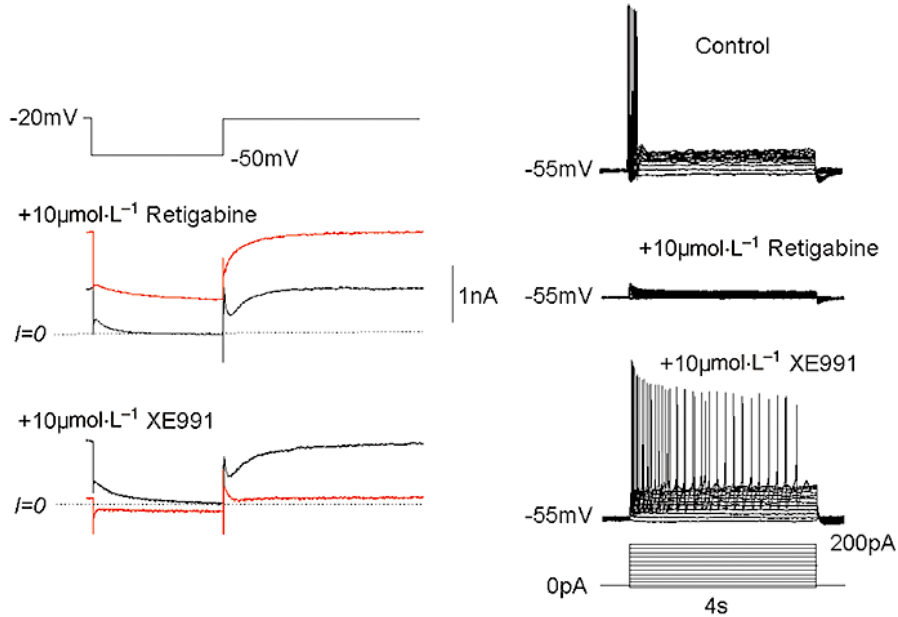
Figure B17. Enhancing or blocking KCNQ channels affect excitability of dissociated rat sympathetic neurons. Retigabine: KCNQ opener. XE991: KCNQ blocker. (Brown and Passmore, 2009)

KCNQ channel dysfunction has been linked to human diseases. Among the five subtypes, KCNQ4 mutation leads to DFNA2 (autosomal dominant deafness locus 2), a nonsyndromic, dominant progressive hearing loss (Kharkovets et al., 2000; Kubisch et al., 1999). KCNQ4 channels are expressed in OHCs and IHCs (Kubisch et al., 1999; Mammano and Ashmore, 1996; Marcotti and Kros, 1999), and were found to be important for IHC resting membrane potential and intracellular calcium levels (Oliver et al., 2003). Immunolabeling for KCNQ2 and KCNQ3 showed expression in spiral ganglion neurons (Jin et al., 2009). Expression of KCNQ4 was also detected in spiral ganglion neurons, and like their expression in the IHCs, there was a basal-to-apical

gradient such that expression was highest at the base of the cochlea (Beisel et al., 2000). Recordings from isolated SGNs revealed a corresponding gradient. A larger KCNQ channel current was recorded in basal SGNs. Inhibition of these channels is thought to promote cell death through elevated intracellular calcium concentration (Lv et al., 2010). These studies on SGNs mostly represent the major population – type I neurons. No report has determined if type II neurons express KCNQ channels or demonstrate KCNQ channel mediated currents.

4.3 Hypersensitivity in tinnitus and hyperacusis

Tinnitus – the phantom perception of sound, refers to conditions involve ringing or buzzing sensation in the ear in the absence of acoustic stimuli. It often co-occurs with hyperacusis, a hypersensitivity to moderate acoustic levels, which in severe cases can be debilitating due to the reduced tolerance and even painful perception in response to normal levels of sound (Andersson et al., 2002; Auerbach et al., 2014). Tinnitus is highly prevalent. One third of people have experienced tinnitus and 10 – 15% of general population had prolonged symptoms for which they seek medical attention (Heller, 2003). Although hyperacusis is less reported than tinnitus, it has been estimated that hyperacusis occurs in ~80% of tinnitus patents (Dauman and Bouscau-Faure, 2005). Despite the large population being affected, understanding of the pathophysiology of tinnitus and hyperacusis is very limited, and currently there is no effective treatment for these diseases.

The induction of the two 'hypersensitive' conditions has been highly correlated with noise exposure. Damage to the cochlea is a known high risk factor for tinnitus and

hyperacusis, and patients often report a prior history of noise trauma (Anari et al., 1999; Auerbach et al., 2014; Ince et al., 1987; Kreuzer et al., 2012). However, noise damages the auditory periphery, reduces the cochlear output from the auditory nerves (mostly type I afferents) and leads to elevated hearing thresholds (Wang et al., 2002). After noise exposure, fusion of the stereocilia of hair cells or the damage to OHCs affects sound transduction as well as tuning and amplification of the signal, so that higher stimulation intensity is needed to drive the responses (Liberman, 1978; Liberman and Kiang, 1978). Some patients who have 'normal' clinical audiograms may also develop tinnitus and hyperacusis (Brandy and Lynn, 1995). Such phenomenon might be related to the damaged IHC-type I afferent synapses and loss of type I SGNs due to relatively mild noise stress (Kujawa and Liberman, 2009), and this noise-induced cochlear neuropathy has been linked to hyperacusis in animal models (Hickox and Liberman, 2014).

The decreased activity of cochlear outputs after noise makes it hard to explain the hypersensitivity to sound in tinnitus and hyperacusis. So, instead of peripheral sensitization, several studies proposed a 'central gain enhancement' mechanism using animal models and human subjects. At multiple levels of the central auditory pathway, including the cochlear nucleus, inferior colliculus and the auditory cortex, enhanced spontaneous and sound-evoked responses were recorded after the induction of tinnitus, which is in sharp contrast to the reduced activity of auditory nerves (Auerbach et al., 2014; Eggermont, 2013). However, the activity of the two classes of auditory nerves – type I and type II afferents has never been examined separately and it is unknown how type II afferents respond to the noise paradigm that induces pathological conditions. What has been known for long time is that type II afferents are resistant to noise or

ototoxic damage to the cochlea. Unlike type I afferents that could retract from the site of damage, type II afferents remain in the cochlea even after the loss of OHCs (Ryan et al., 1980; Spoendlin, 1971b). Whether type II afferents could be involved in pathological conditions would be an interesting question to pursue.

5. Main objectives of this thesis

As summarized above, the function of the unmyelinated type II afferents in the cochlea remained enigmatic for decades. Here, we provide evidence that type II cochlear afferents can report cochlear trauma, a potential trigger for nocifensive behavior. Hyperactivity of type II neurons could contribute as well to the paradoxical hypersensitivity to loud sound that can accompany hearing loss – hyperacusis, despite diminished type I afferent function. In the most severe cases, hyperacusis is described as debilitating "ear pain". The response to trauma by type II afferents may relate most directly to such noxious hearing—"noxacusis," to coin a term. In support of this hypothesis, sparse (~5% of all spiral ganglion neurons) unmyelinated type II afferents can survive cochlear damage, are insensitive to sound, but are activated by the algogenic ligand adenosine triphosphate (ATP). In contrast to the predominant type I afferents that contact IHCs to encode the information content of sound, type II afferents innervate OHCs, which are more sensitive to acoustic trauma. Here, we show that type II afferents are excited by ATP released from supporting cells around damaged OHCs, revealing cellular mechanisms and potential molecular pathways for inner ear pain.

In **Chapter 1**, we describe the general morphology, as well as the features of the synaptic region of type II afferents revealed by biocytin fills of these fibers during electrophysiological recordings.

In **Chapter 2**, we examine the possible postsynaptic receptors at type II afferents. Using more specific pharmacological reagents as well as immunohistochemistry experiments, we were able to identify the GluA2-containing AMPA-type glutamate receptors on type II afferents, which had been controversial previously due to the nonspecific pharmacology used and failure in staining for any glutamate receptors in the OHC region.

In **Chapter 3**, we showed that in contrast to the weak synaptic inputs, ATP potently activated type II afferents. The responses were mediated by two classes of purinergic receptors, ionotropic P2X receptors and metabotropic P2Y receptors. The P2X receptors are nonselective cation channels that depolarize type II afferents in the presence of their agonist ATP. The P2Y receptors are G-protein coupled receptors and signal through second messenger-mediated pathways. We found that KCNQ channels are closed in response to P2Y receptor activation.

In **Chapter 4**, we demonstrated that type II afferents responded robustly to OHC damage. The mechanism involves ATP released from supporting cells triggered by damage, serving as the major source of ATP activating type II afferents in this process. Activation of the P2Y-KCNQ pathway might also lead to increase excitability of type II afferents, which may suggest heightened responses of type II afferents when acoustic

damage occurs and might explain the hypersensitivity associated with pathological

conditions.

Methods

Electrophysiological recordings from type II cochlear afferents

The cochlea was dissected from Sprague Dawley rat pups (Postnatal day P7-P10) according to a protocol approved by the Johns Hopkins Institutional Animal Care and Use Committee. Each animal was put into deep anesthesia by inhalation of isoflurane (Vedco, Inc.), ensured by a foot pinch test. Then the animal was decapitated and the temporal bone was removed. The apical turn of the cochlea was dissected for *ex vivo* recording according to published procedures (Glowatzki and Fuchs, 2002). After removing bone and surrounding tissues, the apical turn of the cochlea was exposed and severed at the modiolus. The stria vascularis and tectorial membrane were removed. The dissected cochlear turn was flattened and secured with an inset pin glued to a coverslip for electrophysiological recordings.

Electrophysiological recordings were done under a microscope (Carl Zeiss Examiner D1) using differential interference contrast (DIC) optics. A cleaning pipette was made by breaking a regular patch pipette at the bottom of the recording chamber. The size of the tip was determined by the pressure against the chamber controlled by a micro-manipulator (Sutter Instruments) along z-axis and breaking of the pipette was visualized with a monitor. 4-to-6 OHCs in row 2 and 3 were removed by the cleaning pipette to expose the dendrites of type II cochlear afferents (Weisz et al., 2009). Very often the Deiters' cells below the removed OHCs died within a few minutes due to the damage to their phalangeal processes that insert between OHC rows. The debris of these

supporting cells was also removed using the same cleaning pipette by gentle inhalation or exhalation. After removal of OHCs and Deiters' cells, two layers of type II afferents could be identified, traveling parallel to the cochlear spiral. The first layer sits right under OHCs, and a second layer is situated deeper at the Deiters' cell level and organized in wider bundles. Most of the recordings (tight-seal intracellular recordings or loose-patch extracellular recordings) were performed at the first layer around the terminal region of the fiber, where type II afferents rise to the base of outer hair cells and form synapses. Recording pipettes (resistances of 6-9 MΩ) were pulled from 1mm borosilicate glass (WPI Instruments). The series resistances of the recordings were less than 35MΩ (membrane test of the pCLAMP 10.3 software - Molecular Devices) and were not corrected. In loose patch recordings, the final seal resistance reaches around 3-4 times the pipette resistance.

Solutions

Extracellular solution contained (in mM): 5.8 KCl, 144 NaCl, 1.3 CaCl$_2$, 0.9 MgCl$_2$, 0.7 NaH2PO4, 5 glucose, 10 HEPES, pH 7.4. The excised cochlear tissue was constantly perfused with the extracellular solution under a rate of two seconds/drop. Intracellular solution contained (in mM): 135 KCl, 0.1 CaCl$_2$, 3.5 MgCl$_2$, 5 K-EGTA, 5 HEPES, 5 NaCl, pH 7.2 (4 mV junction potential, not corrected). During the voltage ramp protocol, 1μM tetrodotoxin was added to the bath to prevent action currents. In some experiments, a high potassium solution was used to depolarize neurons and trigger synaptic transmission, which contains 40 KCl, 110 NaCl, 1.3 CaCl$_2$, 0.9 MgCl$_2$, 0.7 NaH2PO4, 5 glucose, 10 HEPES, pH 7.4. For cell ablation studies, in order to

improve stability, recordings were made with intracellular solution containing organic anions in place of Cl (in mM): 110 K-methanesulfonate, 20 KCl, 0.1 $CaCl_2$, 3.5 $MgCl_2$, 5 K-EGTA, 5 HEPES, 5 Na2phosphocreatine, 0.3 Tris-GTP, pH 7.2. Membrane potentials were corrected for the 10 mV junction potential with this solution. ATP was excluded from all intracellular solutions to prevent desensitization of ATP receptors.

Pharmacological compounds

Pharmacological compounds were applied with a gravity-driven, large bore application pipette placed to cover the spiral branch of the recorded afferent. In some experiments, drugs were loaded in a puffer pipette (with the same tip size as the patch pipette) and applied locally driven by a Picospritzer III (Parker-Hannifin, Irwin PA). All chemical and pharmacological reagents were obtained from Sigma, except for PPADS (Tocris), tetrodotoxin (Tocris), CNQX (Tocris), D-AP5 (Tocris), (RS)-MCPG (Tocris), retigabine (Sigma and Alomone labs), and FM 1-43FX (Life Technologies).

Cell ablation strategy

Cell ablation was performed mechanically, using a sharp needle pulled from 1mm borosilicate glass. The needle was placed parallel to the cochlear spiral, and was moved manually using a micro-manipulator. This ablation procedure started 15-20 outer hair cells apical to the recording site, to encompass the synaptic zone of the fiber. To visualize hair cell ablation, the cochlear tissue was preloaded (25-30 seconds, room temperature) with 5 μM FM1-43, a fluorescent dye that rapidly enters through mechanotransduction channels and partitions into the hair cell membrane. In each trial, one to three OHCs were ruptured by the movement of the needle through the lateral wall of the cell. Rupture was

effected only when the needle was centered on the cell nucleus. After ablation, the damaged outer hair cell swelled immediately and disappeared entirely within 3 – 5 minutes, confirmed by the loss of FM1-43 from the hair cell membrane. There was minimal damage to the surrounding cochlear cells including the afferent neurites, Deiters' cells and Hensen's cells.

Post hoc visualization of biocytin-filled type II afferents

For post hoc visualization of the afferent, 0.25~0.3% biocytin was added to the intracellular solution. The tracer was detected using streptavidin-conjugated horseradish peroxidase, made visible by precipitation of diaminobenzidine (DAB) for light microscopy. After whole-cell patch clamp recording, tissue with biocytin-filled type II afferents was fixed in 4% PFA overnight at 4°C in a 12-well cell culture plate (Corning), and then washed in PBS and stored at 4°C for further batch processing within two weeks. In a new 12-well plate, each tissue was washed in PBS on a shaker (washed twice for 10 min each, and the third time for 30 min) and then quenched in 10% H_2O_2 (with 10% methanol) for 10 minutes. Time has to be controlled precisely (count in seconds) for the critical quenching step. After that the tissue was washed three times in PBS for 10 min each, and permeabilized in 2% Triton in PBS (1 hour, room temperature). Then the tissue was incubated in avidin/biotin complex (Vectastain ABC kit, Vector) overnight at 4°C, washed in PBS (twice for 10 min each time and then 45-60 min for the third time) and reacted with a diaminobenzidine-based peroxide substrate (ImmPACT DAB, Vector) for 10 minutes, until the cell and its arborization were visible under the microscope. The first rinse using PBS was done immediately to stop the reaction, followed by two additional

rounds of wash by PBS for 10 min each. Then the tissue was mounted on a microscope slide for imaging.

Equipment and settings for digital images

After the DAB reaction, the slides for cochlear turns were imaged on a Zeiss LSM 510 Meta microscope. For cell ablation studies, the cochlea was viewed under a microscope (Carl Zeiss Examiner D1) using a 40× water-immersion objective with contrast enhancement (Hamamatsu C2400-62). Images were taken with a digital camera (SONY) attached to the microscope.

Preparation for calcium imaging

To examine the calcium responses of SGN afferents, Advillin-Cre mice were bred into a R26-lsl-GCaMP3 (GCaMP3) mouse line (Paukert et al., 2014) which expresses the genetically encoded calcium sensor GCaMP3 in the Cre recombinase positive cells. The Advillin-Cre mouse line was generated by knocking the transgene *Cre* into the *Advillin* gene locus (da Silva et al., 2011). This construct was found to sparsely label both type I and type II afferents, with increasing numbers of labeled neurons from apex to base (Zhang-Hooks et al., 2016). Although it has been suggested that only male Advillin-Cre mice could be used to achieve specific labeling of sensory neurons (da Silva et al., 2011), by the time for experiments only female Advillin-Cre mice were available for us to cross with the male GCaMP3 mice. Two thirds of the pups in the resulting litter demonstrate nonspecific expression of the Cre recombinase that drives expression in neurons and supporting cells. The rest of the pups have specific expression of the Cre recombinase in the sensory neurons. We found such difference in expression pattern could be easily

identified by looking at the basal fluorescence of GCaMP3 in the animals' tail, where nonspecific vs. specific expression could be distinguished.

The transgenic mice were dissected at postnatal day P5 – P7 and the cochlear explant was obtained as described previously. Segments of cochlea including apical and middle turns were put into culture. They were attached onto cover slips after coating with Cell-Tak (Corning) and incubated in a medium containing Dulbecco's modified Eagle's medium (DMEM), 1 % fetal bovine serum (FBS) and 0.1 % penicillin. After one day in culture, the cochlea with the cover slip was transferred under a laser scanning confocal microscope LSM 710 (Zeiss) for calcium imaging and was superfused with extracellular solution during the experiments. The microscope was equipped with a 20X water-immersion objective, 488 nm laser illumination, and 500–530 nm bandpass filter. DIC images were simultaneously monitored to visualize the sharp needle for ablation studies. Images were collected for one frame/second.

Data acquisition and analysis

Membrane voltage and current were recorded with a MultiClamp 700B amplifier and a Digidata 1440A (Molecular Devices), controlled by pCLAMP 10.3 software (Molecular Devices), sampled at 25 kHz and low-pass filtered at 10 kHz. The data were analyzed in pCLAMP 10.3 (Molecular Devices) and Origin 9.0 (Origin Labs). Statistical analysis (paired or unpaired t-test as appropriate) was performed in Excel (Microsoft) and the results are given as mean ± SD. EPSCs were analyzed using MiniAnalysis software (Synaptosoft) with the criterion three times the root mean square of the noise, and further

accepted or rejected by eye according to their characteristic waveforms. Calcium imaging

data and measurement of type II afferents' morphology were done using ImageJ.

Results

Chapter 1: Morphology of type II cochlear afferents

The morphology of type II neurons, including their somata, peripheral innervation onto multiple OHCs and branching patterns as outer spiral fibers have been characterized by many studies (Berglund and Ryugo, 1987; Brown, 1987a; Echteler, 1992; Ginzberg and Morest, 1983; Ginzberg and Morest, 1984; Huang et al., 2007b; Koundakjian et al., 2007; Liberman et al., 1990; Perkins and Morest, 1975; Simmons and Liberman, 1988a; Simmons and Liberman, 1988b). Among them, informative morphological understanding was gained through the sparse labeling that shows single fibers of type II afferents, using either Golgi staining (e.g. Perkins and Morest, 1975) or HRP fills into the central-going axons of SGNs near the cochlea nucleus. With the latter method the marker has to travel long distance in order to reach the cochlea and label their peripheral processes in the organ or Corti (e.g. Simmons and Liberman, 1988a). In this thesis, we employed a different strategy. We included biocytin directly into the patch pipette. When whole-cell patch clamp recordings were established on type II afferents' dendrite terminals, the biocytin entered through the closest site to the synaptic region and might be ideal for a more complete fill to visualize the finest structures. Combined with streptavidin-conjugated fluorescent labeling, this method could further allow association of type II afferents labeling with immunolabeling for synaptic marker proteins (in Chapter 2), providing more information on the synaptic organization of OHC-type II afferents synapse.

55

1.1 General properties of peripheral innervation

To label the peripheral type II fibers and to understand their specific connectivity with OHCs, giga-ohm-seal intracellular recording was used to fill type II fibers with biocytin in excised apical turns of cochleae from young rats (postnatal days P7 to P9). Before each experiment, biocytin solution was made by mixing 0.0025 – 0.0030 g biocytin into 1 mL intracellular solution. The mixture was made in a 1.5 mL tube and was sonicated for at least 5 minutes, until biocytin was fully dissolved and clear solution was obtained. The biocytin-containing intracellular solution was then filled into the patch pipettes through a capillary attached to a syringe and a micro-filter.

Once giga-ohm seal was established between the patch pipette and the type II afferents' dendrite, a brief suction was applied to rupture the cell membrane and allow diffusion of biocytin into the cytosol of the recorded afferents. The identity of the recorded type II afferents was further confirmed by their characteristic voltage-gated currents elicited by voltage steps (Figure 1.1.1) (Weisz et al., 2009). Remarkably, we found that the dialysis process was fast and biocytin could travel a long distance within the cell. Only five to ten minutes of whole-cell patch clamp recording on a type II afferent was enough to label the entire neuron, including its distal dendrites (the recording site) and synaptic branches, its spiral process under OHCs and supporting cells, its radial process and turning point, their somata in the spiral ganglion and even part of their central-going axons. Because of the difficulty of the recordings on these thin dendrites, multiple trials were made trying to patch onto the type II afferents before a good whole-cell patch clamp recording was achieved. For the unsuccessful trials, sometimes the cell membrane was only partially ruptured that allows in small amount of

biocytin. Therefore, although from trial to trial recordings were made from the same site

on the outer spiral bundle (composed of many type II afferents bundled together) in a

cochlear tissue, in a few cases multiple type II afferents were labeled in the same tissue,

which can be visualized after streptavidin-peroxidase processing. This may cause

difficulty in resolving single fibers for quantitative analysis of their morphology. In other

cases, the soma of the recorded fiber was severed during the initial dissection of the

apical turn, so that the biocytin labeling yielded type II fibers filled until the cut edge of

their radial branch without showing their soma.
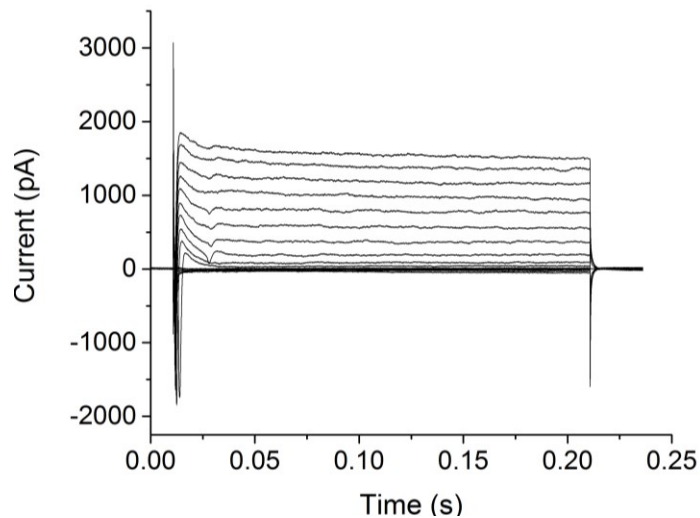
Figure 1.1.1. Currents evoked by voltage steps in type II afferents (10mV steps from -90mV). Cell# A_CL_010913

Among the 40 whole-mounts with filled type II afferents, we selected 15 of them

using the criteria including (1) single fiber are clearly labeled in each tissue; (2) a good

signal-to-noise ratio and high quality of the image, allowing identification of the fine

synaptic branches under OHCs; (3) helicotrema (the very apex of the cochlea) is seen in

the tissue in order to decide the tonotopic location of the labeled fiber. These 15 slides

were used for quantitative morphological characterization. Important parameters of the

57

fiber including the length of their processes, their location along the cochlea's tonopic map, and characters of their synaptic regions were measured and counted with the software ImageJ. The length measurement in ImageJ was made by drawing the lines faithfully following the shape of the fiber using a computer mouse. Some of the remaining slides that provide interesting information were also described in the later part of this chapter. Most of my recordings were made on type II afferents under row 3 OHCs in the apical turn of young rat (P7-P10), so this study only reflects the morphology of type II afferents under these specific conditions.

1. 'Single arbor' fibers

Among the 15 quantified type II neurons, 8 of them gave off a single peripheral process without any major branching. The peripheral neurite leaves the soma in the spiral ganglion to cross the floor of the tunnel of Corti and turns ~ 90 degrees to travel toward the cochlear base (representing higher frequency regions) along the outer spiral bundle (Figure 1.1.2 A). Close to its turning point, the fiber often switches between OHC rows. After traveling several hundred microns, the spiral process seems to innervate mostly one row of OHCs, rising from under the Deiters' cells to the base of the OHCs. The single spiral process averaged 714 ± 229 (SD) μm (n=8 fibers, see Table 1.1.1) from the turning point to the basal-most tip. At the terminal region where the type II afferent rises to travel right under OHCs, an average of 17 ± 4 (SD) short branches off the spiral process formed *en passant* and terminal swellings (Figure 1.1.2. B), presumably the site of synaptic transmission. The somata of type II neurons can also be visualized with great detail (Figure 1.1.2. C), sending the radial process toward the organ of Corti and a central

58

process projecting to the cochlear nucleus. The recording site of the biocytin-containing patch pipette often can be identified by a darker surrounding region, likely caused by the leakage of biocytin before giga-ohm-seal was established (Figure 1.1.2.A arrowhead). This location was seen close to the distal (basal) end of the fiber usually within one third of the length of the entire spiral process. Figure 1.1.3 and Figure 1.1.4 shows two other examples of labeled type II afferents with varying length and synaptic features. The shorter afferents in Figure 1.1.3 have only one major synaptic input region and the morphological synaptic branches were more clustered. The longer afferents in Figure 1.1.4 had a spiral process that averaged 1194.7 µm and a more dispersed synaptic input region. Among the 21 synaptic branches observed, 11 of them clustered to form a major synaptic input region and 3 clustered to form a secondary synaptic region. There were also some 'orphan' branches along its long spiral process.
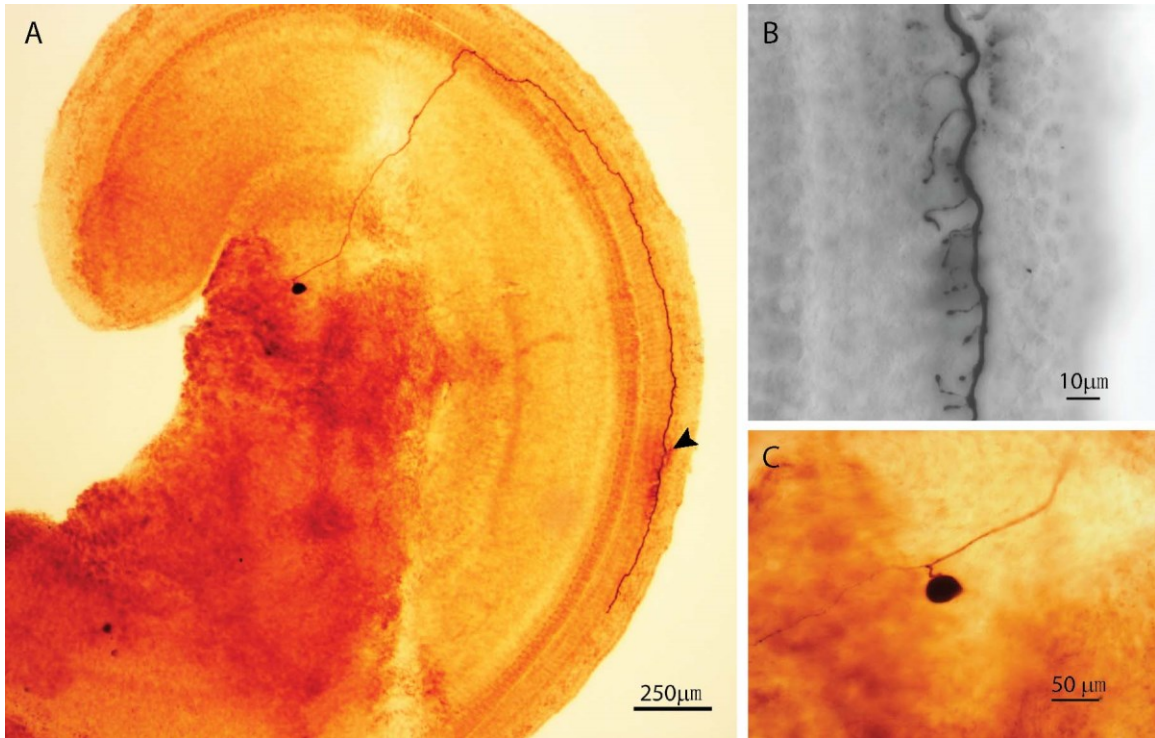
Figure 1.1.2. A. Whole-mount view of a biocytin-filled type II spiral ganglion neuron in the apical turn of P8 rat cochlea. Recording site (arrowhead) was located on the terminal of the spiral branch, where type II afferent forms synaptic contacts with multiple outer hair cells. B. Confocal image of the type II afferent in A near recording site. Branches extend from the shaft onto the row of OHCs above it. C. The biocytin-filled soma of type II neuron, with a pseudo-unipolar morphology. (Cell# B CL 092412)

Slide number	Length of spiral process (μm)	Distance from fiber turning point to cochlear apex (μm)	Arbor	Total synaptic branches	Major synaptic area			synaptic area2		
					Length from apex	length	No. of branches	Length from apex	length	No. of boutons
BCL 9-24-12	899.2	843	1	21	1532	97.3	13	1456.198	30.754	4
A CL 040114	516.4	1121	1	13	1448.3	150.2	9	1416.496	48.409	4
ACL 032714	1194.7	566.5	1	21	1618.3	165.2	11	1237.851	38.181	3
ACL 012214	617.8	613.5	1	12	1082.2	160.5	12			-
3-17-13 Cell B CL	585.5	997.8	1	15	1109	52.8	9			-
9-9-13 Cell A	733.9	658.1	1	22	1108.3	161.3	12	1336.511	104.051	8
ACL 03-28-14	549.1	608	1	17	920.3	224.8	17			-
A CL 10-03-12	612.8	NA	1	13	NA	101.3	12			-
Average ± STD	**714±229**			**17±4**		**139±53**	**12±3**			

Table 1.1.1. Morphological Analysis of eight single arbor type II afferents.

Figure 1.1.3. A single arbor type II afferent in the apical turn of young rat cochlea. Cell# A-CL 012214. Spiral process length was 617.8 μm. This afferent has one single synaptic input area that gave off 12 synaptic branches.
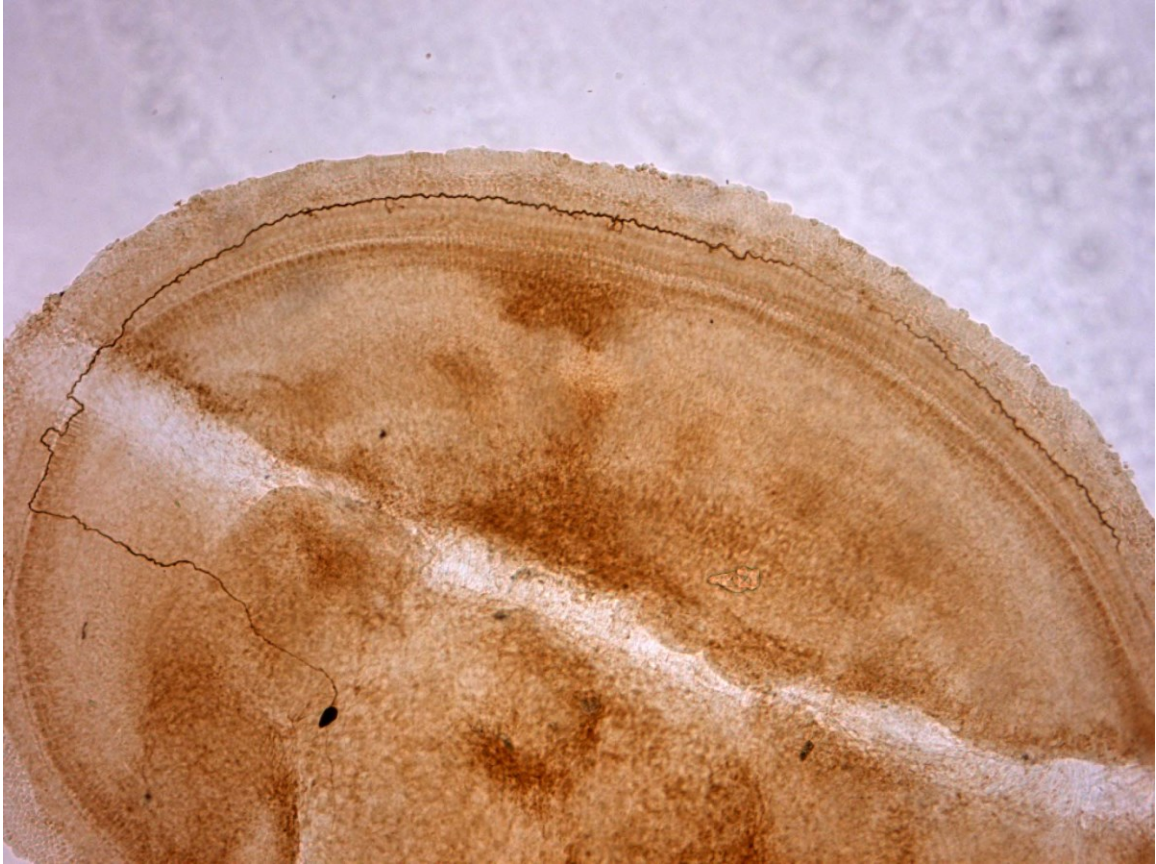
Figure 1.1.4. A single arbor type II afferent in the apical turn of young rat cochlea. Cell # A CL 032714. Total length of the spiral process is 1194.7 µm. The major synaptic area has 11 synaptic branches and a secondary synaptic region has 3 branches.

2. Multiple arbor fibers

The spiral dendrite also could split into 2 (6/15 fibers) or 3 (1 fiber) major basally-projecting arbors. More often, 5 out of 7 multiple arbor fibers showed major branched arbors on their basalward going spiral processes in the OHC region (e.g. Figure 1.1.5). The two exceptions include one fiber with a branched arbor on its radial process (Figure 1.1.6), and one fiber with bifurcated arbors extending both basally and apically. In the second case, synaptic branches were only detected in the basal going arbor but not

the apical going arbor. The apical going arbor also showed a 'ball-like' structure at its terminal that seems to suggest some developmental defect during the neurite growth (Figure 1.1.7).

Despite some morphological diversity, the overall length of the spiral process, the number of synaptic branches and terminal arborization zones were similar among single vs multiple arbor fibers. Multiple arbor fibers had a spiral process averaging 619 ± 208 μm in length (Table 1.1.2, n=7 fibers), not significantly different from that of single arbor fibers (averaged 714 ± 229 μm, Table 1.1.1, n=8 fibers). Although the multiple arbor type II afferents have one or two more major processes, in 5 of 7 such cases, terminal branches arose from only one of the arbors, or prior to the branch point (Figure 1.1.5.Two exceptions in Figure 1.1.8). Morphological analysis revealed an average of 16 ± 7 synaptic branches and a major synaptic region stretching 140 ± 41 μm in multiple arbor type II afferents (Table 1.1.2), similar to these parameters quantified for single arbor type II afferents (Table 1.1.1). Therefore, all the analyzed fibers, whether possessing one or more major arbors, had similar numbers and distribution of terminal branches, and presumably equivalent numbers of synaptic inputs.
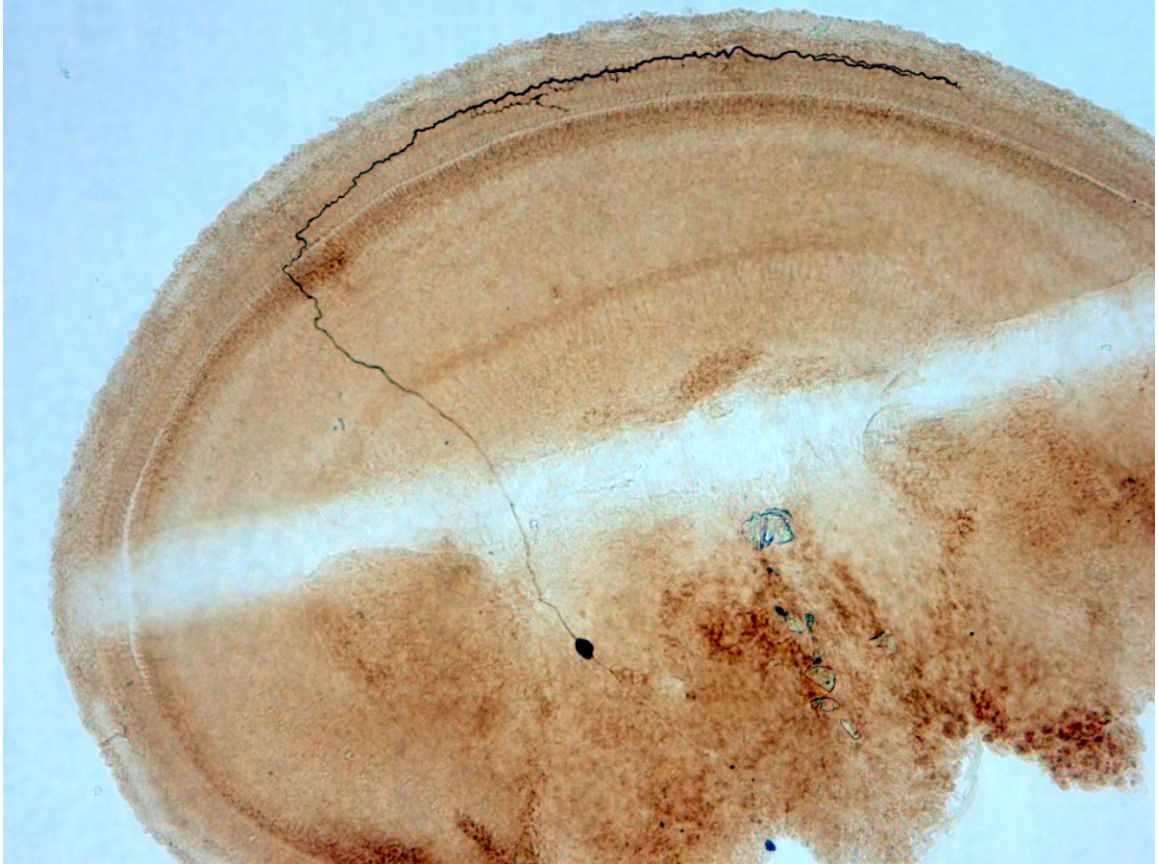
Figure 1.1.5. A multiple arbor type II afferent in the apical turn of young rat cochlea. Fiber branches and the distal terminal. Synaptic branches were found on the dendrite before the branching point. Cell # C_CL031113.
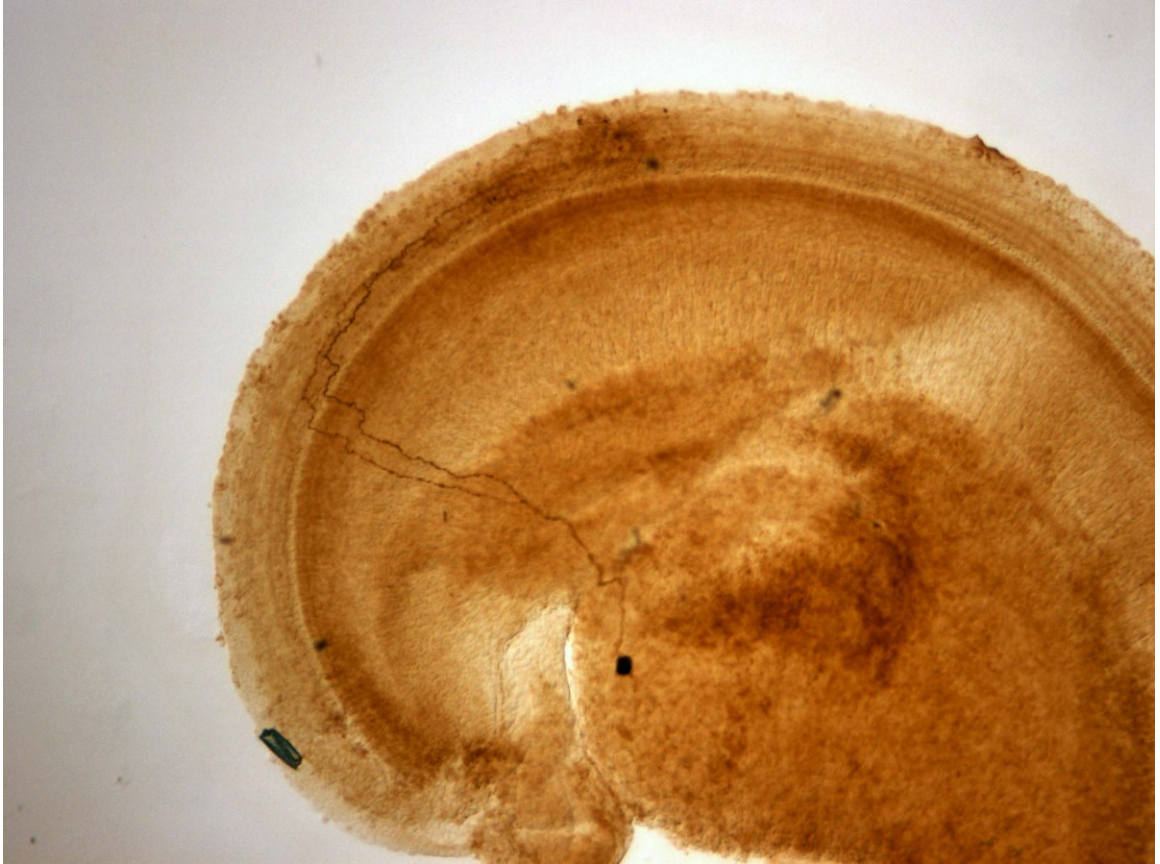
Figure 1.1.6. A multiple arbor type II afferent branched at the radial portion. Cell# A_CL012414

Figure 1.1.7. A cochlear tissue with two labeled fibers – one single arbor type II afferent and one multiple arbor type II afferent projecting bi-directionally. Cell# A CL 9-17-12.
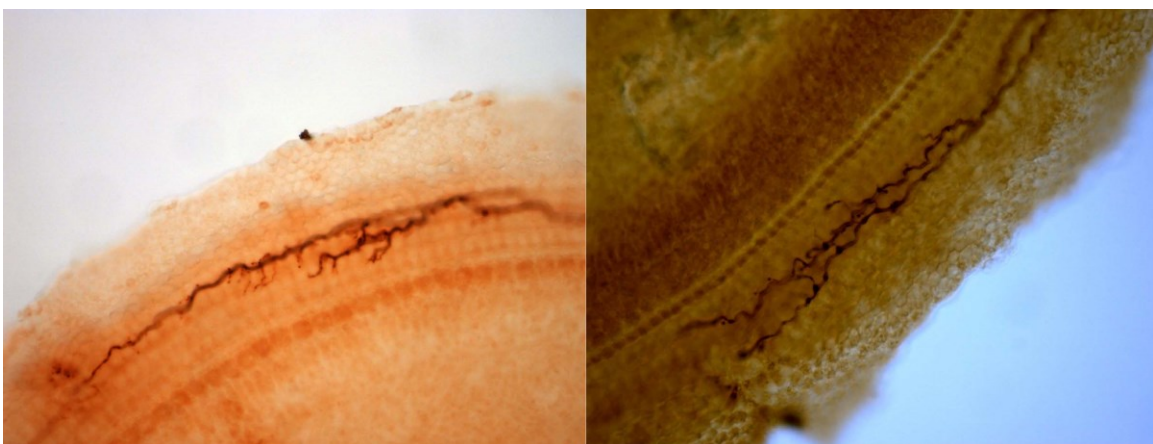
Figure 1.1.8.The only 2 out of 15 labeled fibers showing synaptic branches on multiple arbors.Cell# A_CL_092412 and B_CL082913.

Slide number	Length of spiral process (µm)	Distance from fiber turning point to cochlear apex (µm)	Arbor	Total synaptic branches	Major synaptic area			Other features
					Length from apex	length	No. of branches	
A Cl 012414	400.65	488.8	2	8	692	60.9	8	Synaptic area on one arbor
3-11-13 Cell C	720.1	983	2	14	1243.4	168	11	Synaptic area on major shaft
B CL 9-26-12	983	577	2	7	1255.2	139.6	7	Synaptic area on one arbor, bidirectional
9-9-13 Cell B	689.1	613	2	20 +/- 2	1095.4	135.2	15 +/-2	Synaptic area on both arbor
A CL 9-24-12	413.5	479.5	3	24	700	130.245	18	Synaptic area on one arbor
8-29-2013 Cell B	475.5	919	2	13	1107.8	149.5	13	Synaptic area on both arbor
8-29-13 Cell A (branch at the end)	649.7	924	2	23	1423.4	193.4	20	Synaptic area on major shaft and one arbor
Average ± STD	619±208			16±7		140±41	13±5	

Table 1.1.2. Morphological Analysis of seven multiple arbor type II afferents.

3. Somata of type II neurons

The biocytin fills also enable labeling of somata of type II neurons in the spiral ganglion. Examples of six type II neurons are shown in Figure 1.1.9. One of them showed a typical peudounipolar morphology, which has a bifurcating axon with branches going in opposite directions, one centrally and one peripherally. The rest of them (5 cells) seem to adopt a bipolar morphology, with one central and one peripheral branch directly linked with the soma. However, it is also possible that they could be peudounipolar cells viewed from different angles. The central and peripheral processes are similar in diameter, consistent with previous reports (Berglund and Ryugo, 1986; Kiang et al., 1982)
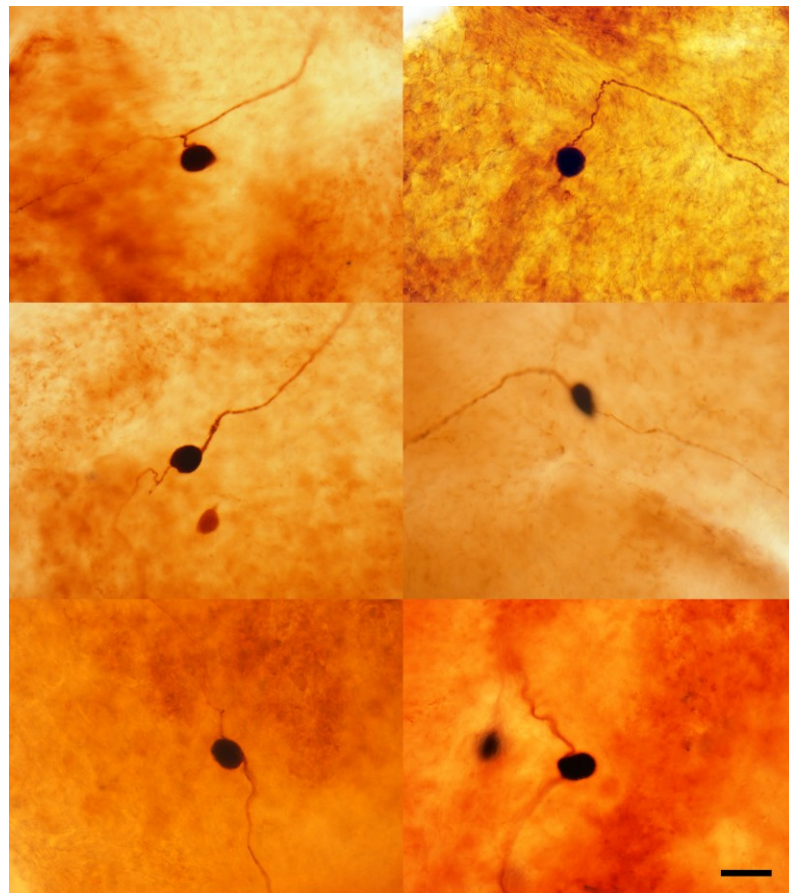
Figure 1.1.9. Somata of six different type II neurons in the apical coil of young rats, showing peudounipolar or bipolar morphology. Scale bar: 50μm.

1.2 Synaptic regions of type II afferents

Since morphological analysis showed no significant differences among any of the measurements between single and multiple arbor type II afferents, all the labeled afferents (8 single-arbor and 7 multiple-arbor fibers) were grouped together for a summary of their features. The number of synaptic branches within the terminal arbors of all fibers averaged 16 ± 5.5 (SD, n = 15). These synaptic branches had an average length of 10.88 ± 6.48 μm (SD). They tend to cluster (12 ± 4 (SD) branches, forming a major synaptic input region that spans a distance of 139 ± 46 (SD) μm (n=15) with smaller secondary clusters 100 μm or more distant in some cases. The secondary synaptic region usually had fewer synaptic branches compared to the major region. In one special case of the eight 'single arbor' fibers, two synaptic zones 228 μm apart were nearly equal (12 and 8 branches).

When examining the detailed morphology using confocal microscopy, we found that each synaptic branch not only has a terminal bouton at the end (Figure 1.2.1, white arrowhead), but also contains *en passant* swellings along the thin synaptic branch (Figure 1.2.1, red arrow). Each branch had an average of 2.04 ± 0.7 (SD) en passant swellings in addition to the terminal bouton. Each branch contacted 1-3 OHCs in the same row and the average number of OHCs contacted by each type II fiber was 23.71 ± 5.82 (SD). Some branches showed arching shapes (Figure 1.2.1, bottom images), that could correspond to the 'pearl chain' postsynaptic densities described in Chapter 2.
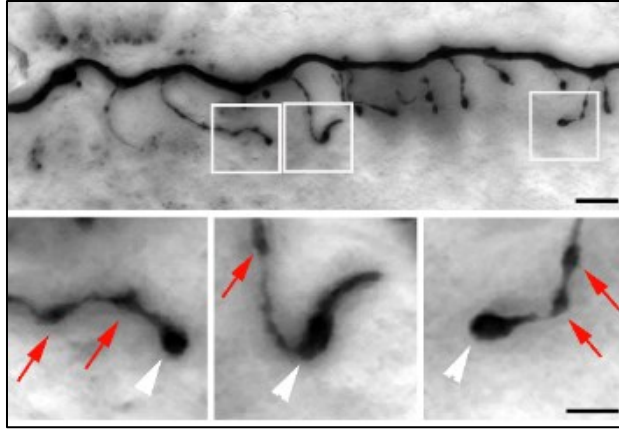
Figure 1.2.1. Higher magnification of synaptic branches. Bottom images are expanded boxed area. Red arrows indicate en passant swellings and white arrowhead shows the terminal bouton.

The location of the major synaptic input zone ranged from 700 to 1600 μm (average 1167 ± 280 μm; SD, n = 15 fibers) from the cochlear apex, placing the synaptic area in a frequency range of ~ 9 kHz (Muller, 1991a; Muller, 1991b). On the other hand, the 90 degree turning point of the fibers was located at 500 to 1000 μm (average 742 ± 213 μm; n = 15 fibers) from the apex, placing it in the frequency range of 7 kHz. Thus, as noted previously (Brown, 1987), type II afferents, if sufficiently sensitive, would report vibrations one quarter to one half an octave higher in frequency than type I afferents projecting in parallel to the same tonotopic zone of the cochlear nucleus.

Besides the synaptic branches contacting OHCs, some small branches were also observed as type II afferents bypassed inner hair cells or traveled under the supporting cells (Deiters' cells). These branches however looked very different from a typical synaptic branch seen in type II afferents. They were much shorter, and without any terminal or *en passant* swellings (Figure 1.2.2). Another interesting observation was made by accidentally labeling two neighboring type II afferents in the same tissue (Figure

71

1.2.3). Radial processes of these two afferents seemed overlapping and projected together to the same tonotopic region of the cochlea. In the spiral ganglion, the two type II neurons were located close to each other. Their 90 degree turning points shared a similar location. Although they sometimes switched to different rows at the apical portion of the spiral process, they finally targeted the same row of OHCs at their terminal region. However, their synaptic input regions were neighboring but non-overlapping. One of them terminated more apically, forming a clustered synaptic region (Figure 1.2.3.B white arrowhead). The other fiber extended further and gave off synaptic branches in a wider region more basally (Figure 1.2.3.B black arrows). Although more repetition is needed, this suggests that type II afferents project to similar frequency regions and can form synaptic contacts with neighboring but non-overlapping sets of OHCs.
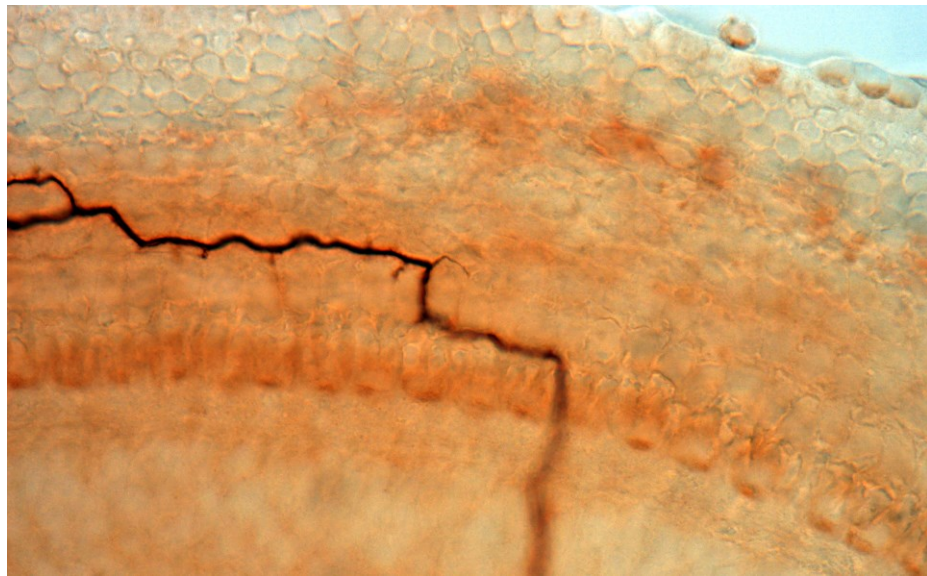
Figure 1.2.2.A type II afferent gave off short branches as it crossed the tunnel of Corti. Cell# A_CL_092412

72
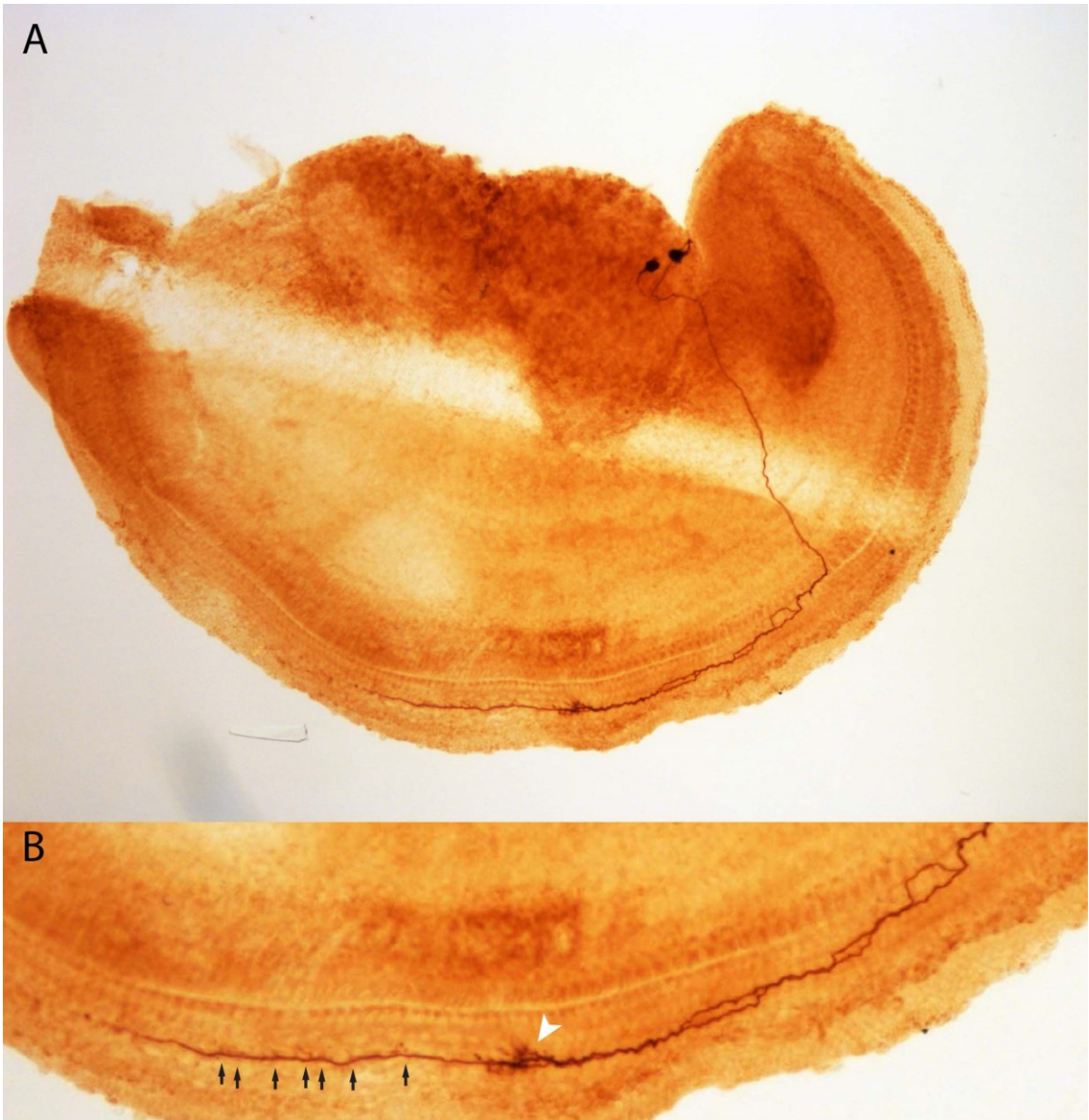
Figure 1.2.3. Differential synaptic regions of two neighboring type II afferents. A. Two neighboring type II afferents turn at a similar location. B. Higher magnification of the synaptic regions. White arrowhead: clustered synaptic region for one fiber. Black arrow: synaptic branches for the second fiber. Cell # AB_CL_031113

To associate the tonotopic location of type II afferents with their morphological features, I plotted the measured parameters in Table 1.1.1 and Table 1.1.2 against the distance from fiber turning point to apex (Figure 1.2.4). It seems that at more apical regions, the length of the spiral process was more variable (Figure 1.2.4 A). A similar observation was made for the number of total synaptic branches (Figure 1.2.4 B), in that apical fibers have a more variable number of morphological synapses. The location of the major synaptic area, measured by the distance from the cochlear apex to the most apical synaptic branch of the area, has a positive correlation with the tonotopic location (turning point) of the afferent (Figure 1.2.4 C). This reflects that the relative distance between the turning point and the major synaptic region is quite stable. There seems to be a weak positive correlation between the length of the major synaptic area and the location of the fiber for single-arbor afferents, but this trend was not observed in multiple-arbor afferents (Figure 1.2.3 D).
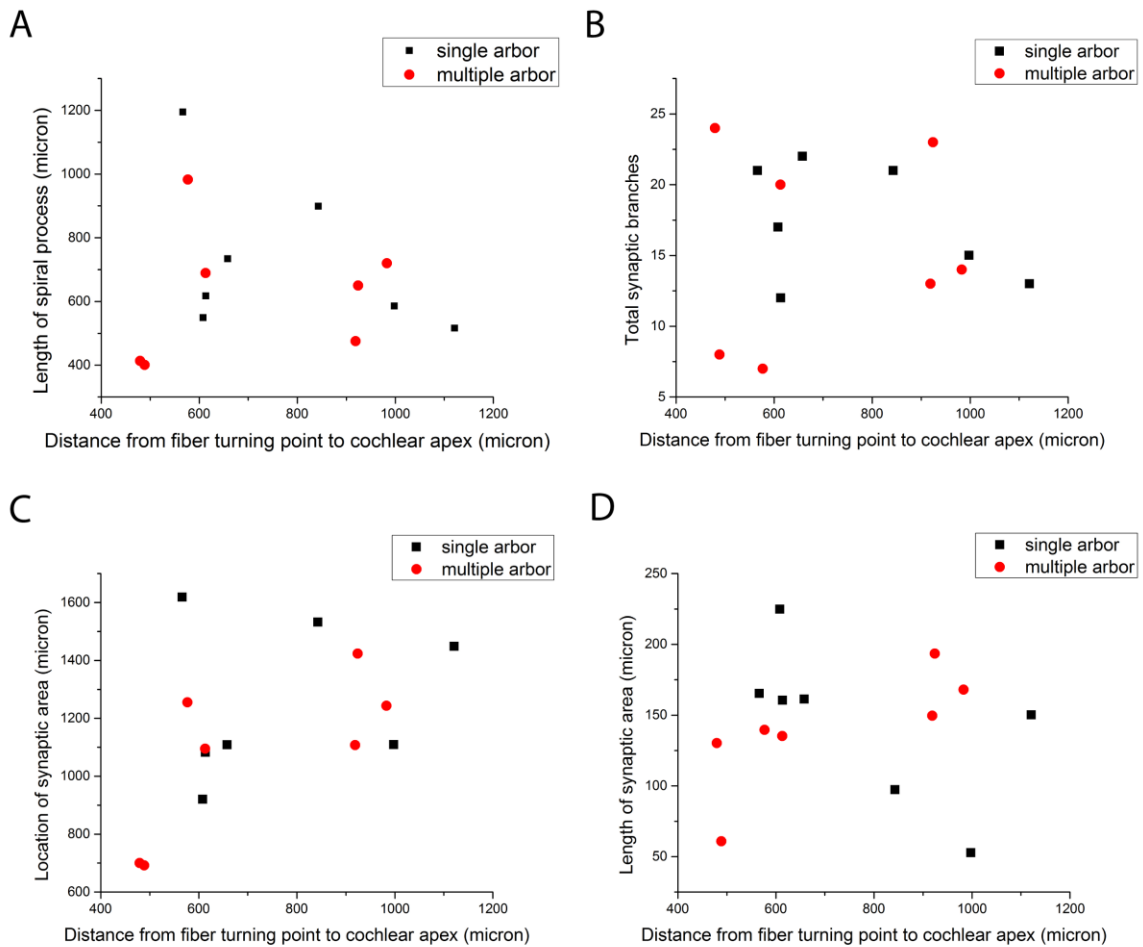
Figure 1.2.4. Morphological features plotted against the location of the type II afferents, measure by the distance from apex to their turning point. Data include seven single-arbor afferents and seven multiple-arbor afferents in Table 1.1.1 and Table 1.1.2.

Discussion:

    Morphological characterization of type II afferents has been done by studies on

young and adult animals of many species, including mouse, rat, cat and guinea pigs

(Berglund and Ryugo, 1987; Brown, 1987a; Echteler, 1992; Ginzberg and Morest, 1983;

Ginzberg and Morest, 1984; Huang et al., 2007b; Koundakjian et al., 2007; Liberman et

al., 1990; Perkins and Morest, 1975; Simmons and Liberman, 1988a; Simmons and

Liberman, 1988b). The contact between type II afferent and OHC has been described as a discrete bouton in some studies ((Ginzberg and Morest, 1984; Nadol, 1983), but can be more extensive, forming en passant synapses as it travels past the OHC (Francis and Nadol, 1993; Nadol, 1988; Sobkowicz et al., 1993). We found that such *en passant* synapses likely occur in the form of *en passant* swelling on the fine synaptic branches, forming a chain of possible postsynaptic sites together with the terminal bouton. The average number of OHCs contacted by each type II fiber was 23.71 ± 5.82 counted in our experiments. This number is similar to that predicted to be required for threshold stimulation of type II afferents (Weisz et al., 2012).

Although we focused only on the apical coil of the cochlea, small differences of recording site revealed that type II afferents located more apically tended to be more variable in morphology compared with those closer to the middle turn. It has been reported that apical type II afferents have more elaborated patterns of innervation, whereas middle fibers are the longest and have larger synaptic areas. Synapses of the basal type II afferents were found to have more terminal bouton instead of *en passant* swellings (Brown, 1987a; Fechner et al., 2001; Simmons and Liberman, 1988a). It may be interesting to address such differences in synaptic transfer by recording type II afferents at varying cochlear locations.

All the HRP stainings were done *post-hoc*, after the electrophysiological experiments described in later chapters. This enabled us to confirm the successful recording on type II afferents, and have a better understanding about the morphology of the recorded cells. The finding that the recording site is always located at the distal end of

76

the fiber helped us designing the experiments. For example, for cell ablation studies, OHCs apical to the recording sites should be situated right above the recorded fibers. And to record the synaptic inputs from OHCs to type II afferents, the location of recording should better move away from the terminal region to keep the synaptic input area intact.

Chapter 2: Postsynaptic receptors of type II afferents

In the mammalian cochlea, inner hair cells release glutamate to excite AMPA-type receptors (AMPARs) on the predominant (95%) type I afferents (Glowatzki and Fuchs, 2002; Ruel et al., 2000) that provide all acoustic input to the brain. The synaptic arrangement of type I afferents with IHCs has been well-characterized. In particular, the single dendrite of each type I afferent forms a compact bouton ending opposite to a presynaptic ribbon of the IHC (Ginzberg and Morest, 1984; Hafidi et al., 1990; Khimich et al., 2005; Kiang et al., 1982; Liberman et al., 2011; Wang and Green, 2011). In contrast, connections between individual type II afferents and OHCs remain to be fully elucidated. In particular, it is not known whether ribbon synapses comprise the main or the only sites of signaling, since non-ribbon-associated contacts between OHCs and type II afferents were reported (Dunn and Morest, 1975; Nadol, 1983). Recently it has been suggested that AMPA receptors may also mediate outer hair cell transmission to the scant and enigmatic type II afferents (Glowatzki and Fuchs, 2002; Weisz et al., 2009). However, the pharmacology used was AMPA/kainate receptor antagonist – NBQX, and this could not rule out the role of kainate receptors present at this synapse found by immunolabel (Fujikawa et al., 2014). The physiological result also runs counter to the conclusion, based on immunolabeling of GluA2/GluA3 and GluA2 subunits, that OHC synapses are not AMPAR-dependent (Chen et al., 2009; Flores-Otero and Davis, 2011; Khimich et al., 2005; Liberman et al., 2011; Matsubara et al., 1999). More recently it has been reported that antibodies to GluA2 label type II contacts to OHCs in the immature but not adult rat cochlea (P8), and that the adult synapse may be mediated only by kainate

receptors (Fujikawa et al., 2014). Thus, the present study was undertaken to explore this issue further and to elucidate the relationship between ribbons, postsynaptic glutamate receptors and postsynaptic density markers in afferent fibers at the OHC synapses.

2.1 Type II afferent innervation and synaptic markers

Additional background

Unpublished data from my colleague Dr. Rodrigo Martinez Monedero showed for the first time that among the 4 subunits of AMPA receptors (GluA1 − GluA4), only anti-GluA2 produced localized, specific labeling at the OHC regions of excised <u>adult</u> rat cochlear whole-mounts. Double labeling with an antibody against CtBP2, a protein found in presynaptic ribbons (Lenzi and von Gersdorff, 2001; Wagner, 1997), was performed to relate postsynaptic GluA2 labeling to the location of presynaptic ribbons in hair cells (Figure 2.1.1). CtBP2 and GluA2 puncta were closely aligned in most cases (Figure 2.1.1A, magnified inset. Quantification in Figure 2.1.1C). Assuming that the GluA2 puncta represent functional synapses, this high level of juxtaposition suggests that AMPAR-mediated synaptic transmission occurs at ribbon synapses of OHCs, with 2-3 such ribbon synapses per OHC. As a positive control, GluA2 antibody was also tested in the inner hair cell region. Many more presynaptic CtBP2-labeled ribbons and postsynaptic GluA2 receptor clusters were found among IHCs and they were consistently juxtaposed (Figure 2.1.1B. Quantification in Figure 2.1.1D), consistent with previous reports regarding the number of synapses per IHC and the close correspondence between CtBP2-labeled ribbons and GluA2/3 or GluA2 receptor clusters (Beutner and Moser,

2001; Brandt et al., 2003; Fuchs et al., 2003; Khimich et al., 2005; Liberman et al., 2011; Meyer et al., 2009; Neef et al., 2007).
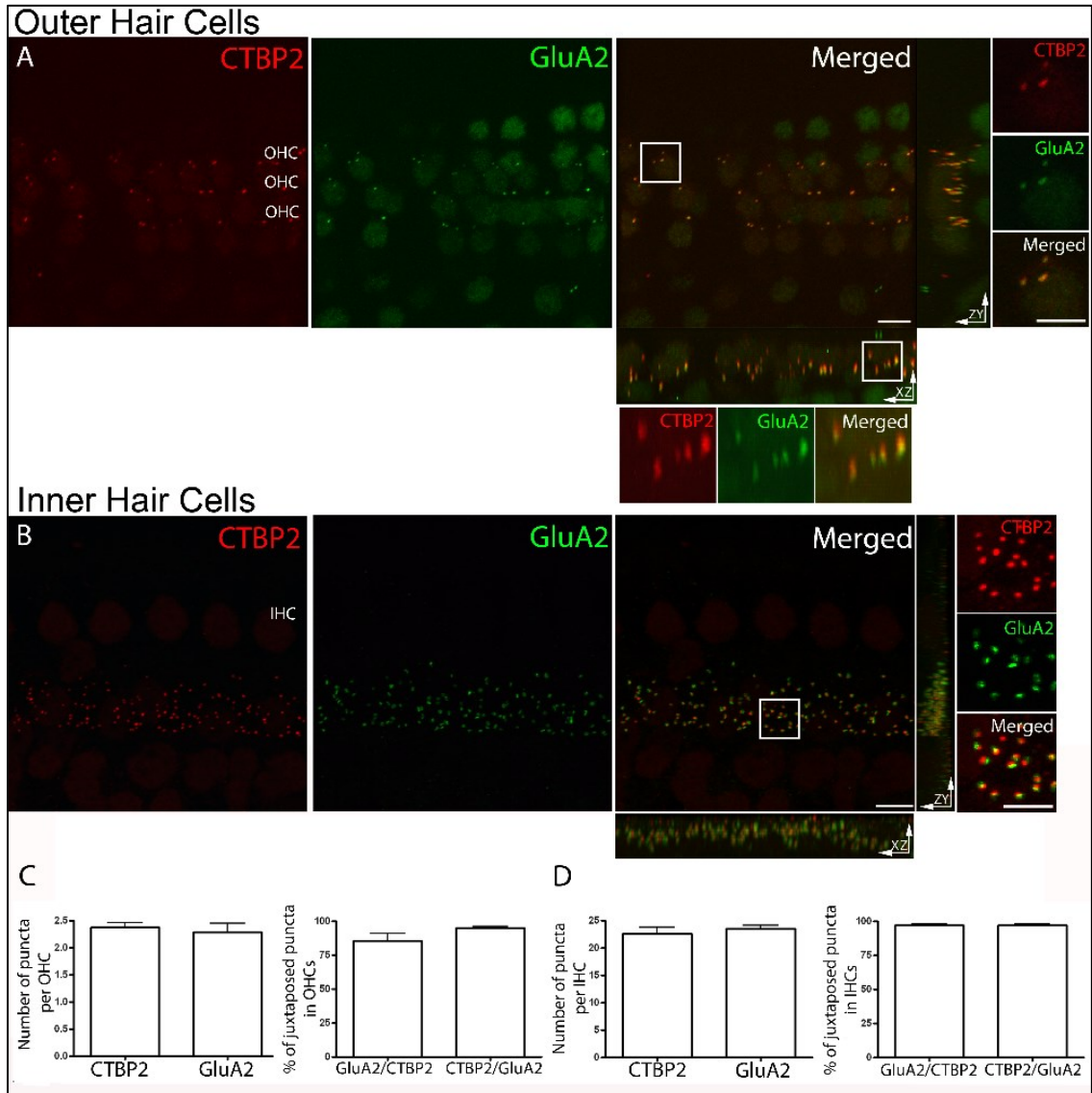
Figure 2.1.1. Maximum intensity projections of confocal z-stacks of the medial region of the organ of Corti from an adult rat viewed from the endolymphatic surface including 24 adjacent OHCs and 5 IHCs.
A. Immunolabel for the presynaptic ribbon marker (CtBP2: red channel). Immunolabel for the postsynaptic marker glutamate receptor A2 (GluA2: green channel). Magnified inserts: CtBP2 and GluA2 puncta were closely juxtaposed in the X-Y plane. Rotation to the Z-X or Z-Y planes reveals spatial displacement between pre- and postsynaptic markers. B. Pre- and postsynaptic immunolabels IHCs as in A. CtBP2 and GluA2 immunopuncta were consistently juxtaposed at the IHCs. Magnified insert in the X-Y

80

plane shows clear separation of pre- and postsynaptic labels. C. Quantification of the number and the percentage of juxtaposed CTBP2 and GluA2 puncta in OHCs. In a single OHC there was 2.28 ± 0.17 GluA2 puncta and 2.37 ± 0.08 CtBP2 puncta per OHC. 85.52 ± 5.48% of CtBP2 puncta were juxtaposed to individual GluA2 puncta and 94.86 ± 1.1% of GluA2 puncta were juxtaposed to CtBP2 puncta . D. Quantification of the number and the percentage of juxtaposed CtBP2 and GluA2 puncta in the IHCs. At individual IHCs there were 23.3 ± 0.6 GluA2 puncta and 22.4 ± 1.0 CtBP2 puncta. 96.84 ± 1% of CtBP2 puncta were juxtaposed to individual GluA2 puncta and 96.59 ± 1.1% of GluA2 puncta were juxtaposed to CtBP2 puncta. 1A-D: n=3-9 independent preparations; 50 IHCs, 72 OHCs. There were no statistically significant differences in number or correlation among the immunolabels (one way-ANOVA test; p>0.05). Scale bar is 5 μm and 2.5 μm in magnifications. From Martinez-Monodero et al., in preparation.

Further insight into the synaptic arrangements of type II afferent neurons was gained using antibodies directed against postsynaptic density proteins PSD95, Shank and Homer. In the central nervous system, PSD95 participates in synaptic targeting of AMPA receptors (Colledge et al., 2000; El-Husseini et al., 2000; Harms and Craig, 2005; Hirbec et al., 2003; Ives et al., 2004; Naisbitt et al., 1997; Sheng, 1997). In contrast to the near membrane location of PSD95, Shank and Homer serve as postsynaptic density organizing proteins that extend further into the cytoplasm to link cytoskeletal components (Brandstatter et al., 2004). Antibodies to these postsynaptic markers were applied to cochlear whole mounts and their labeling compared to that of GluA2 clusters and presynaptic ribbons at outer hair cell afferent contacts.

Interestingly, PSD95, Shank and Homer revealed complex patterns that could extend several microns along the synaptic pole of the OHC. These postsynaptic structures appeared as an irregular cluster or as an interconnected series, like a short 'pearl chain' (Figure 2.1.2A, B, F, G). PSD95 and Shank immunolabels were closely colocalized (Figure 2.1.2A, insets). Homer showed the same clustered patterns as did PSD95 and

Shank (Figure 2.1.2D). The pattern of postsynaptic density markers had an especially interesting relationship to the CtBP2-labeled presynaptic ribbons, as shown here for Shank (Figure 2.1.2B, F). Most CtBP2-positive ribbons were juxtaposed to Shank, PSD95 or Homer (Figure 2.1.2H). However, roughly half of the postsynaptic densities had no associated CtBP2 puncta. A similar relationship between GluA2 and postsynaptic density proteins were observed, reflecting the strong correspondence between GluA2 and CtBP2 immunolabeling (Figure 2.1.1). The number of postsynaptic density protein puncta (PSD95, Shank and Homer) was nearly twice the number of CtBP2 or GluA2 puncta in the OHC area.
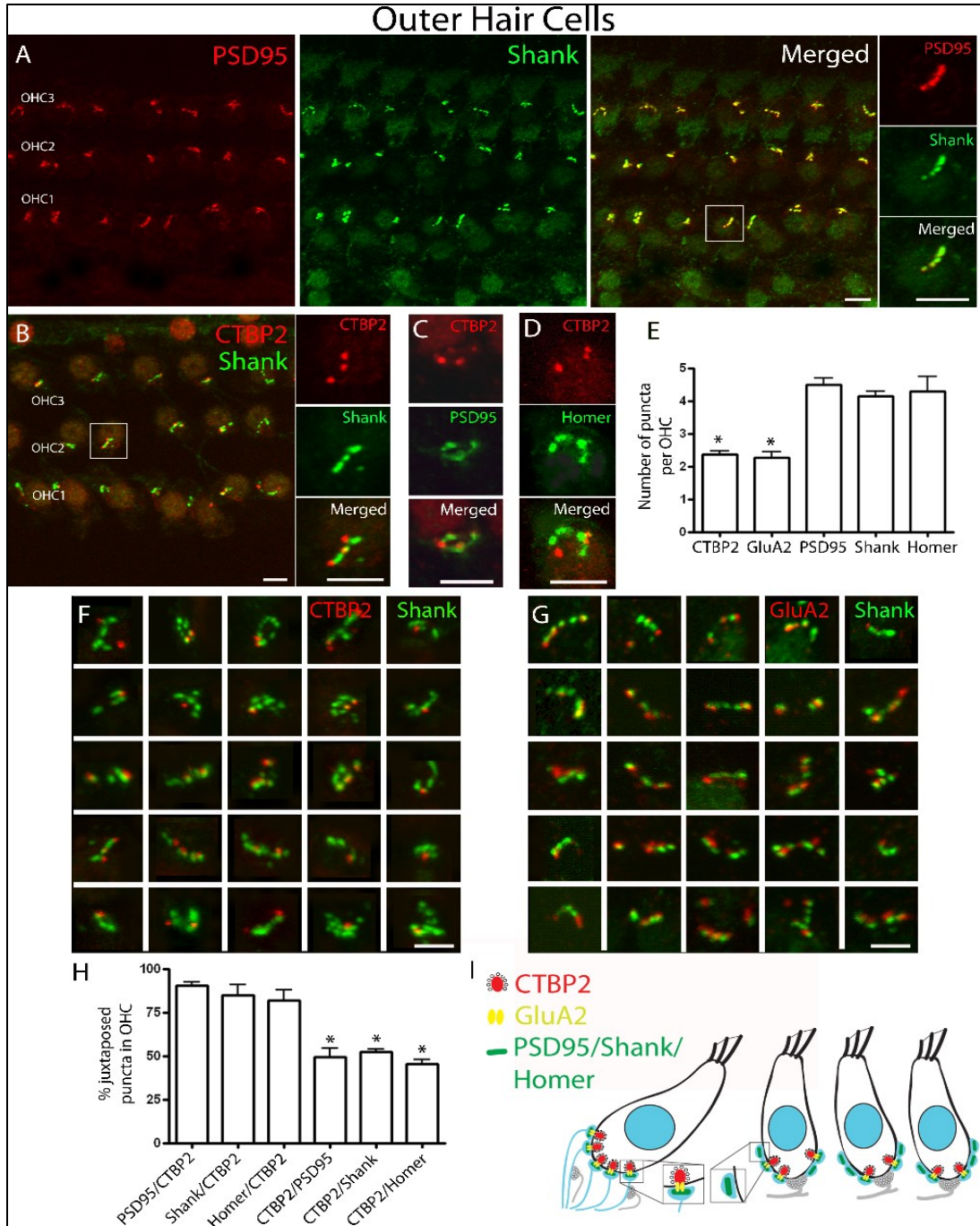
Figure 2.1.2. Confocal z-stack of the OHCs of the medial region of the organ of Corti from an adult rat viewed from the endolymphatic surface.
A. Immunolabeling with the postsynaptic density proteins PSD95 (red channel) and Shank (green channel) show an interconnected series of puncta along the base of the OHCs. Both PSD95 and Shank puncta are closely coincident (magnification insert, X-Y plane).
B, Immunolabeling with the presynaptic ribbon marker CtBP2 (red channel) and

postsynaptic markers Shank
C. Immunolabel for CtBP2 and PSD95.
D. Immunolabel for CtPB2 and Homer. Magnified inserts (X-Y plane) in each case show more extensive postsynaptic density distribution than presynaptic.
E. Pre- and postsynaptic immunopuncta at the OHCs. The number of CtBP2 or GluA2 puncta was significantly smaller than that of postsynaptic density markers (PSD95, Shank or Homer) (one way-ANOVA, p = 0.01; Bonferroni's multiple comparison test; n = 3-7; 72-168 OHCs).
F. Thumbnails of the base of individual OHCs immunolabeled for CtBP2 (red channel) and Shank (green channel). Many the Shank immunopuncta had no CtBP2 associated with them.
G. Thumbnails of the base of individual OHCs immunolabeled for GluA2 (red channel) and Shank (green channel). Many of the Shank immunopuncta had no GluA2 associated with them.
H. Percent Juxtaposition of the CtBP2 and postsynaptic density proteins. The ratio of PSD95, Shank or Homer puncta juxtaposed to CTBP2 was significantly from the ratio of CTBP2 puncta juxtaposed to the postsynaptic density proteins (one way-ANOVA test; p ≤ 0.01; Bonferroni's multiple comparison test). Scale bar is 5 µm or 2.5 µm in magnified inserts and thumbnails.
I. Schematic drawing of OHC and IHC synapses. At the IHC afferent synapse CtBP2/GluA2 relates closely in number to postsynaptic density markers. At the OHC afferent synapse, only a subset of postsynaptic density proteins relate to CtBP2/GluA2 synaptic markers. From Martinez-Monodero et al., in preparation.

Additional Methods

0.3% biocytin (3.0mg/mL) was added to the intracellular solution of the patch pipettes for delivery into the spiral branch of type II afferents via whole-cell gigaohm-seal recordings. The tracer was detected using streptavidin-conjugated horseradish peroxidase, or streptavidin-conjugated fluorescent labeling. In some experiments, the cochlear tissue was preloaded (30 second, room temperature) with 5µM FM1-43FX (Invitrogen), a fluorescent dye that rapidly enters through mechanotransduction channels and partitions into the hair cell membrane. HRP staining was done as previously described. In a second set of experiments we combined fluorescent labeling of the fiber (biocytin – streptavidin conjugated AF488) with immunofluorescent labeling of synaptic

markers in OHCs. The tissue with the filled type II afferent fiber was fixed in 4 % PFA for 10-60 minutes at 4°C. Then the tissue was exposed to 1% BSA and 10% heat inactivated goat serum in PBS for 1 hour at RT to reduce non-specific labeling. Streptavidin-Alexa Fluor 488 conjugate was applied overnight at 4°C in 5% heat inactivated goat serum and 1% BSA. Streptavidin-Alexa Fluor 488 conjugate and CtBP2 or PSD95 antibodies were applied overnight at 4°C in 5% heat inactivated goat serum and 1% BSA. Samples were washed and incubated for 1 hour at RT with the secondary antibodies (that had been centrifuged at high speed and diluted at 1:1000 in 1xPBS). Alexa Fluor 568 goat anti-rabbit and Alexa Fluor 633 goat anti-mouse (Invitrogen) were used as secondary antibodies. Samples were rinsed three times for 10 min each in PBS at RT before mounting and viewing.

Results

In order to further relate the synaptic marker proteins with postsynaptic terminals on type II afferents, we combined fluorescently labeled biocytin fills of type II afferents with immunolabel for pre- and postsynaptic markers CtBP2 and PSD95. Tissue with biocytin-filled fibers was treated with streptavidin conjugated Alexa Fluor 488 as described in the additional method of this session. Similar to the HRP label shown in Chapter 1 (Figure 2.1.3A and B), morphology of fluorescently labeled type II afferents was revealed in great detail, clearly showing the structure of the fine synaptic branches including a terminal bouton and en passant swellings (Figure 2.1.3C, D, E, F). These experiments were done in young rat cochleas (~P8) due to the difficulty of biocytin injection in adult cochlea.

85

To locate type II terminals on individual OHCs, we tried two methods to label OHCs. In one set of experiments, OHC nuclei were counterstained with DAPI (Figure 2.1.3C). In a second set of experiments, the tissue was perfused with 5μM FM1-43 for 30 seconds, a fluorescent dye that is taken up by hair cells through the transduction channel (Nishikawa and Sasaki, 1996) (Figure 2.1.3D). The main terminal zone of a filled fiber was investigated with confocal microscopy. Again, synaptic branches with bouton endings and *en passant* swellings were visible and branches appeared to arc around the synaptic pole of the OHC (Figure 2.1.3C and D, insets). Interestingly, *en passant* swellings and bouton endings together form a structure that resembles the 'pearl chain' pattern observed for postsynaptic maker proteins (PSD95, Shank and Homer, Figure 2.1.2). Most of the synaptic branches innervate a single OHC. Occasionally small processes could branch or extend to contact multiple OHCs. In this dataset, the number of OHCs contacted by one fiber was 23 ± 6.48 (SD, n = 9), identical to the result in preparations with unlabeled OHCs counted in the HRP fills (Chapter 1).

Combination of pre- or postsynaptic immunolabel with fiber filling was only occasionally successful. This may be a result of tissue condition after the time required for the intracellular recording protocol, and/or a reflection of less robust expression of synaptic proteins in the 8-10 day-old animals needed for successful fiber recording. In any event even this low success rate provides qualitative, if not quantitative description. CtBP2 immunopuncta were located near to some, but not all terminal branches as well as en passant swellings of a filled fiber (Figure 2.1.3E). One or two CtBP2 puncta were associated with multiple swellings on each synaptic branch. The small ratio between CtBP2 and the morphological swellings resemble that between CtBP2 and the 'pearl

chain'-like postsynaptic markers (e.g. Shank in Figure 2.1.2F), suggesting these morphological swellings may correspond to the postsynaptic structures, and are likely the sites for functional synapses. However, when antibody for PSD95 was tested in this young age (~P8), not every swelling was colocalized with the postsynaptic marker, suggesting the possibility that type II synapses were still under development. Some, but not every, terminal branch of a filled fiber could be found in near proximity to juxtaposed immunopuncta for CtBP2 and PSD-95 (Figure 2.1.3F), suggesting that more than one type II afferent may innervate the same OHC so that the 'orphan' CtBP2/PSD-95 cluster may be attributed to a different type II afferent that was not filled. Since immunolabel proved extremely difficult for filled fiber tissue and this method only allowed fiber filled at younger age limited by the recording technique, further immunolabeling was carried out on young cochlear whole-mounts (~P8) that were processed similarly to the adult tissues to examine possible developmental differences. Double-immunolabel for CtBP2 and PSD-95 gave an intermittent 'pearl chain' association like that of the adult OHC (Figure 2.1.3G), suggesting that some adult features are already present in the cochlear synapses of young rats. Therefore these results may still partially reflect the organization of OHC-type II afferent synapses in adult cochlea.
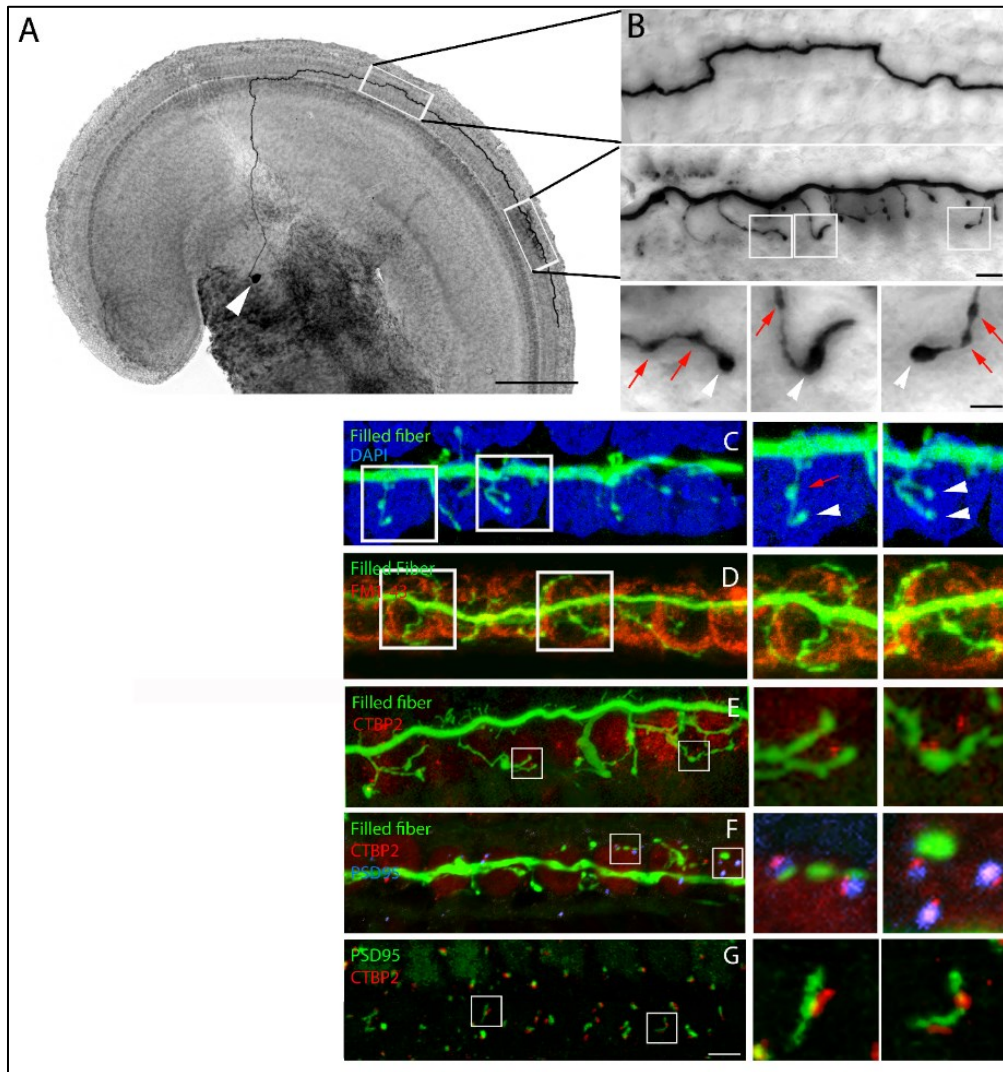
Figure 2.1.3. Single type II fibers with intracellular labeling.
A. Apical turn of a young (P8) rat organ of Corti with biocytin filled type II fiber after Streptavidin-peroxidase reaction. Scale bar 125 μm.
B. Higher magnification of boxed areas in A – showing trajectory and terminal branches.
C. Biocytin-filled type II fiber reacted with streptavidin-AlexaFluor488 (green). OHC nuclei labeled with DAPI (blue). Magnifications show en passant (red arrows) and terminals (white arrowheads) of branches from boxed regions.
D. Biocytin-streptavidin-AlexaFluor488 filled fiber combined with FM1-43-labelled OHCs (red). Magnifications show terminal branches enwrapping the base of outer hair cells.
E. Biocytin-streptavidin-AlexaFluor488 filled fiber combined with CtPB2 immunolabel (red). Magnifications show approximation of some terminal branches to CtBP2 puncta.
F. Biocytin-streptavidin-AlexaFluor488 filled fiber combined with immunolabel for CtBP2 (red) and PSD95 (blue). Magnifications show approximation of some (but not all) terminal boutons to juxtaposed pre- and postsynaptic immunopuncta.

G. Combined immunolabel for PSD95 (green) and CtBP2 (red) among OHCs of young rat cochlea. Magnification shows 'pearl chain' pattern found in adult cochlea. Scale bar 5µm in B, C, D, E, F, G. From Martinez-Monodero et al., in preparation.

2.2 AMPA receptors mediate OHC-type II synaptic transmission

The identity of neurotransmitter and receptors at the OHC to type II contact has been debated for some years. The absence of GluR2/3 immunoreactivity led to the conclusion that some mechanism other than AMPAR-mediated transmission operated there (Matsubara et al., 1996a; Thiers et al., 2008). Initial studies of synaptic currents in type II afferents showed that these were blocked by the AMPA/kainate antagonist NBQX, leaving open the possibility that postsynaptic kainate receptors shown by immunohistochemistry study (Fujikawa et al., 2014) might mediate the response to glutamate release from OHCs. On the other hand, our work described here revealed that the AMPA receptor subunit GluA2 were present in the outer hair cell region, juxtaposed with the CtBP2-labeled ribbons and co-localized with around half of the more extensive postsynaptic markers (Martinez-Monedero et al.; in preparation).

Further support for the involvement of GluA2 AMPA receptors was obtained by intracellular recording from type II afferents in excised apical turns of young rat cochlea (P7-P9). The highly potent AMPA-specific noncompetitive antagonist CP-465022 was applied while recording potassium-evoked excitatory post-synaptic currents (EPSCs). CP-465022 shares a similar binding site on AMPARs with its earlier precedent GYKI, but is much more potent on AMPA receptors (Lazzaro et al., 2002; Menniti et al., 2000) and highly selective for AMPA over kainite receptors (Lazzaro et al., 2002; Paternain et

al., 1995). At 100 μM (2 fibers) and 10 μM (3 fibers) CP-465022 completely eliminated EPSCs induced by the elevated external potassium (40 mM) that depolarized OHCs, suggesting AMPA receptors mediate the synaptic transmission between OHC and type II afferents (Figure 2.2.1A and B). To further support this observation, CP465022 was applied at a lower concentration (1 μM) that partially blocked EPSCs recorded in type II afferents (Figure 2.2.1B). The distribution of EPSC amplitudes was shifted to smaller numbers in 1 μM CP465022 (Figure 2.2.1D) compared with control condition (Figure 2.2.1C). Average EPSC amplitude was reduced to 64.3% and a cumulative plot is shown in Figure 2.1.4E (n=2 afferents). To further probe for kainate or other non-AMPA receptors, the residual current in CP-465022 was normalized and its waveform compared to that before block. Interestingly, no difference in EPSC kinetics was found before and during block by CP-465022 (Figure 2.2.1F). Given the known kinetics differences between AMPA and kainite receptors (Lerma and Marques, 2013), our result suggests that a single kinetically homogenous population of glutamate receptors is functional at this synapse. The relatively fast deactivation kinetics of EPSCs suggests a role for AMPA receptors, rather than the normally much slower kainite receptors.

Inclusion of the GluA2 subunit renders AMPARs impermeable to calcium (Hollmann et al., 1991; Mishina et al., 1991), suggesting that synaptic currents in type II afferents flow through calcium-impermeant channels. This finding was further supported by data from the doctoral thesis of Catherine Weisz. Cat showed that intracellular spermine did <u>not</u> cause rectification of the current-voltage relation of EPSCs, indicating the presence of the calcium impermeant GluA2 subunit. She also showed that the compounds philanthotoxin and Naspm, which cause conductance block of GluA2-<u>lacking</u>

AMPA receptors had no effect on EPSCs recorded in type II afferents. Taken together, these results suggest that GluA2-containing AMPARs most likely mediate rapid glutamatergic excitation at the OHC to type II afferent synapse in the rat cochlea.
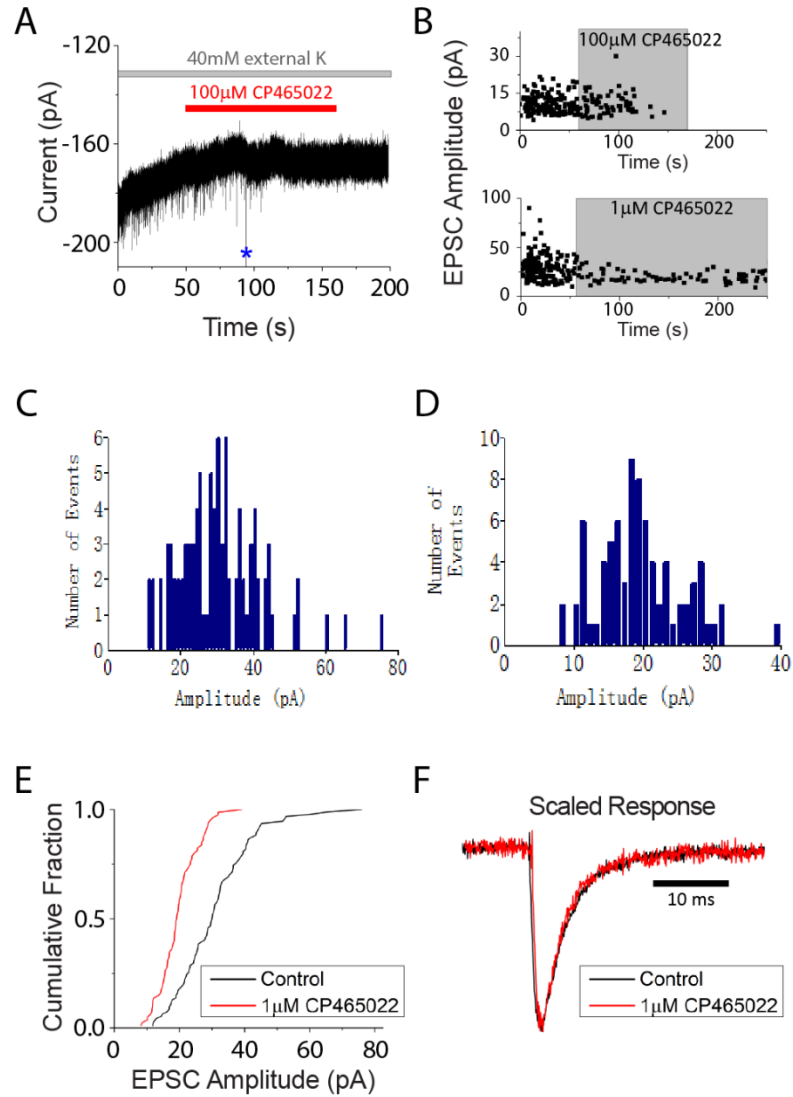
Figure 2.2.1. AMPA receptors mediate the synaptic transmission from OHC to type II afferents.
A. Representative trace showing the complete block of EPSCs by 100µM CP465022. Blue star indicate an action current occasionally recorded in this fiber. Recordings were made in 40mM external potassium to increase EPSC frequency.
B. Diary plot of EPSCs showing a complete block by 100µM CP465022 and partial block by 1µM CP465022.
C. Distribution of EPSC amplitude in control (n=3 afferents).

D. Distribution of EPSC amplitude in 1μM CP465022 (n=3 afferents).
E. Representative cumulative plot of EPSCs. EPSC amplitudes decreased in the presence of 1μM CP465022 (red).
F. Scaled EPSC waveforms in control (black) and in 1μM CP465022 (red) showing similar kinetics Modified from Martinez-Monodero et al, in preparation.

2.3 Acetylcholine responses of type II afferents

Besides the OHC to type II afferent synapse, it has been proposed that type II afferents may serve as the postsynaptic targets for cholinergic medial olivocochlear efferents that innervate the cochlea. Ultrastructural studies suggested that axodendritic efferent to type II afferent synapses may be possible (Nadol, 1983; Thiers et al., 2002). Although terminal endings of both medial olivocochlear efferents (MOC efferents) and type II afferents were clustered at the base of OHCs, morphological synapses between MOC efferents and type II afferents were identified on the dendritic 'shaft' of outer spiral bundle fibers that were further away from their OHC contacts. Evidence for such morphological synapses was the appearance of a few vesicles found close to the cell membrane on the efferent side. Since the major transmitter released from MOC efferent is acetylcholine (ACh) (Eybalin, 1993), we tried to probe if this axodendritic synapse is functional by testing ACh responses in type II afferents.

Whole-cell voltage clamp recordings were made in 5 type II afferents from young rat (P7-P10) cochlea. Applying 1 mM ACh consistently induced very small responses (1-4pA) which were hardly measurable. When I switched to current clamp recordings, a small depolarization by 1 mM ACh was recorded, averaged 2.9 ± 1.7 mV (n=7 cells). Figure 2.3.1 shows the biggest ACh induced response recorded in a type II afferents. No correlation was found between the response amplitude and the age (within the range of

P7-P10) of the animal. Because of the insignificant ACh response at the young ages limited by our preparation, this question was not pursued further in this thesis.
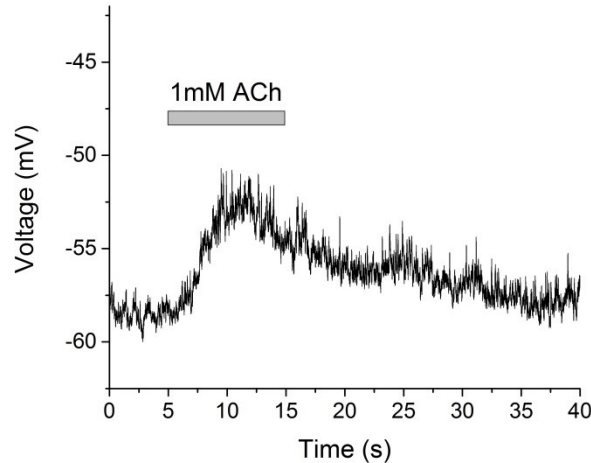
Figure 2.3.1. Small ACh responses recorded in a type II afferent from a P9 rat.

Discussion

The synaptic organization of OHC-type II afferents was poorly understood. Although EPSCs triggered by OHC depolarization were recorded in type II afferents, this finding was confounded by the lack of immunolabel of GluA2/3 AMPA receptors at this synapse (Eybalin et al., 2004; Fujikawa et al., 2014; Knipper et al., 1997b; Liberman et al., 2011; Matsubara et al., 1996b; Meyer et al., 2009). Only one study localized very weak GluA2/3 puncta in outer hair cells but they were not associated with the presynaptic ribbon labeled by CtBP2 (Huang et al., 2012). Non-ribbon-associated contacts between OHCs and type II afferents were also reported (Dunn and Morest, 1975; Nadol, 1983). Therefore, the type of postsynaptic receptors, as well as whether ribbons serve as the major site of synaptic transmission was still controversial. The present work shows that

postsynaptic GluA2 expression corresponded highly with the presynaptic ribbons labeled by CtBP2, with a nearly 1:1 ratio. Although the PSD-95, Shank and Homer antibodies revealed extensive 'pearl chain'-like postsynaptic densities, the AMPA receptor subunit GluA2 was expressed specifically at only two or three spots in the 'pearl chain' where a presynaptic ribbon was juxtaposed, forming discrete sites of synaptic contacts. The 'pearl chain'-like postsynaptic structures were related to the morphological swellings on type II dendrites through biocytin fills. On each synaptic branch of type II afferents, the *en passant* and terminal swellings were also arranged in a chain structure, and the distances between these swellings were similar to the distances between puncta of the postsynaptic markers. CtBP2 immunolabeling was further found juxtaposed to the swellings on type II dendrites, suggesting these are the sites for GluA2-containing AMPA receptor mediated synaptic transmission. These findings not only confirmed the previous observation of discrete boutons (Ginzberg and Morest, 1984; Nadol, 1983) or more extensive, en passant synapses between OHC and type II afferents (Francis and Nadol, 1993; Nadol, 1988; Sobkowicz et al., 1993), but also associated these morphological features with a highly specialized organization of pre- and postsynaptic proteins.

Our electrophysiological experiments suggest that synaptic transmission is most likely mediated by GluA2-containing AMPA receptors. CP-465022 has been shown to serve as a selective antagonist for AMPA over kainate or NMDA receptors (Lazzaro et al., 2002). The concentration used in our experiments (1, 10, 100 µM) has a minimal effect on GluK2 receptors tested by heterologous expression in *Xenopus* oocytes (Balannik et al., 2005). Analysis of EPSC waveforms before and after partial blocks (Figure 2.2.1F) suggests that synaptic currents were contributed by a single kinetic group,

which is faster than the typical kainate receptor mediated EPSCs identified in other native neurons (Lerma and Marques, 2013). Together with the pharmacological experiments on calcium permeant and impermeant AMPARs, this evidence further supports the presence and function of GluA2-containing AMPARs at OHC-type II afferent synapses.

It was intriguing to identify 'empty slots' on the extensive postsynaptic densities on type II afferents. These slots were revealed by antibodies to postsynaptic proteins, but were negative for ribbon (CtBP2) and AMPA receptors (all of the subunits GluA1-A4 were tested). One possibility is that these 'empty slots' are not completely free of receptors, but can be occupied by postsynaptic receptors other than the AMPARs. Kainate receptors had been colocalized to a similar postsynaptic density structure (named 'C shape') identified in type II afferents (Fujikawa et al., 2014) and immunogold labeling of P2X2 receptors was found at the OHC-type II synapse (Housley et al., 1999). It is unclear if NMDA receptors and metabotropic glutamate receptors are present at this synapse. However, our physiological studies showed that EPSCs recorded in type II afferents were most likely mediated by GluA2-containing AMPARs. These results did not reveal any residual components of EPSCs that might be mediated by other receptors. Therefore even if other receptors coexist at the same synapse, they might be playing a modulatory role instead of directly contributing to the synaptic currents. A second possibility is that such 'empty slots' may be sites of silent synapses that allows plasticity to occur. It would be interesting to examine this hypothesis and investigate what kind of stimulation could induce changes of synaptic strength at the OHC-type II afferent contacts.

Chapter 3: Purinergic signaling in type II afferents

Although synaptic inputs from OHCs have been recorded and carefully characterized (Weisz et al., 2009; Weisz et al., 2012), whether acoustic stimulation of outer hair cells could serve as the adequate stimulus for type II afferents is still a remaining question. Sound drives OHCs and the depolarization could reach ~0mV (Johnson et al., 2011). However, tested in vivo, broad band sound could not activate type II afferents, whereas the same condition faithfully triggered responses of type I afferents (Brown, 1994; Robertson, 1984; Robertson et al., 1999). The lack of sound-driven responses of type II afferents may be explained by the weak synaptic transfer function. Release probability of OHCs was low so that each action potential has ~1/4 chance to trigger single vesicular release, which causes a small EPSP (3.8±2.0 mV) compared to the action potential threshold (~25 mV from the resting membrane potential). Even though each type II afferent connects with over ten OHCs and summation of EPSPs is likely, by calculation, synaptic activation of type II afferents is difficult, unless loud or even traumatic level of sound maximally activates all the presynaptic OHCs (Weisz et al., 2009; Weisz et al., 2014; Weisz et al., 2012).

Another phenomenon accompanying loud sound stimulation is the increased concentration of ATP in the cochlear fluid (Munoz et al., 1995). ATP strongly depolarized type II afferents and elicited action potentials in extracellular recordings. Although some EPSCs were also recorded, the large slow component of the ATP-triggered responses in type II afferents was unchanged when synaptic transmission was blocked, suggesting that such response was intrinsic to the type II afferents and was

independent of synaptic transmission (Weisz et al., 2009). It was speculated that the sensitivity to ATP might enable robust responses of type II afferents during acoustic damage. However, purinergic signaling in type II afferents was poorly understood and it was unclear which receptors mediated the responses. In this chapter, we investigated the types of purinergic receptors expressed in type II neurons, and revealed both ionotropic and metabotropic components of ATP and UTP induced responses.

3.1 Characterization of the ionotropic P2X receptors

In order to examine the presence of the ionotropic P2X receptors, 50 µM ATP was applied using a large-bore gravity-driven application pipette. For all the experiments, the application pipette was positioned parallel to the cochlear spiral so that perfusion could cover a longer distance of the type II afferents' spiral dendrites. Inward current was induced in type II afferents by ATP, averaging 55.3 ± 17.7 pA at peak (voltage clamp at -60 mV, 10 experiments in 7 afferents) and a large depolarization could also be recorded in current clamp recordings (Figure 3.1.1 A and B). The ATP evoked response was significantly reduced by the P2X antagonist, PPADS (Fig. 3.1.1 A, 3.5 ± 3.4 pA, $p < 0.05$, compared to controls, 4 experiments in 4 afferents) and could be partially recovered.
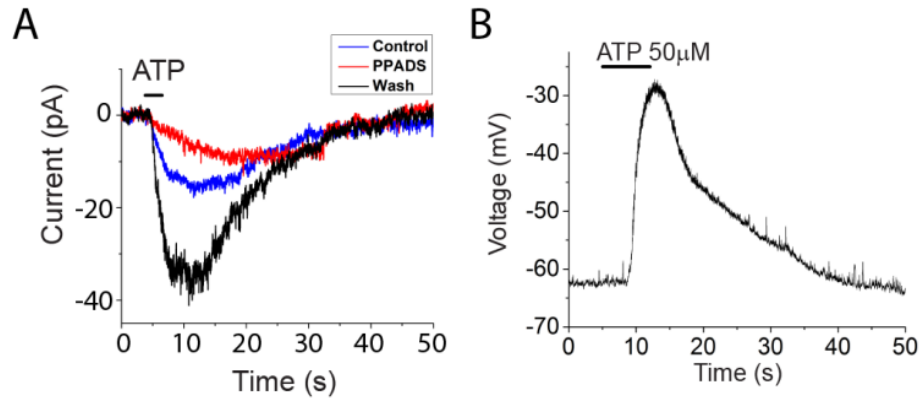
Figure 3.1.1. ATP evoked inward current and depolarization in type II afferents.
A. ATP induced current can be blocked significantly by the P2X receptor antagonist
PPADS (red trace), with partial recovery (blue trace).
B. 50 µM ATP induced a large depolarization in type II afferents.

PPADS is a known P2X receptor antagonist, but it also partially blocks P2Y4 and

P2Y6 receptors. To further test the contribution of P2X receptors to the ATP-induced

responses in type II afferents, a voltage ramp protocol was employed to unveil the ionic

mechanism. Holding potential was ramped from -90mV to +30mV in normal external

solution or after 50 µM ATP was applied (Figure 3.1.2 A and B). Ramp current in the

absence of ATP (Figure 3.1.2 B, black) was subtracted from that in its presence (Figure

3.1.2 B, red) to obtain the ATP-dependent ramp current (Figure 3.1.2 C). After

subtraction, the resulting ATP-dependent current showed an inward current upon ATP

application, and went outward when voltage was ramped to positive values (Figure 3.1.2

C). The ATP-dependent current–voltage (I-V) relation had a positive slope at its reversal

near 0 mV (Figure 3.1.2D, representative of 5 experiments in 3 cells), consistent with the

activation of non-selective cation channels (P2X receptors). This non-selective

conductance induced by 50 µM ATP further supports the presence of P2X receptors in

type II afferents.
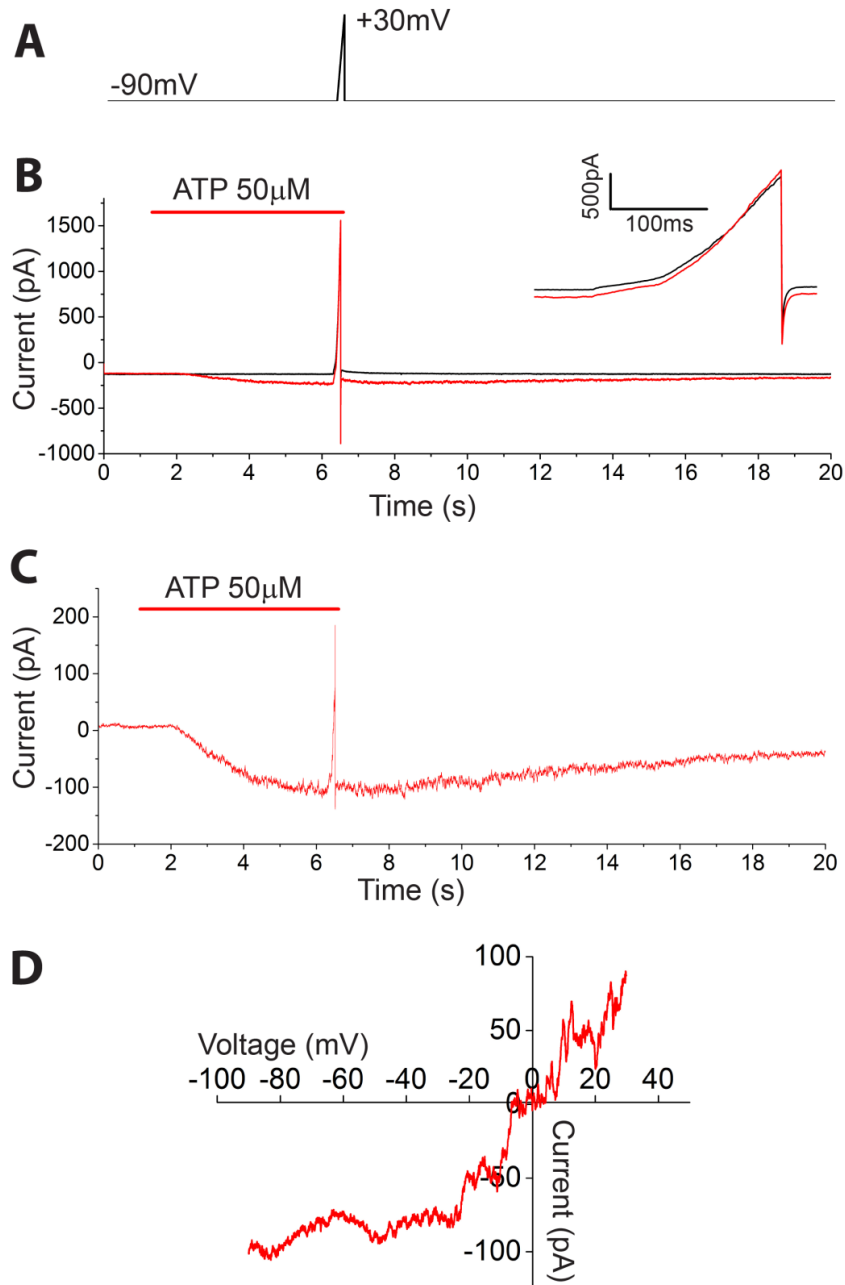
Figure 3.1.2. I-V relation of ATP response revealed by voltage ramp in voltage clamp recordings. A. Voltage command.
B. Overlay of responses from a type II afferent when the holding potential was ramped from -90mV to +30mV in normal external solution (black), or after ATP was applied (red). Inset: expanded trace during voltage ramp with (red) and without (black) ATP application.
C. Subtracted response in B, showing the ATP-dependent component.
D. Plot of I-V relation of ATP response. Reversal potential was around 0 mV (n=3 afferents).

3.2 Characterization of the metabotropic P2Y receptors

Next we examined the presence of the other class of purinergic receptor – the metabotropic P2Y receptor. UTP (100 μM), an agonist of P2Y2, P2Y4 and P2Y6 receptors, evoked a small inward current in voltage-clamp at -60 mV (8.9 ± 4.7 pA, 12 experiments in 8 cells, Figure 3.2.1A). Similarly, in current clamp recordings, 100μM UTP caused a much smaller depolarization (6.8 ± 4.4 mV, n=11 afferents, Figure 3.2.1B) than that induced by 50 μM ATP. The difference in the size of the responses implied that UTP might trigger a distinct ionic mechanism.
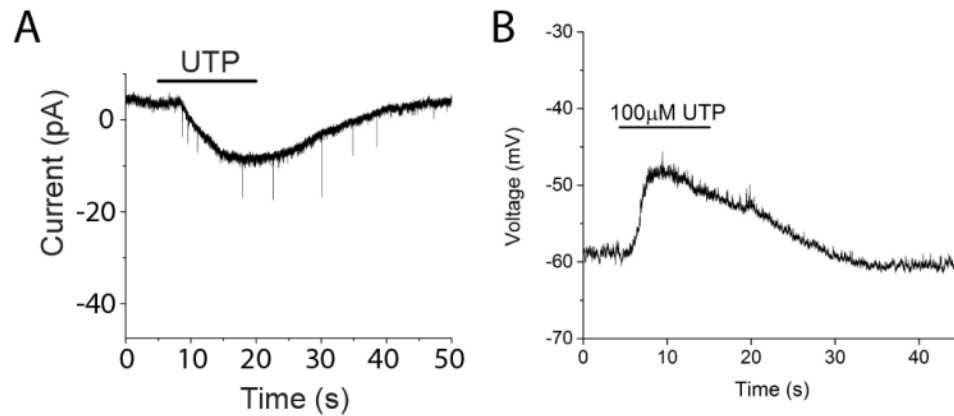
Figure 3.2.1. UTP (agonist for P2Y2, P2Y4 and P2Y6 receptor) induced inward current and depolarization in type II afferents.
A. UTP-evoked inward current in voltage clamp recordings at -60mV. EPSCs (the downward 'spikes') were occasionally recorded, but their frequency was not changed significantly during UTP application.
B. UTP-evoked depolarization was smaller on average than that due to ATP.

The I-V relation of UTP-evoked current revealed a decrease in potassium conductance by P2Y receptor activation. Tested by a similar voltage ramp protocol (Figure 3.2.2 A and B), the UTP-dependent ramp current was distinct from the ATP-dependent ramp current, with an opposite direction during the voltage ramp (Figure 3.2.2

C). The UTP-dependent current was entirely inward, activating positive to -70 mV (Fig. 3.2.2 D, representative of 6 experiments in 6 cells), and the reversal potential can be extrapolated to near E_K, suggesting the closure of voltage-dependent potassium channels by P2Y receptors signaling through second messenger pathways (Lechner and Boehm, 2004).
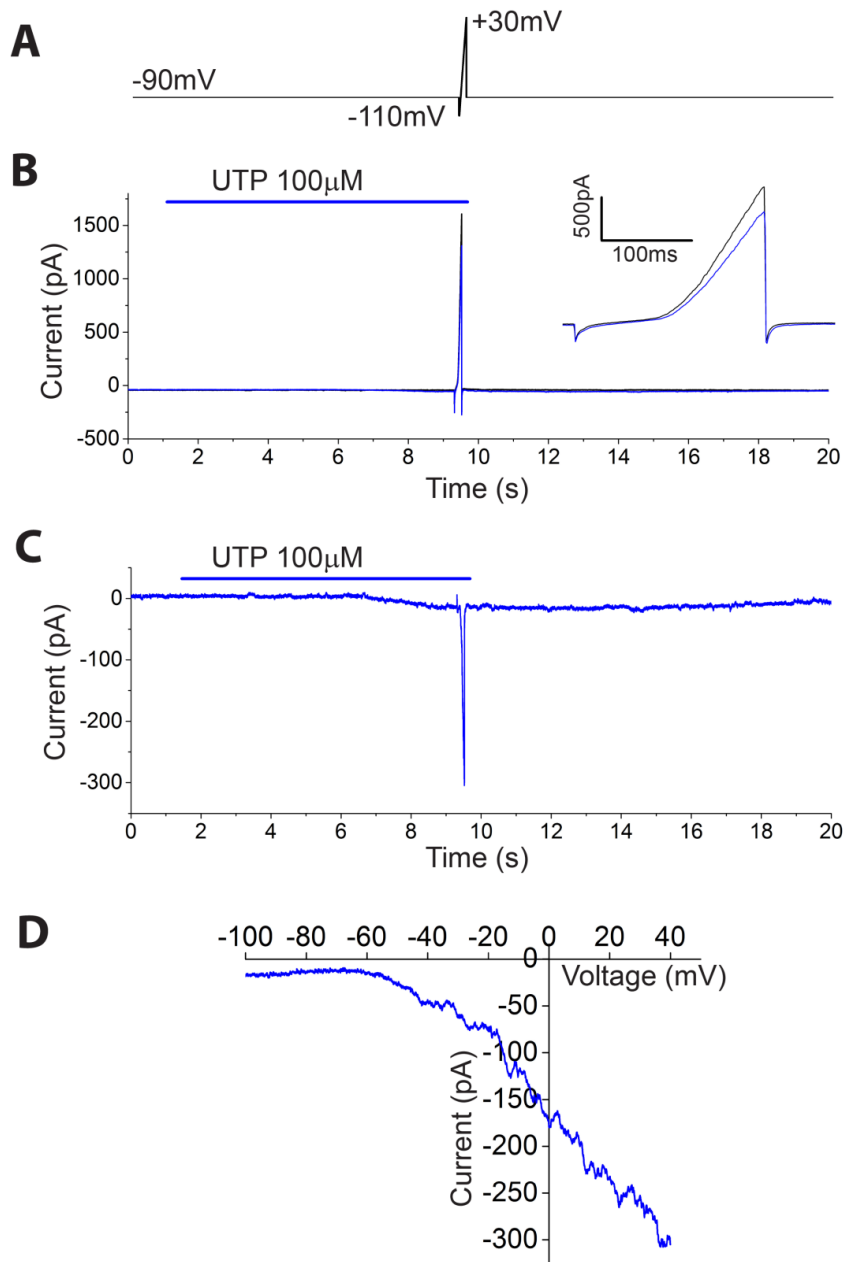
Figure 3.2.2. I-V relation of UTP response revealed by voltage ramp in voltage clamp recordings.
A. Voltage command.
B. Overlay of responses from a type II afferent when the holding potential was ramped from -110mV to +30mV in normal external solution (black), or after UTP was applied (blue). Inset: expanded trace during voltage ramp with (blue) and without (black) UTP application.
C. subtracted responses in B, showing the UTP-dependent component.
D. Plot of I-V relation of UTP response. Reversal potential around -70 mV (n=6 afferents).

Responses to UTP in type II afferents suggest the involvement of P2Y2, P2Y4 or P2Y6 subunits. Among them, P2Y2 and P2Y4 receptors could also be activated by ATP. However, the I-V relation of 50 µM ATP induced current only reflected a P2X receptor-mediated nonselective cation conductance (Figure 3.1.2 D). We found that this may be explained by the differential affinity of P2X and P2Y receptors for ATP. I-V relation of ATP responses in type II afferents showed a transition from 'P2X-like' to 'P2Y-like' behavior when ATP concentration was gradually lowered (Figure 3.2.3). With the lowest concentration tested (1µM), the ATP-dependent ramp current was inward at positive voltages (i.e., reduced outward current) and resembled the I-V relation of UTP responses, suggesting that P2Y receptors may be preferentially activated. With increasing concentration, the ATP-evoked current became more inward at negative voltages, and less so at positive voltages, suggesting the P2X response (increased cation conductance) overwhelms the P2Y response in higher concentrations of ATP (n=2 afferents). Therefore, it seems that the relative contribution of P2X and P2Y-KCNQ pathways depends on the local ATP concentration on type II afferents. At sub micro-molar ATP, the higher-affinity P2Y-KCNQ pathway is preferentially activated. At higher concentrations of ATP the ionotropic P2X receptors predominate.
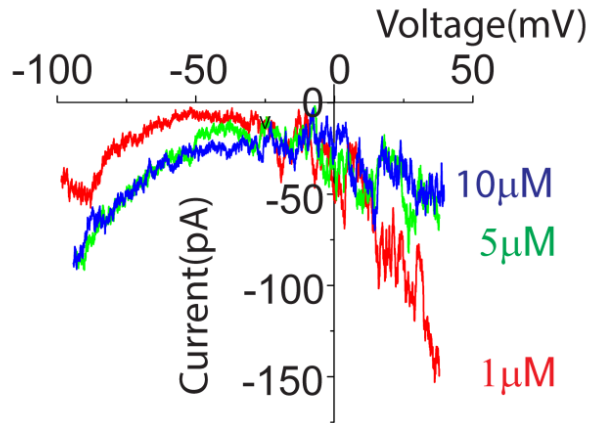
Figure 3.2.3. Low concentrations of ATP preferentially activate 'P2Y-like' ramp currents. A voltage-ramp protocol (as in Fig. 3.2.2) was used to examine membrane currents evoked in type II fibers by lower concentrations of ATP (1 μM, 5 μM and 10 μM) that might differentially activate lower (P2X) and higher affinity (P2Y) receptors. As ATP concentration was decreased the evoked ramp current changed from 'P2X-like' to 'P2Y-like'. With the lowest concentration tested (1 μM), the ATP-dependent current was inward at positive voltages (i.e., reduced outward current), suggesting that P2Y receptors may be preferentially activated. With increasing concentration the ATP-evoked current became more inward at negative voltages, and less inward at positive voltages, suggesting the P2X response (increased cation conductance) overwhelms the P2Y response in higher concentrations of ATP (2 experiments in 2 cells).

3.3 P2Y receptor activation closes KCNQ potassium channels

The potassium conductance closed by UTP reflected voltage dependency at positive voltages (Figure 3.2.2 D), suggesting that the signaling pathway involved voltage-gated potassium channels inhibited by metabotropic receptors. A good candidate is the KCNQ (Kv7) family potassium channels that can be regulated by the Gq-PLC pathway. The KCNQ channel antagonist XE-991 reversibly eliminated the UTP-dependent ramp current in type II afferents (Figure 3.3.1A, from 92.7±20.8 to 3.8±4.5 pA, at +40 mV, 4 experiments in 4 cells, p<0.01), and the KCNQ channel opener retigabine reliably activated outward currents (Figure 3.3.1B, 37.9±3.0 pA at -60 mV, 4 experiments

in 4 cells). These effects suggest that P2Y receptor activation depolarized type II afferents through the closure of KCNQ channels. This is consistent with the small effect of UTP at -60mV (Figure 3.2.1A) where few voltage-dependent KCNQ channels are open.

The closure of KCNQ channels by P2Y receptors increased type II fiber excitability. In UTP, the current threshold for type II afferent action potentials was reduced to $78.2 \pm 3.5\%$ of the level required in normal conditions (four experiments in four cells; $P < 0.01$) (Figure 3.3.1C). Thus, UTP caused a small, but significant increase in excitability, despite the fact that these measurements were made at rest where only few KCNQ channels are open (Figure 3.2.2 D). The effect of P2Y-mediated KCNQ closure will be greater still when type II afferents are depolarized as during acoustic trauma. Thus, KCNQ channels serve as a promising target to modulate the damage-sensitive type II afferents.
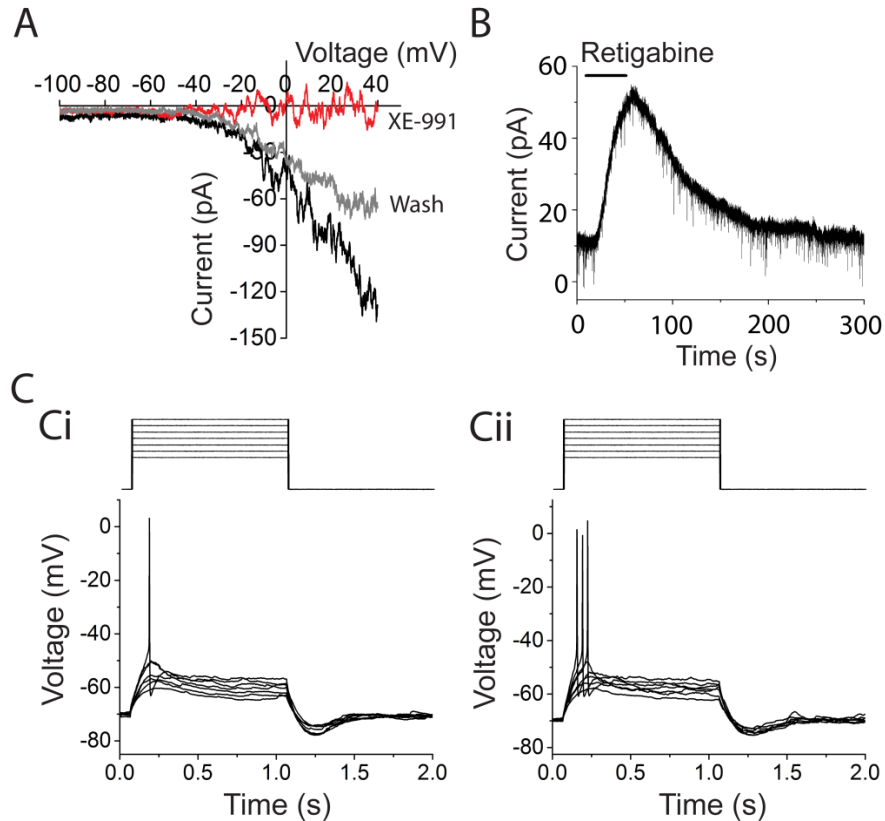
Figure 3.3.1. KCNQ channels were closed upon P2Y receptor activation and regulated excitability of type II afferents.
A. XE-991 (KCNQ blocker) reversibly eliminated the UTP-evoked ramp current. I–V relation of UTP before (black), during (red), and after (gray) XE-991 application.
B. Retigabine (KCNQ opener) induced outward current at −60 mV in type II cochlear afferents.
C. Current step protocol (1pA steps) to evoke action potentials (Ci). In UTP, from the same resting membrane potential, action potentials were evoked by smaller current steps (Cii).

Discussion

These results suggest the presence of two distinct purinergic responses mediated by ligand gated P2X receptors and G protein-coupled P2Y receptors, respectively. Both our pharmacological experiments and the I-V relation studies reflected the P2X receptor mediated responses in type II afferents, consistent with the previous finding that PPADS

106

blocked ATP induced spikes (Weisz et al., 2009). The subtype of P2X receptor expressed

in type II afferents was not further characterized. However, based on the slowly-

desensitizing nature of the ATP responses (Figure 3.1.1 A and Figure 3.1.2 C), the

subtypes involved might be P2X2, P2X4 or P2X7 receptors, according to a similar slow

desensitization kinetics of these receptors in heterologous systems (North, 2002) and

DRG neurons (Burgard et al., 1999; Rae et al., 1998). P2X2 were found to express at the

postsynaptic terminals of type II afferents by immunogold study (Housley et al., 1999)

and P2X7 immunolabel was found in SGNs as well as fiber bundles crossing the tunnel

of Corti (Nikolic et al., 2003). P2X2/P2X3 heteromeric receptors were expressed in

neonatal rat SGNs confirmed by pharmacology (Greenwood et al., 2007). It is unknown

if type II and type I afferents express a different set of P2X receptors that may explain

their difference under physiological and pathological conditions. Recordings from type I

terminals revealed quite small ATP induced responses (Tritsch et al., 2007) compared to

the large depolarization induced by ATP in type II afferents (Figure 3.1.1B). Type I

afferents were more susceptible to acoustic damage, with swollen terminals and soma

degeneration after noise exposure (Kujawa and Liberman, 2009), whereas type II

afferents remained in the damaged cochlea even after the loss of OHCs (Ryan et al.,

1980; Spoendlin, 1971a). Among the purinergic receptors, P2X7 receptor has been

repeatedly suggested to mediate apoptosis due to its calcium permeability (Ferrari et al.,

1999; Kong et al., 2005) and it might be interesting to examine if this receptor is

differentially expressed in type I vs type II afferents.

This was the first demonstration of P2Y receptor mediated responses in type II

afferents (Figure 3.2.1). Like somatosensory pain fibers, type II afferents rarely fired

spontaneous action potentials at rest when tested in vivo (Brown, 1994; Robertson, 1984; Robertson et al., 1999). However, when ATP was released during acoustic trauma, P2Y receptor closes the KCNQ channels and enhanced neuronal excitability in a similar way characterized in many other neuronal types (Brown and Passmore, 2009). This mechanism was preferentially activated when the ATP concentration was low (Figure 3.2.3), consistent with a high affinity of P2Y receptors to ATP (Junger, 2011). The high sensitivity of the P2Y-KCNQ mechanism is meaningful considering the long spiral dendrites of type II afferents. The closure of potassium channels may make the fiber electrically more compact. Even a moderate elevation of ATP concentration might be enough to 'sensitize' type II afferents and enable them to respond more effectively to other stimulation, for example a potentiated synaptic transfer from OHCs, to warn the animals of the nociceptive sound that may cause damage to their hearing.

Chapter 4: Damage induced responses in type II afferents

Having established the ATP receptors and signaling pathways in type II afferents, we next examined whether type II afferents respond to cell damage using an *ex vivo* preparation. After loud noise exposure, the endolymphatic concentration of ATP rises 2-3 fold (Munoz et al.; 2001), presumably as a result of damaged cells (e.g. stria vascularis, hair cells) and the active release of ATP by supporting cells in the damaged outer hair cell region. ATP release also can be induced by mechanical perturbation or hypotonic stress without cell damage *in vitro* (Zhao et al., 2005). In this chapter, we developed a method that allows us to record from type II afferents while outer hair cells were ablated with a sharp glass probe. We dissected the different components that may contribute to the cell damage – induced responses in type II afferents, and tried to address the excitability changes after damage.

4.1 Outer hair cell damage activates type II afferents

To monitor type II afferents, intracellular and extracellular recordings were made from their spiral dendrites under OHCs in the apical turn of the cochlea excised from young rats [postnatal day 7 (P7) to P10]. As a proxy for cochlear trauma, individual OHCs were ruptured with a glass microneedle positioned nearer the cochlear apex than the recording electrode. By rapidly advancing the needle, one to three OHCs were ruptured (Figure 4.1.1A), visualized by the loss of preloaded FM1-43 fluorescence

specifically taken up through hair cells' transduction channels (Meyers et al., 2003) (Figure 4.1.1B). The damaged hair cells became round and swollen, and disintegrated within a few minutes after rupture. Equivalent but off-center punctures failed to rupture hair cells and no change was recorded in type II membrane current or potential, ruling out direct mechanical effects of the needle on the type II afferent (Figure 4.1.2B).
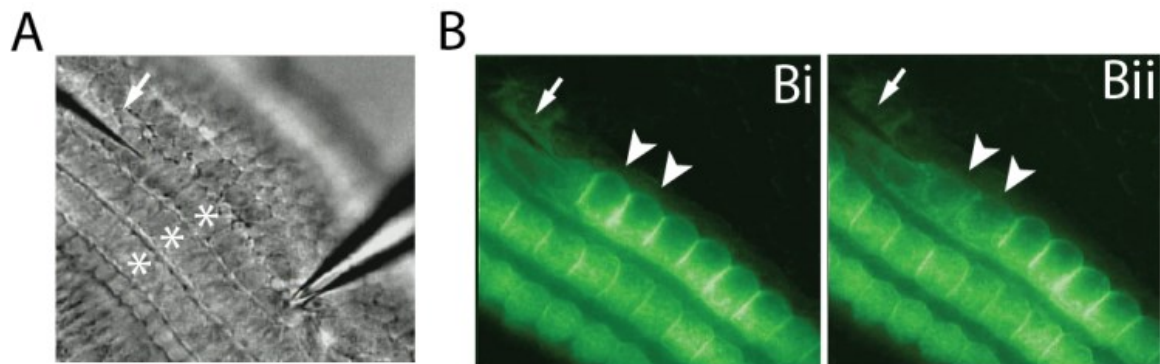
Figure 4.1.1. The experimental preparation to study type II afferents' response to damage.
A. Electrode (Right) recording from a type II afferent (out of focus) under OHC rows (stars). The glass needle (arrow) poised to ablate one to three OHCs per trial.
B. Two FM1-43–loaded OHCs [arrowheads (Bi)] were ruptured and lost fluorescence (Bii).

Upon OHC rupture, a large depolarization (23.8 ± 4.5 mV; 14 trials in seven afferents) was recorded from type II afferents (Figure 4.1.2A). The depolarization had an initial fast phase (rise time 1.36 ± 0.41s), followed by a slow component that lasted tens of seconds. Action potentials were triggered on the rising phase of the depolarization (Figure 4.1.2A, inset). In voltage-clamp recordings, a long-lasting inward current was observed (peak current, 111.9 ± 16.4 pA at -70 mV; 10 trials in six fibers) with a 90% decay time of 58.0 ± 9.5 s (Figure 4.1.2B). OHC ablation also faithfully elicited action

110

potentials in loose-patch extracellular recordings (Figure 4.1.2C, n=7 fibers, 23 of 24

trials induced spikes). The spike trains always appeared within 1s after OHC ablation,

consistent with the intracellular recording showing action potentials on the rising phase of

the depolarization (Figure 4.1.2A).
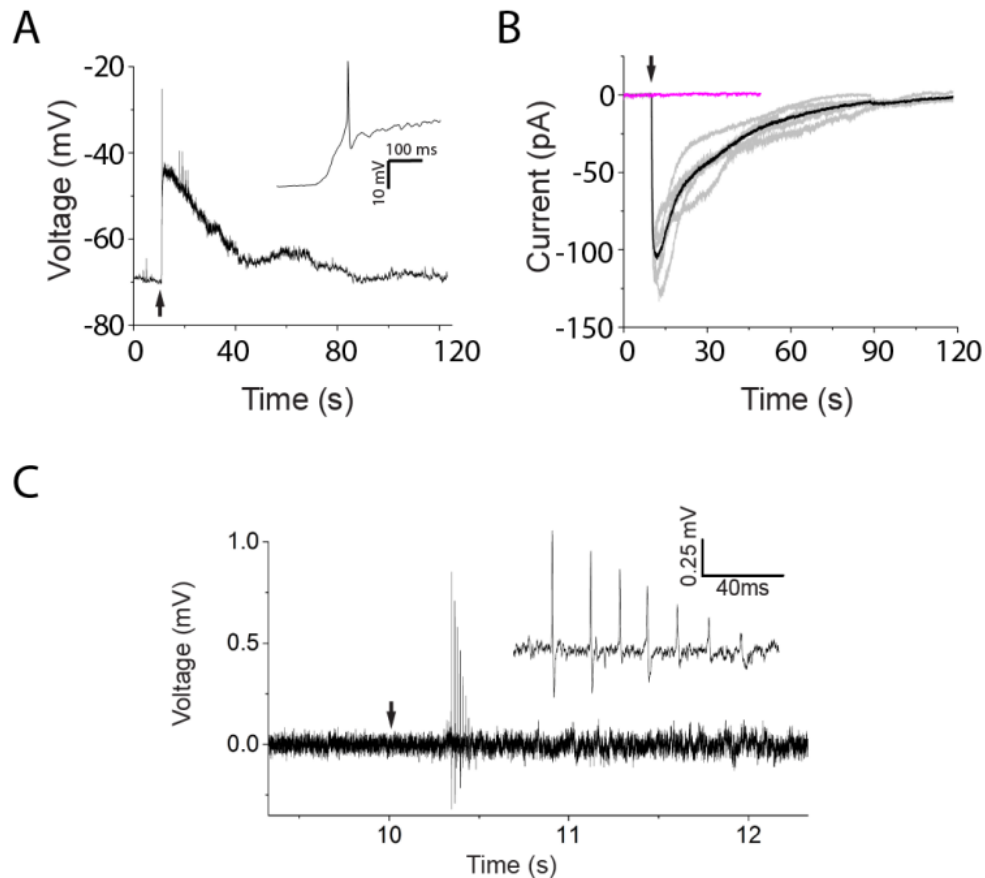
Figure 4.1.2. The cell damage-induced response of type II afferents. Arrow indicates
OHC damage by the sharp needle.
A. OHC ablation depolarized type II afferents and triggered action potentials on the
rising phase (Inset).
B. Representative traces of damage-induced currents (at −70 mV) from five different type
II afferents (gray) and the average (black). Identical needle movement that failed to
ablate OHCs induced no current (magenta).
C. Loose-patch extracellular recording of type II afferent when OHCs were ablated
(arrow). Action potentials were reliably generated by hair cell ablation (n=7 fibers, 23 of
24 trials induced spikes).

111

4.2 ATP from supporting cells contributes to the damage induced response

A role for ATP in this response was shown by the application of pyridoxalphosphate-6-azophenyl-2′,4′-disulfonic acid (PPADS) (50 µM), the P2X receptor antagonist that also partially blocks P2Y4 and P2Y6 receptors. The damage-induced current was greatly abbreviated in PPADS (Figure 4.2.1) (90% decay time, 13.3 ± 7.9 s; $P < 0.001$ compared with control), and charge transfer significantly decreased (from 2.5 ± 0.4 nC in control to 0.8 ± 0.2 nC; $P < 0.001$). Therefore, ATP mediated the slow component of OHC damage induced response in the type II cochlear afferent.
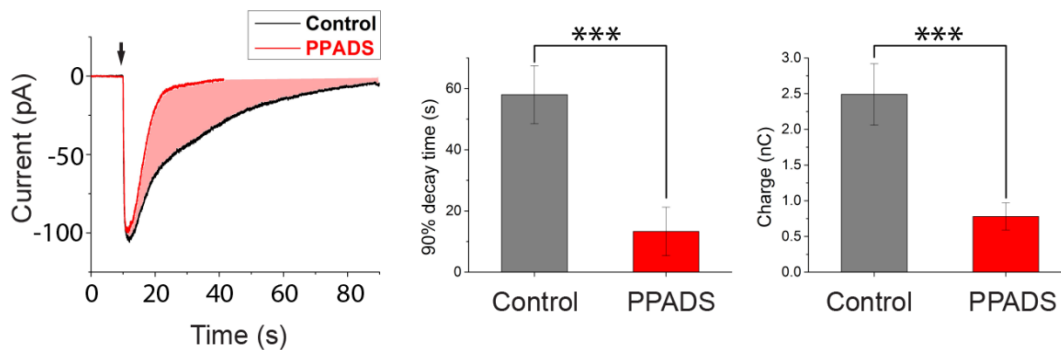
Figure 4.2.1. OHC damage induced response was blocked by PPADS. Average ablation-induced current in PPADS (red, three trials in three afferents) compared with average control current. 90% decay time and charge transfer were significantly decreased.

The prolonged damage-induced response (tens of seconds) is similar in its time course to ATP-dependent calcium waves observed in cochlear supporting cells after hair cell rupture. These minutes-long waves trigger regenerative ATP release through connexin hemichannels on the outer supporting cells, contributing to the rise of ATP concentration in the cochlear fluid after damage (Anselmi et al., 2008; Gale et al., 2004; Lahne and Gale, 2010; Piazza et al., 2007). Accordingly, when the connexin hemichannel

blocker carbenoxolone (CBX) was applied to block ATP release from supporting cells, the type II afferent response to hair cell damage was significantly shortened, with a 90% decay time of 13.8 ± 2.8 s and charge transfer of 0.8 ± 0.1 nC (Figure 4.2.2; $P < 0.001$ for both measures compared with control), suggesting supporting cells as a major source of ATP acting on type II afferents.
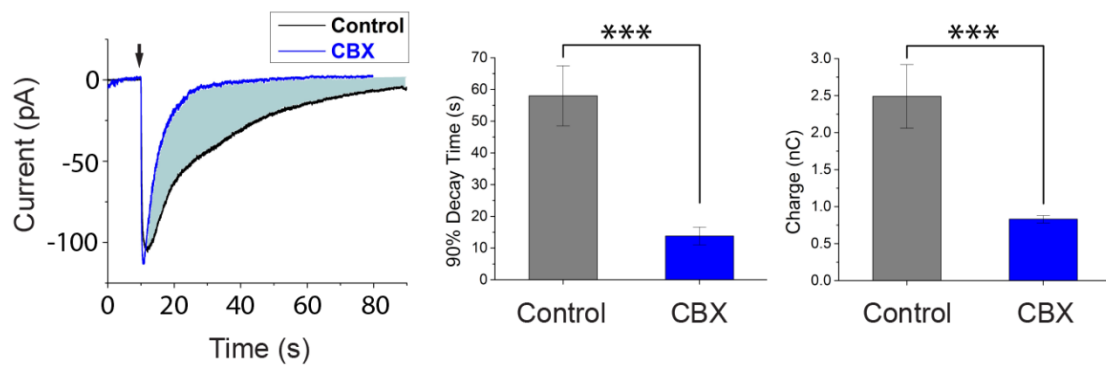
Figure 4.2.2. Connexin hemichannel blocker reduced the slow component of damage induced response. Average ablation-induced current in CBX(blue, five trials in three afferents) compared with average control current. 90% decay time and charge transfer were significantly decreased.

4.3 Characterization of other components mediating type II afferent responses to damage

In these experiments, the peak current amplitude in PPADS and CBX was not significantly different from that of control responses (Figure 4.2.1 and 4.2.2). This residual early peak was responsible for the damage induced action potentials recorded in loose-patch extracellular recordings (Figure 4.1.2C), due to the short latency (spikes appeared within 1s after OHC damage) and that the spikes were not blocked by PPADS (n=2 afferents). To test the possibility that glutamate released from damaged hair cells

might contribute to the early peak, a cocktail of glutamate receptor blockers, including 50μM APV, 50μM CNQX and 1mM MCPG to block AMPA, NMDA, kainate and metabotropic glutamate receptors, was perfused into the bath solution prior to outer hair cell ablation. However, the cell damage induced responses, reflected by the spike trains in extracellular recordings, was not affected by glutamate receptor block (Figure 4.3.1; n=4 afferents). The average number of spikes produced was 6.94±3.58 per OHC ablation in the blocker mixture, not significantly different from 5.53±0.58 spikes per OHC ablation in control (p = 0.415).
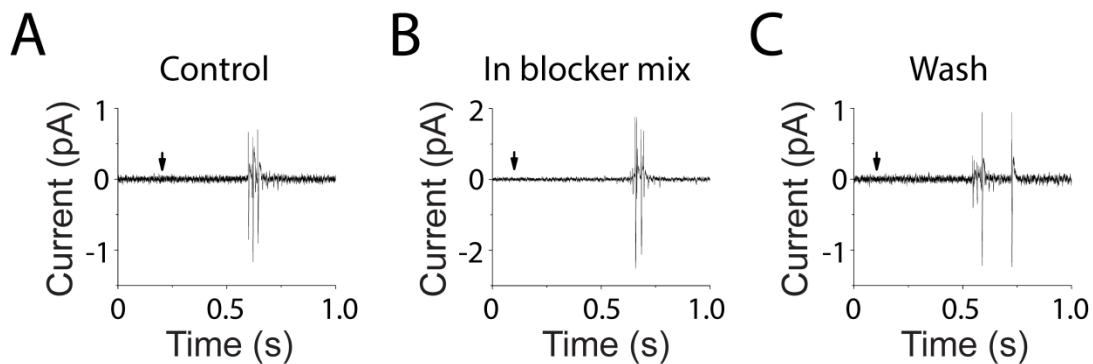
Figure 4.3.1. Damage-induced responses of type II afferents were insensitive to block of glutamate receptors.
A. Loose-patch extracellular recording of action potentials from a type II afferent following OHC ablation (at arrow).
B. A mixture of glutamate receptor blockers, including 50 μM APV, 50 μM CNQX, and 1 mM MCPG to block NMDA, AMPA/kainate, and metabotropic glutamate receptors had no effect (n = 4 afferents).
C.Type II response to OHC ablation after removal of glutamate receptor blockers.

A second possibility is that the remaining fast component is caused by the release of cytoplasmic potassium from the damaged hair cells. We have taken two approaches to test this hypothesis. First, we used ion substitution to change the driving force on potassium current. External potassium was elevated from 5.8 to 40 mM by substitution

with sodium, shifting the potassium equilibrium (E_K) potential from −80 to −31 mV.

Thus, the effect of any additional potassium released by hair cell damage will be reduced

in this condition. In normal saline, hair cell rupture might expose nearby tissue to ~150

mM K^+, producing an inward current due to the change in E_K from −80 to 0 mV. In the

presence of 40 mM potassium, the same bolus of high potassium will change the driving

force from −31 to 0 mV. Assuming the induced inward current is purely due to K^+, the

evoked current should be 2.6-fold smaller. The peak amplitude of the fast component was

reversibly decreased 1.7-fold (from 94.1 ± 14.1 to 54.5 ± 5.9 pA; three experiments in

three afferents) by prior exposure to 40 mM K^+. Given that the actual changes in

potassium concentration are unknown, this result supports the suggestion that the early

inward current is carried at least in part by potassium ions.

A second approach we took was to puff 150 mM K^+ saline (110 K-

methanesulfonate, 20 KCl, 0.1 $CaCl_2$, 3.5 $MgCl_2$, 5 K-EGTA, 5 HEPES, 5

Na2phosphocreatine, 0.3 Tris-GTP, pH 7.2) that does not contain ATP but mimics other

ionic composition inside of a neuron. In 10 trials in 3 afferents, the maximum response

induced by puffing internal solution averaged 97.4±6.7 pA (Figure 4.3.2), not

significantly different from the peak current induced by OHC ablation (Figure 4.1.2 B;

p=0.103). Taken together, the fast early peak of the cell ablation induced responses might

due to a rapid potassium depolarization when cells were ruptured, which is probably a

feature unique to this experimental paradigm, but less likely to happen *in vivo* because

sound progressively damages OHCs over a longer time course.

A

5.8 mM K⁺ 40 mM K⁺ Wash

B
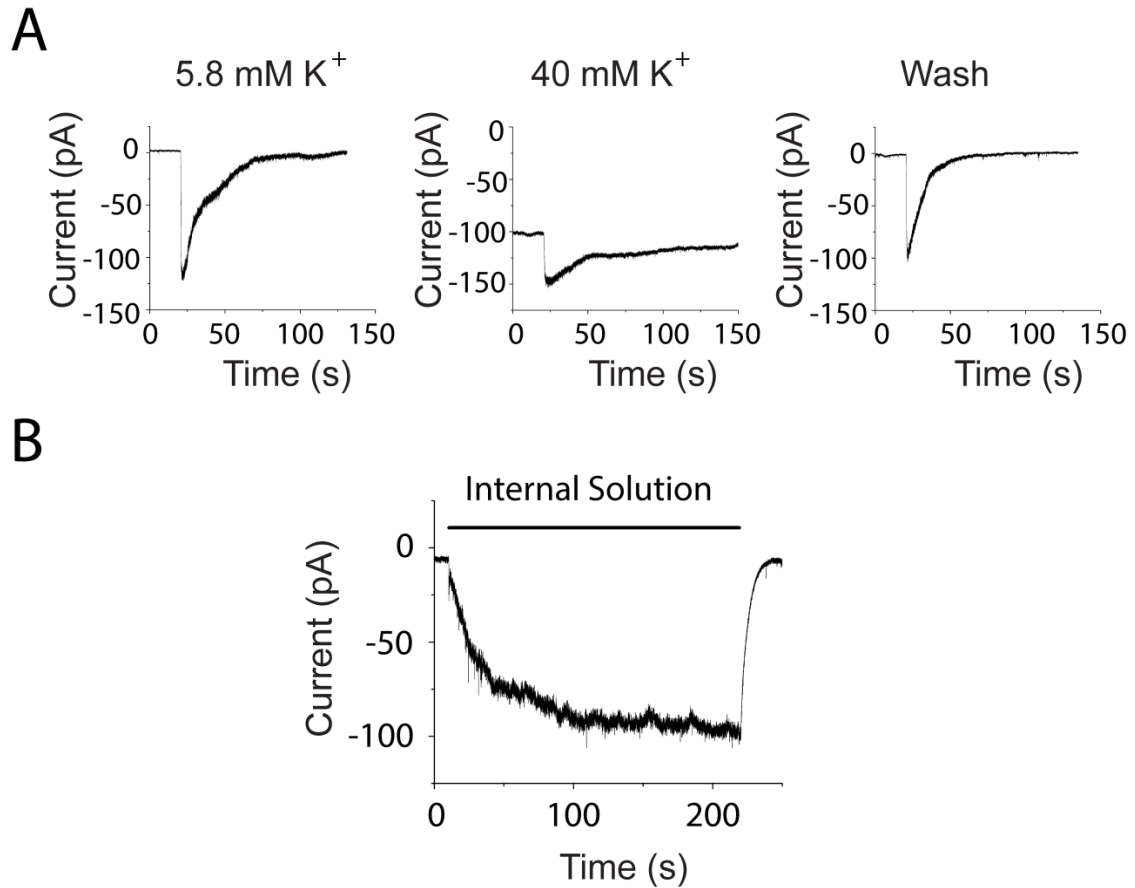
Internal Solution

Figure 4.3.2. Potassium ions contribute to the peak damage-induced current.
A. Damage induced responses were decreased in amplitude when the driving force for potassium ions was reduced.
B. Superfusion with "internal solution" (150 mM K-methanesulfonate, buffered calcium, no ATP) induced large inward currents in type II afferents.

4.4 Hypersensitivity of type II afferents during damage

In Chapter 3 we showed that the excitability of type II afferents can be regulated by P2Y-KCNQ pathway. During OHC cell ablation, ATP released from supporting cells could act on type II afferents for tens of seconds. To address if excitability changes during cell ablation, we delivered a series of current injection pulses to test the firing threshold of type II afferents at different time points during cell ablation (Figure 4.4.1). In

116

two afferent recordings, the firing thresholds (measured by the minimum current to induce action potentials) were lowered during or even after the cell ablation responses, from 10 pA to 5 pA, and from 17pA to 13 pA, respectively. However, due to the movement of the sharp needle, the recordings became less stable after cell ablation, making the result difficult to repeat when tested in another six type II afferents.
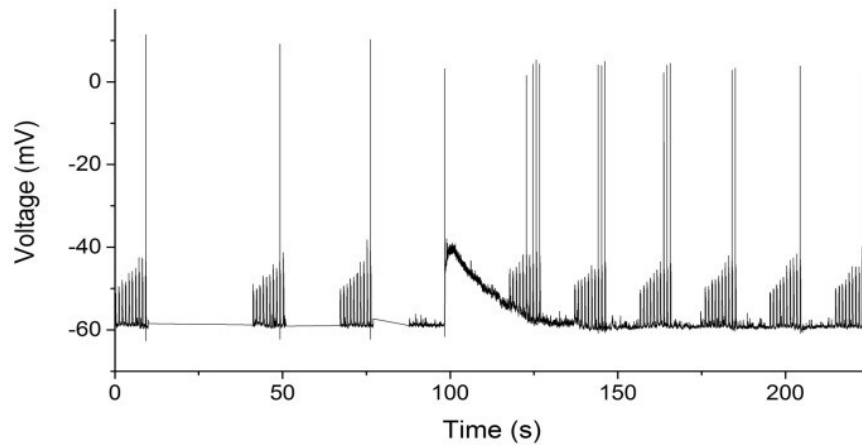
Figure 4.4.1. Type II afferents might become more excitable during OHC damage. The same series of current injection steps were delivered before, during and after OHC ablation at 100s, to test the excitability changes of type II afferents.

We next tried to assess the role of KCNQ channels directly by pharmacological manipulation. The KCNQ activator retigabine (10µM) was applied to the tissue during extracellular recordings from type II afferents. OHC damage was used as a means to trigger action potentials in type II afferents (Figure 4.4.2 Control). Repeated hair cell ablation in the presence of retigabine (KCNQ channel opener) failed to elicit any action potentials in five type II fibers (Figure 4.4.2; n=5 afferents), echoing the analgesic effect

117

of retigabine on somatic pain pathways (Brown and Passmore, 2009).
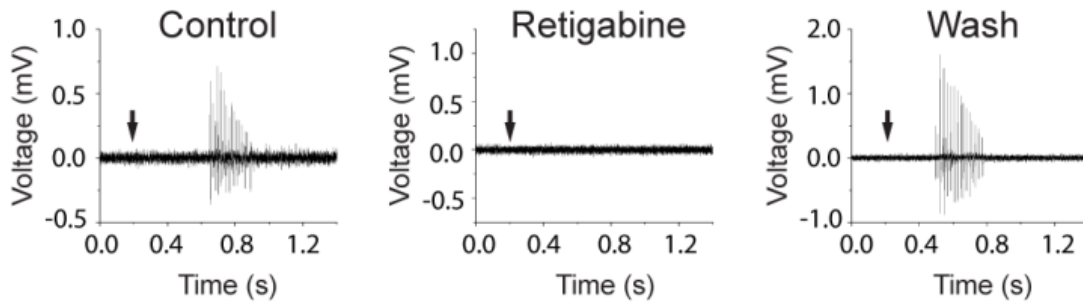
Figure 4.4.2. The KCNQ channel activator retigabine reversibly prevented the response of type II afferents to OHC ablation (n = 5 afferents).

4.5. Calcium imaging on type II afferents using a cultured preparation.

The electrophysiological experiments examined the response of one single type II afferents at a time. In order to study population responses to cell damage, preliminary calcium imaging experiments were conducted on both type I and type II cochlear afferents. A Cre line for advillin, an actin regulatory protein of the gelsolin/villin family that is expressed almost exclusively in peripheral sensory neurons, was bred into a conditional GCaMP3 mouse line, causing expression of the genetically encoded calcium sensor in type I and type II neurons. Cochlear explants were dissected out at P5-P7 then kept an additional day in culture. Due to the limited availability of the transgenic mice, in the initial experiments, female Advillin-Cre mice was crossed with male GCaMP3 mice, causing 2/3 of their progeny to express GCaMP3 nonspecifically in all cells. These nonspecific expression tissues served as a control to test the cell ablation paradigm. A characteristic, long-lasting calcium wave was induced by outer hair cell damage (Figure 4.5.1A), which propagated in a regenerative way (Figure 4.5.1A; arrow at 70s). The rest

118

of the progeny showed specific labeling of type I and type II afferents as reported (Zhang-Hooks et al., 2016). With specific expression of GCaMP3, a type II afferent fiber and a type I afferent terminal was found to respond to high potassium stimulation (Figure 4.5.1B). This "proof of principle" experiment could inform further experiments to monitor type II afferents' activity on a longer time scale, to combine with hair cell damage strategies in culture (e.g. ototoxins that kills hair cells), and to address whether hypersensitivity occurs after damage.
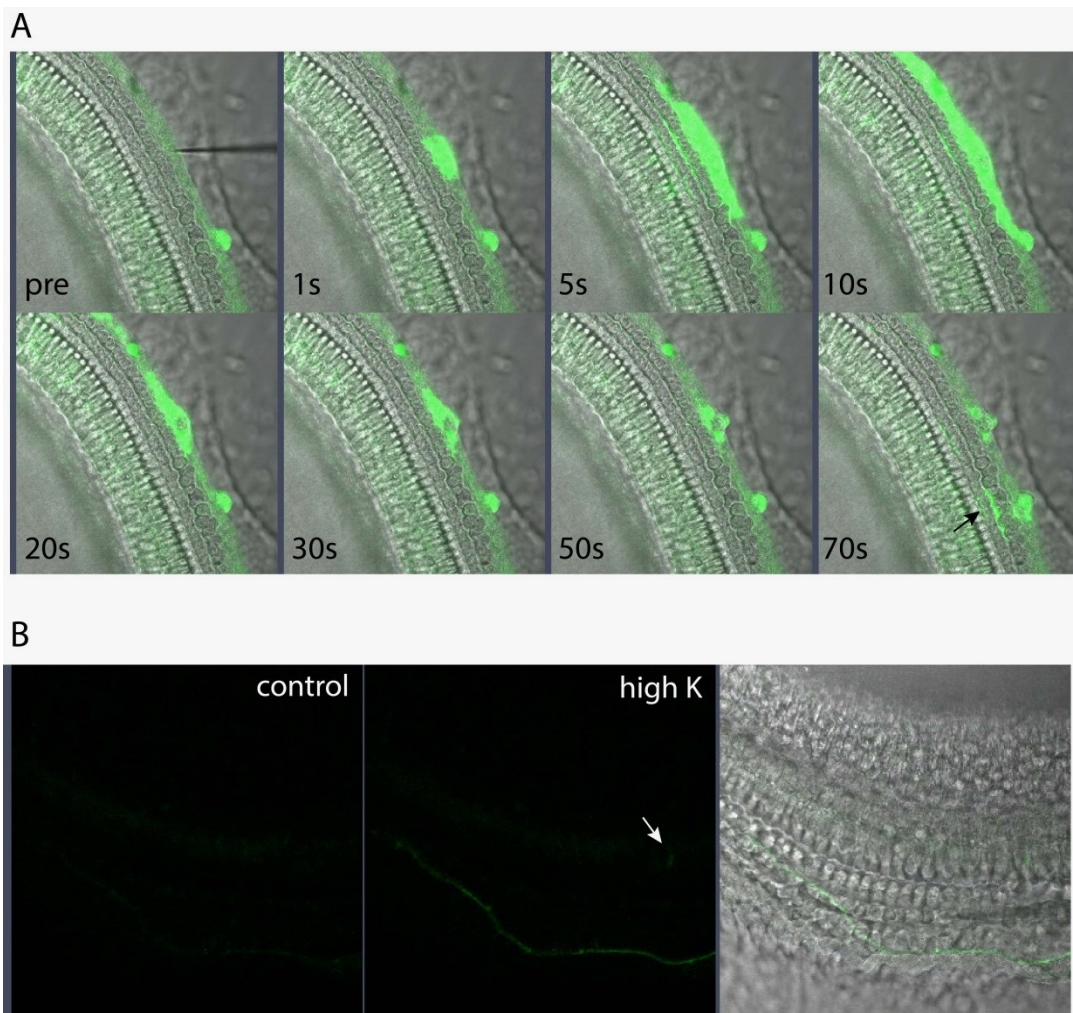
Figure 4.5.1. Calcium imaging on type II afferents.
A. Non-selective expression of GCaMP3 in all cells. A sharp needle was targeted on a

row-3 OHC (pre). After the OHC was ablated, a regenerative calcium wave was observed in outer supporting cells. The wave shrank back the ablation site at 70s, indicated by black arrow.
B. GCaMP3was specifically expressed in type I and type II neurons. High potassium solution triggered increased calcium signals in a type II afferent fiber and a type I terminal (indicated by the white arrow). Image on the right shows overlay of the activated cells with DIC image.

Discussion

Here we demonstrated that OHC damage could depolarize type II afferents. OHCs are among the most sensitive structures in the cochlea that could be damaged by sound (Wong and Ryan, 2015). Here cell ablation by a sharp needle was used as a proxy for the *in vivo* damage of OHCs. After the penetration of the sharp needle, OHCs immediately became swollen and ultimately ruptured, characteristic for a necrotic death pathway. Necrotic death of OHCs was also observed in the noise exposed cochlea (Hu and Zheng, 2008). Membrane leakage was found 5 minutes after noise exposure, allowing the passage of 3kDa and 40kDa membrane tracers (FITC-dextrans). The different aspect of noise-induced OHC death is that apoptosis could also occur (Hu et al., 2006; Hu and Zheng, 2008; Yang et al., 2004). Following membrane leakage, some OHC nuclei became swollen, but other OHCs might have condensed nuclei and their apoptotic death was confirmed by TUNEL assay and caspase staining.

The leakage of OHCs boosted a secondary mechanism that actively released ATP from outer supporting cells, making the effect last tens of seconds for each single OHC ablation *in vitro* (Anselmi et al., 2008; Gale et al., 2004; Lahne and Gale, 2010; Piazza et al., 2007). Our experiments revealed a similar time course of damage induced responses

of type II afferents. ATP contributed up to ~70% of the total charge transfer and elicited a long lasting slow response in type II afferents as a result of only 1-3 OHCs ablation. This effect might be greater with noise damage to a large area of the organ of Corti. Tested *in vivo*, ATP concentration was found increased after acoustic damage (Munoz et al., 1995). Our study also suggested a role for potassium ions in the damage induced responses of type II afferents. In other studies, OHC membrane leakage was observed 5 min after noise exposure (Hu and Zheng, 2008) that may lead to potassium ion exit from the cell. The endolymphatic potential, maintained by high K^+ in the endolymph, was also found to decrease after noise exposure as a result of a shunting effect (Housley et al., 2013). Whether the K^+ concentration could increase in the perilymph to affect type II afferents is unclear. The potassium mechanism may contribute to type II afferents' response to cell damage, but whether this could happen *in vivo* still needs more investigation.

Our experiments showed some possible excitability changes of type II afferents during cell ablation. In Figure 4.4.1, current steps revealed lowered firing threshold not only during the depolarization, but also lasted for tens of seconds after the damage induced response. Because of the difficulty of the experiments, this was found in only 2 out of 8 afferents and needs more experiments to confirm. Retigabine blocked action potentials induced by cell damage. However, this may not reflect the excitability changes produced by ATP, since the spikes appeared in the early peak whereas the ATP effect appeared later as a slow component. To address this effect, a similar experiment applying the KCNQ channel blocker XE991 may be more informative to determine the physiological influence of the P2Y-KCNQ pathway.

Chapter 5: Discussion and Future Work

This work provides direct evidence that type II afferents, in addition to sensing glutamate release from outer hair cells, are activated by cochlear damage in the young rat's cochlea. This observation may help to resolve the decades-long conundrum that type II afferents *in vivo* are very <u>in</u>sensitive to sound (Brown, 1994; Robertson, 1984) and yet presumably carry some information to the auditory brainstem. Likewise, measured *ex vivo*, synaptic excitation is weak and could activate type II afferents only if all the presynaptic outer hair cells were maximally stimulated (Weisz et al., 2012). Alternatively, ATP potently activates type II afferents (Weisz et al., 2009) and serves as a major contributor to the damage-induced response. Possible enhancement of excitability may also lead to robust responses of type II afferents to acoustic stress or cell damage.

5.1 Synaptic structure of OHC-type II afferent synapses

Although it has been established that OHCs and type II afferents form functional glutamatergic synapses (Weisz et al., 2009; Weisz et al., 2012), the identity of the postsynaptic glutamate receptor in type II afferents was still controversial. Using antibodies against AMPA receptor subunits GluA2/GluA3 or GluA2 alone, most of the previous studies failed to reveal immunolabel of AMPA receptors at this synapse (Knipper et al., 1997a; Liberman et al., 2011; Matsubara et al., 1996a; Meyer et al., 2009). Two recent publications successfully demonstrated GluA2 subunit expression in the OHC region (Fujikawa et al., 2014; Huang et al., 2012). However, their results did not suggest

a functional synapse mediated by GluA2 receptors. In one study, the GluA2 subunit was found associated with presynaptic ribbons in the P8 rat cochlea. However, this is only seen in the apical portion but not often in the basal portion, and the labeling was completely missing in the adult cochlea (Fujikawa et al., 2014). The basal cochlea is known to be more advanced than the apical portion in developmental maturation (Waguespack et al., 2007). Therefore, GluA2 expression was interpreted as a transient developmental effect since it was only detected in apical cochlea of neonatal rats. A second study in mouse cochlea revealed GluA2/GluA3 puncta in OHC region only in early postnatal days, however, the expression was permanently lost after P6, also revealing a developmental effect (Huang et al., 2012). Using two different antibodies to the GluA2 subunit and an improved immunostaining protocol, work from Rodrigo Martinez-Monedero in the lab demonstrated juxtaposition of GluA2 and presynaptic ribbon marker (CtBP2) in the OHC region, not only in young rat cochlea as previously reported, but also in the mature adult cochlea. The labeling was highly correlated with a ~1:1 ratio, and our work further found CtBP2 puncta were associated with the swellings on type II afferents, revealing the site for synaptic transmission at this ribbon synapse. The organization of *en passant* and terminal swellings on the synaptic branches of type II afferents corresponded well with the 'pearl-chain' like structure of postsynaptic density proteins, discovered in this work (Martinez-Monedero et al., unpublished) and previously (Fujikawa et al., 2014). AMPA receptor mediated synaptic transmission was further supported by the blocking effect of the AMPA specific antagonist CP-465,022, as well as the fast kinetics observed for EPSCs, since kainate receptor mediated synaptic currents

are normally slow and have a time constant of decay similar to that of NMDA receptors (Lerma and Marques, 2013).

The 'empty-slot' on postsynaptic densities of type II afferents leads to an interesting hypothesis that plasticity may occur at this normally weak synapse. Within the 'pearl-chain' postsynaptic structure, nearly half of the slots were found without GluA2 or CtBP2. The extensive postsynaptic structure with weaker GluA2 immunolabeling, as well as less well-organized presynaptic vesicles surrounding the ribbons (Fuchs and Glowatzki, 2015; Weisz et al., 2012) may explain the much weaker synaptic transmission at OHC-type II afferents synapse, compared to the efficient IHC-type I afferents synaptic transmission (Glowatzki and Fuchs, 2002). The weak synaptic transmission is normally insufficient to activate type II afferents, and it may be interesting to study if the empty slots provide sites of receptor insertion, enabling experience-dependent changes of synaptic strength (for example, before and after acoustic damage). Tightly regulated AMPA receptor trafficking in and out of synaptic regions is crucial for synaptic plasticity in central neurons, and this process is NMDAR and calcium/calmodulin dependent (Anggono and Huganir, 2012; Kerchner and Nicoll, 2008). Currently there is no evidence for a role of NMDA receptors in type II afferents, but this may be worth exploring. On the other hand, our work demonstrated large responses of type II afferents mediated by P2X receptors, and such responses might occur during acoustic trauma. P2X receptors could account for substantial calcium entry into the cell upon activation. P2X receptor calcium permeability is comparable with that for NMDA receptors and is much higher than that for AMPA and kainate receptors (Pankratov et al., 2009). P2X receptors might regulate synaptic strength upon brain injury when ATP was released in a pathological

condition. The effect is still controversial due to other factors that may play a role in the process (Fujii, 2004; Yamazaki et al., 2003; Zhang et al., 2006). Some studies showed in central neurons that ATP could promote LTP probably due to the calcium permeability of P2X receptors (Sim et al., 2006; Wang et al., 2004), but other studies showed a negative effect of P2X receptor activation on LTP (Pankratov et al., 2002). The precise mechanism of P2X receptor mediated plasticity change is still elusive.

5.2 Type II afferents as nociceptive fibers

While synaptic transmission from each OHC triggers single vesicular release and causes an average EPSP of only ~4mV (Weisz et al., 2012), direct application of ATP strongly depolarized type II afferents (~30mV) that made the fiber cross the firing threshold (Weisz et al., 2009). ATP can be released into cochlear fluid after mechanical or hypotonic stress (even without outer hair cell ablation) *in vitro* (Zhao et al., 2005) or noise exposure *in vivo* (Munoz et al., 2001). ATP concentration increase in the cochlea is not only caused by the damage to neural and non-neural structures (Wong and Ryan, 2015), but also triggers active release of ATP in the organ of Corti by supporting cells. Experimental ablation of OHCs was shown to initiate ATP-dependent calcium waves in nearby Hensen's cells that further triggers release of ATP through their connexin hemi-channels, which lasts for tens of seconds (Anselmi et al., 2008; Gale et al., 2004; Lahne and Gale, 2010; Piazza et al., 2007). This enabled a large and long-lasting response caused by ATP recorded in type II afferents. Our work is the first to show the coexistence of the ionotropic P2X mechanism and the metabotropic P2Y pathway in type II cochlear

afferents. P2X2 receptors have been located to the postsynaptic junction in the OHC

region in adult guinea pig (Housley et al., 1999), and P2Y2 receptors have been identified

in a small population of spiral ganglion neurons but their identity was not confirmed

anatomically (Huang et al., 2010). It may be interesting to further investigate the

subcellular localization of purinergic receptors in type II afferents. The distribution of

these receptors may define a 'nociceptive receptive field' of type II afferents, that is, the

frequency range of the cochlea spiral that is monitored by each type II afferent fiber. In

our experiments, sequential cell ablation started from the 15th OHC apical to the

recording site which is usually located at the terminal of type II afferents' spiral dendrite.

Ablation of these OHCs almost never failed to induce responses in type II afferents,

indicating that the 'nociceptive receptive field' at least covers 15 OHCs from the end of

the fiber. In one study though, ablation of the 20th OHC failed to induce responses but as

the sharp needle advanced closer to the recording site, the damage induced responses

were faithfully recorded from ~15th to 1st OHC ablation. It is known that apical to the

synaptic region, type II afferents traveled at lower levels below the supporting cells with

distance up to 0.5mm away from the OHC base (Berglund and Ryugo, 1987; Ginzberg

and Morest, 1983; Perkins and Morest, 1975; Simmons and Liberman, 1988a). This part

of fiber may not be close enough to sense the damage-induced ATP release or may not

express the purinergic receptors. Most of the recordings in this study were made on type

II afferents under row 3 OHCs. It is also unknown if type II afferents under different

OHC rows may have varying size of damage induced responses, since row 3 is closer to

the Hensen's cells region which contains numerous supporting cells with damage induced

calcium waves and the potential to release great amounts of ATP (Anselmi et al., 2008; Gale et al., 2004; Lahne and Gale, 2010; Piazza et al., 2007).

Before hearing onset, type I afferents also can be activated by periodic ATP released from inner supporting cells of Kolliker's organ, generating spontaneous activity that is crucial for cochlear maturation (Tritsch et al., 2010; Tritsch et al., 2007; Wang et al., 2015). This process differs from the ATP-dependent activation of type II afferents in many aspects. First, purinergic signaling between inner supporting cells and the sensory neurons was only observed during a limited period in the immature cochlea. After the onset of hearing (around P12), Kolliker's organ degenerated and the ATP-driven firing of auditory nerves ceased. Second, direct response to ATP was small and insufficient to activate type I afferents. Action potentials in type I afferents were triggered indirectly through synaptic transmission from activated IHCs (Tritsch et al., 2007; Wang et al., 2015). In contrast, type II afferents are insensitive to synaptic transmission from OHCs but strongly activated by direct effects of ATP. These distinctions suggest that type I and type II afferents serve different functional roles. Type I afferents receive inputs from the auditory receptor neurons (IHCs) and convey acoustic information, whereas type II afferents detect trauma via purinergic sensitivity along more extensive dendrites. This is analogous to the somatosensory system that large-diameter, myelinated mechanosensory fibers provide analytical sensation, while small-caliber, unmyelinated C-fibers transmit pain. Similar to the purinergic C-fibers, type II afferents express P2X receptors and can be excited by ATP released during tissue damage (Cook and McCleskey, 2002). Type II afferents have low basal activity at normal conditions (Brown, 1994; Robertson, 1984), a property shared by nociceptors to respond promptly when algogenic agents are present.

127

Finally, KCNQ channels can serve as a potential target for silencing both type II afferents and somatosensory pain fibers (Brown and Passmore, 2009).

To further strengthen this proposal, it is important to know if type I afferents also respond to cell damage, since P2X receptors are expressed in IHCs (Housley et al., 1999; Sugasawa et al., 1996) so that ATP released during cell damage might activate type I afferents by synaptic transmission from IHCs. However, based on current observations, cell-damage induced regenerative calcium wave spread in the OHC region along the cochlear spiral, but barely reached the IHC region (Lahne and Gale, 2010). This might be due to the separation by the tunnel of Corti that may serve as fluid buffer to attenuate the spreading of ATP. This question can be examined by the calcium imaging preparation described in Chapter 4. What is certain at this point is that the normally 'silent' type II afferents (Brown, 1994; Robertson, 1984) may have an increased activity during acoustic damage. This imbalance of type II vs type I inputs to the brainstem may underlie induction of central plasticity changes in pathological conditions such as tinnitus or hyperacusis.

The activation of P2Y-KCNQ pathway may enhance excitability of type II afferents. UTP application reduced the current threshold for spikes to $78.2 \pm 3.5\%$ of that in normal conditions, therefore the effect was mild under these conditions. This is also true for somatosensory fibers. The KCNQ channel blocker XE991 itself did not change the membrane potential of primary afferents, showing a minimal effect when the afferents were at rest (Rivera-Arconada and Lopez-Garcia, 2006). However, the KCNQ effect is greater when cells are depolarized, as when Aδ fibers were activated by thermal

or mechanical stimulation (Brown and Passmore, 2009). Therefore the regulation of excitability may be manifested when type II afferents are activated during acoustic damage or under pathological conditions. Previous studies also reported that sensitivity to ATP is reduced in type II afferents after the onset of hearing (Weisz et al., 2009), consistent with the fact that loud sound is not usually painful to normal ears. However, purinergic signaling in the cochlea is upregulated after noise exposure (Wang et al., 2003), raising the possibility that type II afferents become more sensitive after damage, in part by increased sensitivity to ATP.

5.3 Function of type II afferents

Our results demonstrated that type II afferents can be activated by acoustic damage. In support of this finding, recent work has shown that damaging sound increased activity-dependent c-Fos expression in the granule cell region of the cochlear nucleus (Flores et al., 2015), the presumed target of type II afferents in the auditory brainstem identified by morphological studies (Benson and Brown, 2004; Brown et al., 1988a; Brown and Ledwith, 1990; Brown et al., 1988b; Hurd et al., 1999). In this study, a Vglut3-/- mouse line was used to silence the IHC-type I pathway whereas the type II afferents pathway may be preserved. However, these mice did not show avoidance to noise even with high sound pressure levels that damaged OHCs, therefore inconclusive for a role of type II afferents in sensing acoustic trauma (Flores et al., 2015). A previous study also showed lack of startle reflexes to sound in Vglut3-/- mice (Seal et al., 2008). More effort is needed to find out the proper behavioral paradigm that reveals the function

of type II afferent pathway. It also has been suggested that activation of type II afferents by noise could drive medial olivocochlear efferents to suppress cochlear sensitivity (Froud et al., 2015); although that hypothesis is difficult to reconcile with the fact that medial olivocochlear efferents have acoustic tuning and sensitivity similar to those of type I afferents (Liberman and Brown, 1986). This conclusion was controversial also because the peripherin-/- mice used in this study may affect both type II and type I afferents, at least found in early development (Hafidi et al., 1993). A more specific marker is desired to isolate the function of type II afferents.

If type II afferents are nociceptors then that information should reach central targets mediating withdrawal, or nocifensive behavior, distinct from the standard auditory pathways through inferior colliculus to medial geniculate that serve cognitive hearing. Type I and type II axons arborize in parallel to the dorsal and ventral cochlear nuclei in the brainstem; but only type II endings are found within the small cell cap and granule cell layers that envelope the principal nuclei (Benson and Brown, 2004; Brown et al., 1988a; Brown and Ledwith, 1990; Brown et al., 1988b; Hurd et al., 1999). Postsynaptic targets of type II afferents in this area were identified morphologically but without functional evidence. The granule cell domain is thought to be a site for multi-modal integration as well as the target of collaterals from olivocochlear efferents (Benson and Brown, 1990; Benson and Brown, 2004; Brown et al., 1988b; Brown et al., 1991; Paloff and Usunoff, 1992; Shore and Zhou, 2006; Wright and Ryugo, 1996; Zhan and Ryugo, 2007). Whether components of the small cell cap or granule cell layers project to central pain pathways remains to be determined. The central pathway for type II afferents could be determined by the Cre-dependent virus tracing experiments, using a specific mouse

line recently discovered in the lab that labels type II afferents. Such mouse lines also enable selective manipulation of type II afferents, either by channel rhodopsin to examine their postsynaptic target in the auditory brainstem by electrophysiological recordings, or by the chemogenetic tools such as DREADDs (Designer Receptors Exclusively Activated by Designer Drugs) to study the behavioral consequence of activating or silencing the type II afferent pathway.

Noise causes cochlear neuropathy and cell death, reducing cochlear output to the central auditory pathway (Hickox and Liberman, 2014; Wang et al., 2002). Paradoxically, noise exposure has been highly correlated with the 'gain of function' auditory pathologies (Anari et al., 1999; Auerbach et al., 2014; Ince et al., 1987; Kreuzer et al., 2012), such as tinnitus and hyperacusis, where phantom sound is perceived, or loud sound becomes painful despite acoustic responses of the auditory periphery is reduced. The elevated activity of damage-resistant type II afferents (Ryan et al., 1980; Spoendlin, 1971b), like the peripheral sensitization of somatic nociceptors in hyperalgesia(Treede et al., 1992), may contribute to the painful perception in hyperacusis or may be responsible for the induction of central hyperactivity in tinnitus (Auerbach et al., 2014; Eggermont, 2013). A reduction in KCNQ channel activity in central neurons has been shown to be important for tinnitus induction (Li et al., 2013), and systematic administration of KCNQ activators were found to prevent the development of tinnitus in mice (Kalappa et al., 2015; Li et al., 2013) where type II afferents might be silenced among other targets. It will be of interest to examine type II fibers in the adult cochlea to determine if synaptic connections, KCNQ channel expression, purinergic sensitivity, or other aspects of excitability undergo long-

term changes after acoustic trauma, which may provide insights for therapeutic targets to treat hyperacusis and other sequelae of hearing loss.

Bibliography

Abbracchio, M. P., Burnstock, G., Boeynaems, J. M., Barnard, E. A., Boyer, J. L., Kennedy, C., Knight, G. E., Fumagalli, M., Gachet, C., Jacobson, K. A., and Weisman, G. A. (2006). International Union of Pharmacology LVIII: update on the P2Y G protein-coupled nucleotide receptors: from molecular mechanisms and pathophysiology to therapy. Pharmacol Rev *58*, 281-341.

Abbracchio, M. P., Burnstock, G., Verkhratsky, A., and Zimmermann, H. (2009). Purinergic signalling in the nervous system: an overview. Trends Neurosci *32*, 19-29.

Adams, P. R., Brown, D. A., and Constanti, A. (1982). Pharmacological inhibition of the M-current. J Physiol *332*, 223-262.

Akasu, T., Hirai, K., and Koketsu, K. (1983). Modulatory actions of ATP on membrane potentials of bullfrog sympathetic ganglion cells. Brain Res *258*, 313-317.

Anari, M., Axelsson, A., Eliasson, A., and Magnusson, L. (1999). Hypersensitivity to sound--questionnaire data, audiometry and classification. Scand Audiol *28*, 219-230.

Andersson, G., Lindvall, N., Hursti, T., and Carlbring, P. (2002). Hypersensitivity to sound (hyperacusis): a prevalence study conducted via the Internet and post. Int J Audiol *41*, 545-554.

Anggono, V., and Huganir, R. L. (2012). Regulation of AMPA receptor trafficking and synaptic plasticity. Curr Opin Neurobiol *22*, 461-469.

Anselmi, F., Hernandez, V. H., Crispino, G., Seydel, A., Ortolano, S., Roper, S. D., Kessaris, N., Richardson, W., Rickheit, G., Filippov, M. A., *et al.* (2008). ATP release

through connexin hemichannels and gap junction transfer of second messengers propagate Ca2+ signals across the inner ear. Proc Natl Acad Sci U S A *105*, 18770-18775.

Auerbach, B. D., Rodrigues, P. V., and Salvi, R. J. (2014). Central gain control in tinnitus and hyperacusis. Front Neurol *5*, 206.

Balannik, V., Menniti, F. S., Paternain, A. V., Lerma, J., and Stern-Bach, Y. (2005). Molecular mechanism of AMPA receptor noncompetitive antagonism. Neuron *48*, 279-288.

Barclay, M., Julien, J. P., Ryan, A. F., and Housley, G. D. (2010). Type III intermediate filament peripherin inhibits neuritogenesis in type II spiral ganglion neurons in vitro. Neurosci Lett *478*, 51-55.

Barclay, M., Ryan, A. F., and Housley, G. D. (2011). Type I vs type II spiral ganglion neurons exhibit differential survival and neuritogenesis during cochlear development. Neural Dev *6*, 33.

Beisel, K. W., Nelson, N. C., Delimont, D. C., and Fritzsch, B. (2000). Longitudinal gradients of KCNQ4 expression in spiral ganglion and cochlear hair cells correlate with progressive hearing loss in DFNA2. Brain Res Mol Brain Res *82*, 137-149.

Benson, T. E., and Brown, M. C. (1990). Synapses formed by olivocochlear axon branches in the mouse cochlear nucleus. J Comp Neurol *295*, 52-70.

Benson, T. E., and Brown, M. C. (2004). Postsynaptic targets of type II auditory nerve fibers in the cochlear nucleus. J Assoc Res Otolaryngol *5*, 111-125.

Berglund, A. M., Benson, T. E., and Brown, M. C. (1996). Synapses from labeled type II axons in the mouse cochlear nucleus. Hear Res *94*, 31-46.

Berglund, A. M., and Brown, M. C. (1994). Central trajectories of type II spiral ganglion cells from various cochlear regions in mice. Hear Res *75*, 121-130.

Berglund, A. M., and Ryugo, D. K. (1986). A monoclonal antibody labels type II neurons of the spiral ganglion. Brain Res *383*, 327-332.

Berglund, A. M., and Ryugo, D. K. (1987). Hair cell innervation by spiral ganglion neurons in the mouse. J Comp Neurol *255*, 560-570.

Berglund, A. M., and Ryugo, D. K. (1991). Neurofilament antibodies and spiral ganglion neurons of the mammalian cochlea. J Comp Neurol *306*, 393-408.

Bernard, P. A., and Spoendlin, H. (1973). Unmyelinated fibers in the cochlea. JFORL J Fr Otorhinolaryngol Audiophonol Chir Maxillofac *22*, 39-42.

Beurg, M., Safieddine, S., Roux, I., Bouleau, Y., Petit, C., and Dulon, D. (2008). Calcium- and otoferlin-dependent exocytosis by immature outer hair cells. J Neurosci *28*, 1798-1803.

Beutner, D., and Moser, T. (2001). The presynaptic function of mouse cochlear inner hair cells during development of hearing. J Neurosci *21*, 4593-4599.

Beutner, D., Voets, T., Neher, E., and Moser, T. (2001). Calcium dependence of exocytosis and endocytosis at the cochlear inner hair cell afferent synapse. Neuron *29*, 681-690.

Blackburn-Munro, G., and Jensen, B. S. (2003). The anticonvulsant retigabine attenuates nociceptive behaviours in rat models of persistent and neuropathic pain. Eur J Pharmacol *460*, 109-116.

Bland-Ward, P. A., and Humphrey, P. P. (1997). Acute nociception mediated by hindpaw P2X receptor activation in the rat. Br J Pharmacol *122*, 365-371.

Bleehen, T., and Keele, C. A. (1977). Observations on the algogenic actions of adenosine compounds on the human blister base preparation. Pain *3*, 367-377.

Bodin, P., and Burnstock, G. (2001). Purinergic signalling: ATP release. Neurochem Res *26*, 959-969.

Bradbury, E. J., Burnstock, G., and McMahon, S. B. (1998). The expression of P2X3 purinoreceptors in sensory neurons: effects of axotomy and glial-derived neurotrophic factor. Mol Cell Neurosci *12*, 256-268.

Brandstatter, J. H., Dick, O., and Boeckers, T. M. (2004). The postsynaptic scaffold proteins ProSAP1/Shank2 and Homer1 are associated with glutamate receptor complexes at rat retinal synapses. J Comp Neurol *475*, 551-563.

Brandt, A., Striessnig, J., and Moser, T. (2003). CaV1.3 channels are essential for development and presynaptic activity of cochlear inner hair cells. J Neurosci *23*, 10832-10840.

Brandy, W. T., and Lynn, J. M. (1995). Audiologic Findings in Hyperacusic and Nonhyperacusic Subjects. Am J Audiol *4*, 46-51.

Brask, T. (1979). The noise protection effect of the stapedius reflex. Acta Otolaryngol Suppl *360*, 116-117.

Brawer, J. R., and Morest, D. K. (1975). Relations between auditory nerve endings and cell types in the cat's anteroventral cochlear nucleus seen with the Golgi method and Nomarski optics. J Comp Neurol *160*, 491-506.

Brown, D. A. (1988). M currents. Ion Channels *1*, 55-94.

Brown, D. A., and Adams, P. R. (1980). Muscarinic suppression of a novel voltage-sensitive K+ current in a vertebrate neurone. Nature *283*, 673-676.

Brown, D. A., and Passmore, G. M. (2009). Neural KCNQ (Kv7) channels. Br J Pharmacol *156*, 1185-1195.

Brown, M. C. (1987a). Morphology of labeled afferent fibers in the guinea pig cochlea. J Comp Neurol *260*, 591-604.

Brown, M. C. (1987b). Morphology of labeled efferent fibers in the guinea pig cochlea. J Comp Neurol *260*, 605-618.

Brown, M. C. (1994). Antidromic responses of single units from the spiral ganglion. J Neurophysiol *71*, 1835-1847.

Brown, M. C., Berglund, A. M., Kiang, N. Y., and Ryugo, D. K. (1988a). Central trajectories of type II spiral ganglion neurons. J Comp Neurol *278*, 581-590.

Brown, M. C., and Ledwith, J. V., 3rd (1990). Projections of thin (type-II) and thick (type-I) auditory-nerve fibers into the cochlear nucleus of the mouse. Hear Res *49*, 105-118.

Brown, M. C., Liberman, M. C., Benson, T. E., and Ryugo, D. K. (1988b). Brainstem branches from olivocochlear axons in cats and rodents. J Comp Neurol *278*, 591-603.

Brown, M. C., Pierce, S., and Berglund, A. M. (1991). Cochlear-nucleus branches of thick (medial) olivocochlear fibers in the mouse: a cochleotopic projection. J Comp Neurol *303*, 300-315.

Burgard, E. C., Niforatos, W., van Biesen, T., Lynch, K. J., Touma, E., Metzger, R. E., Kowaluk, E. A., and Jarvis, M. F. (1999). P2X receptor-mediated ionic currents in dorsal root ganglion neurons. J Neurophysiol *82*, 1590-1598.

Burgess, B. J., Adams, J. C., and Nadol, J. B., Jr. (1997). Morphologic evidence for innervation of Deiters' and Hensen's cells in the guinea pig. Hear Res *108*, 74-82.

Burnstock, G. (2009). Purinergic receptors and pain. Curr Pharm Des *15*, 1717-1735.

Burnstock, G. (2013). Purinergic mechanisms and pain--an update. Eur J Pharmacol *716*, 24-40.

Castillo, P. E., Malenka, R. C., and Nicoll, R. A. (1997). Kainate receptors mediate a slow postsynaptic current in hippocampal CA3 neurons. Nature *388*, 182-186.

Chen, C. C., Akopian, A. N., Sivilotti, L., Colquhoun, D., Burnstock, G., and Wood, J. N. (1995). A P2X purinoceptor expressed by a subset of sensory neurons. Nature *377*, 428-431.

Chen, Z., Peppi, M., Kujawa, S. G., and Sewell, W. F. (2009). Regulated expression of surface AMPA receptors reduces excitotoxicity in auditory neurons. J Neurophysiol *102*, 1152-1159.

Cockayne, D. A., Dunn, P. M., Zhong, Y., Rong, W., Hamilton, S. G., Knight, G. E., Ruan, H. Z., Ma, B., Yip, P., Nunn, P*., et al.* (2005). P2X2 knockout mice and P2X2/P2X3 double knockout mice reveal a role for the P2X2 receptor subunit in mediating multiple sensory effects of ATP. J Physiol *567*, 621-639.

Colledge, M., Dean, R. A., Scott, G. K., Langeberg, L. K., Huganir, R. L., and Scott, J. D. (2000). Targeting of PKA to glutamate receptors through a MAGUK-AKAP complex. Neuron *27*, 107-119.

Collier, H. O., James, G. W., and Schneider, C. (1966). Antagonism by aspirin and fenamates of bronchoconstriction and nociception induced by adenosine-5'-triphosphate. Nature *212*, 411-412.

Cook, S. P., and McCleskey, E. W. (2002). Cell damage excites nociceptors through release of cytosolic ATP. Pain *95*, 41-47.

da Silva, S., Hasegawa, H., Scott, A., Zhou, X., Wagner, A. K., Han, B. X., and Wang, F. (2011). Proper formation of whisker barrelettes requires periphery-derived Smad4-dependent TGF-beta signaling. Proc Natl Acad Sci U S A *108*, 3395-3400.

Dauman, R., and Bouscau-Faure, F. (2005). Assessment and amelioration of hyperacusis in tinnitus patients. Acta Otolaryngol *125*, 503-509.

Delmas, P., and Brown, D. A. (2005). Pathways modulating neural KCNQ/M (Kv7) potassium channels. Nat Rev Neurosci *6*, 850-862.

Dost, R., Rostock, A., and Rundfeldt, C. (2004). The anti-hyperalgesic activity of retigabine is mediated by KCNQ potassium channel activation. Naunyn Schmiedebergs Arch Pharmacol *369*, 382-390.

Dunn, R. A., and Morest, D. K. (1975). Receptor synapses without synaptic ribbons in the cochlea of the cat. Proc Natl Acad Sci U S A *72*, 3599-3603.

Echteler, S. M. (1992). Developmental segregation in the afferent projections to mammalian auditory hair cells. Proc Natl Acad Sci U S A *89*, 6324-6327.

Egan, T. M., and Khakh, B. S. (2004). Contribution of calcium ions to P2X channel responses. J Neurosci *24*, 3413-3420.

Eggermont, J. J. (2013). Hearing loss, hyperacusis, or tinnitus: what is modeled in animal research? Hear Res *295*, 140-149.

El-Husseini, A. E., Schnell, E., Chetkovich, D. M., Nicoll, R. A., and Bredt, D. S. (2000). PSD-95 involvement in maturation of excitatory synapses. Science *290*, 1364-1368.

Eybalin, M. (1993). Neurotransmitters and neuromodulators of the mammalian cochlea. Physiol Rev *73*, 309-373.

Eybalin, M., Caicedo, A., Renard, N., Ruel, J., and Puel, J. L. (2004). Transient Ca2+-permeable AMPA receptors in postnatal rat primary auditory neurons. Eur J Neurosci *20*, 2981-2989.

Fechner, F. P., Burgess, B. J., Adams, J. C., Liberman, M. C., and Nadol, J. B., Jr. (1998). Dense innervation of Deiters' and Hensen's cells persists after chronic deefferentation of guinea pig cochleas. J Comp Neurol *400*, 299-309.

Fechner, F. P., Nadol, J. J., Burgess, B. J., and Brown, M. C. (2001). Innervation of supporting cells in the apical turns of the guinea pig cochlea is from type II afferent fibers. J Comp Neurol *429*, 289-298.

Fekete, D. M., Rouiller, E. M., Liberman, M. C., and Ryugo, D. K. (1984). The central projections of intracellularly labeled auditory nerve fibers in cats. J Comp Neurol *229*, 432-450.

Ferrari, D., Los, M., Bauer, M. K., Vandenabeele, P., Wesselborg, S., and Schulze-Osthoff, K. (1999). P2Z purinoreceptor ligation induces activation of

caspases with distinct roles in apoptotic and necrotic alterations of cell death. FEBS Lett *447*, 71-75.

Flores-Otero, J., and Davis, R. L. (2011). Synaptic proteins are tonotopically graded in postnatal and adult type I and type II spiral ganglion neurons. J Comp Neurol *519*, 1455-1475.

Flores, E. N., Duggan, A., Madathany, T., Hogan, A. K., Marquez, F. G., Kumar, G., Seal, R. P., Edwards, R. H., Liberman, M. C., and Garcia-Anoveros, J. (2015). A Non-canonical Pathway from Cochlea to Brain Signals Tissue-Damaging Noise. Curr Biol *25*, 606-612.

Francis, H. W., and Nadol, J. B., Jr. (1993). Patterns of innervation of outer hair cells in a chimpanzee: I. Afferent and reciprocal synapses. Hear Res *64*, 184-190.

Frerking, M., Malenka, R. C., and Nicoll, R. A. (1998). Synaptic activation of kainate receptors on hippocampal interneurons. Nat Neurosci *1*, 479-486.

Froud, K. E., Wong, A. C., Cederholm, J. M., Klugmann, M., Sandow, S. L., Julien, J. P., Ryan, A. F., and Housley, G. D. (2015). Type II spiral ganglion afferent neurons drive medial olivocochlear reflex suppression of the cochlear amplifier. Nat Commun *6*, 7115.

Fuchs, P. A. (2005). Time and intensity coding at the hair cell's ribbon synapse. J Physiol *566*, 7-12.

Fuchs, P. A., and Glowatzki, E. (2015). Synaptic studies inform the functional diversity of cochlear afferents. Hear Res *330*, 18-25.

Fuchs, P. A., Glowatzki, E., and Moser, T. (2003). The afferent synapse of cochlear hair cells. Curr Opin Neurobiol *13*, 452-458.

Fujii, S. (2004). ATP- and adenosine-mediated signaling in the central nervous system: the role of extracellular ATP in hippocampal long-term potentiation. J Pharmacol Sci *94*, 103-106.

Fujikawa, T., Petralia, R. S., Fitzgerald, T. S., Wang, Y. X., Millis, B., Morgado-Diaz, J. A., Kitamura, K., and Kachar, B. (2014). Localization of kainate receptors in inner and outer hair cell synapses. Hear Res *314*, 20-32.

Gale, J. E., Piazza, V., Ciubotaru, C. D., and Mammano, F. (2004). A mechanism for sensing noise damage in the inner ear. Curr Biol *14*, 526-529.

Gerevich, Z., and Illes, P. (2004). P2Y receptors and pain transmission. Purinergic Signal *1*, 3-10.

Ginzberg, R. D., and Morest, D. K. (1983). A study of cochlear innervation in the young cat with the Golgi method. Hear Res *10*, 227-246.

Ginzberg, R. D., and Morest, D. K. (1984). Fine structure of cochlear innervation in the cat. Hear Res *14*, 109-127.

Glowatzki, E., and Fuchs, P. A. (2002). Transmitter release at the hair cell ribbon synapse. Nat Neurosci *5*, 147-154.

Glowatzki, E., Ruppersberg, J. P., Zenner, H. P., and Rusch, A. (1997). Mechanically and ATP-induced currents of mouse outer hair cells are independent and differentially blocked by d-tubocurarine. Neuropharmacology *36*, 1269-1275.

Gonzales, E. B., Kawate, T., and Gouaux, E. (2009). Pore architecture and ion sites in acid-sensing ion channels and P2X receptors. Nature *460*, 599-604.

Goutman, J. D., and Glowatzki, E. (2007). Time course and calcium dependence of transmitter release at a single ribbon synapse. Proc Natl Acad Sci U S A *104*, 16341-16346.

Grant, L., Yi, E., and Glowatzki, E. (2010). Two modes of release shape the postsynaptic response at the inner hair cell ribbon synapse. J Neurosci *30*, 4210-4220.

Greenwood, D., Jagger, D. J., Huang, L. C., Hoya, N., Thorne, P. R., Wildman, S. S., King, B. F., Pak, K., Ryan, A. F., and Housley, G. D. (2007). P2X receptor signaling inhibits BDNF-mediated spiral ganglion neuron development in the neonatal rat cochlea. Development *134*, 1407-1417.

Guinan, J. J., Jr. (2006). Olivocochlear efferents: anatomy, physiology, function, and the measurement of efferent effects in humans. Ear Hear *27*, 589-607.

Guo, C., Masin, M., Qureshi, O. S., and Murrell-Lagnado, R. D. (2007). Evidence for functional P2X4/P2X7 heteromeric receptors. Mol Pharmacol *72*, 1447-1456.

Hafidi, A. (1998). Peripherin-like immunoreactivity in type II spiral ganglion cell body and projections. Brain Res *805*, 181-190.

Hafidi, A., Despres, G., and Romand, R. (1990). Cochlear innervation in the developing rat: an immunocytochemical study of neurofilament and spectrin proteins. J Comp Neurol *300*, 153-161.

Hafidi, A., Despres, G., and Romand, R. (1993). Ontogenesis of type II spiral ganglion neurons during development: peripherin immunohistochemistry. Int J Dev Neurosci *11*, 507-512.

Hafidi, A., and Dulon, D. (2004). Developmental expression of Ca(v)1.3 (alpha1d) calcium channels in the mouse inner ear. Brain Res Dev Brain Res *150*, 167-175.

Hamernik, R. P., Turrentine, G., and Wright, C. G. (1984). Surface morphology of the inner sulcus and related epithelial cells of the cochlea following acoustic trauma. Hear Res *16*, 143-160.

Hamilton, S. G., McMahon, S. B., and Lewin, G. R. (2001). Selective activation of nociceptors by P2X receptor agonists in normal and inflamed rat skin. J Physiol *534*, 437-445.

Hamilton, S. G., Wade, A., and McMahon, S. B. (1999). The effects of inflammation and inflammatory mediators on nociceptive behaviour induced by ATP analogues in the rat. Br J Pharmacol *126*, 326-332.

Harms, K. J., and Craig, A. M. (2005). Synapse composition and organization following chronic activity blockade in cultured hippocampal neurons. J Comp Neurol *490*, 72-84.

Hashimoto, S., and Kimura, R. S. (1988). Computer-aided three-dimensional reconstruction and morphometry of the outer hair cells of the guinea pig cochlea. Acta Otolaryngol *105*, 64-74.

Hattori, M., and Gouaux, E. (2012). Molecular mechanism of ATP binding and ion channel activation in P2X receptors. Nature *485*, 207-212.

Heller, A. J. (2003). Classification and epidemiology of tinnitus. Otolaryngol Clin North Am *36*, 239-248.

Hernandez, C. C., Zaika, O., and Shapiro, M. S. (2008). A carboxy-terminal inter-helix linker as the site of phosphatidylinositol 4,5-bisphosphate action on Kv7 (M-type) K+ channels. J Gen Physiol *132*, 361-381.

Hickox, A. E., and Liberman, M. C. (2014). Is noise-induced cochlear neuropathy key to the generation of hyperacusis or tinnitus? J Neurophysiol *111*, 552-564.

Hirbec, H., Francis, J. C., Lauri, S. E., Braithwaite, S. P., Coussen, F., Mulle, C., Dev, K. K., Coutinho, V., Meyer, G., Isaac, J. T.*, et al.* (2003). Rapid and differential regulation of AMPA and kainate receptors at hippocampal mossy fibre synapses by PICK1 and GRIP. Neuron *37*, 625-638.

Hollmann, M., Hartley, M., and Heinemann, S. (1991). Ca2+ permeability of KA-AMPA--gated glutamate receptor channels depends on subunit composition. Science *252*, 851-853.

Housley, G. D., Bringmann, A., and Reichenbach, A. (2009). Purinergic signaling in special senses. Trends Neurosci *32*, 128-141.

Housley, G. D., Greenwood, D., and Ashmore, J. F. (1992). Localization of cholinergic and purinergic receptors on outer hair cells isolated from the guinea-pig cochlea. Proc R Soc Lond B Biol Sci *249*, 265-273.

Housley, G. D., Kanjhan, R., Raybould, N. P., Greenwood, D., Salih, S. G., Jarlebark, L., Burton, L. D., Setz, V. C., Cannell, M. B., Soeller, C.*, et al.* (1999). Expression of the P2X(2) receptor subunit of the ATP-gated ion channel in the cochlea: implications for sound transduction and auditory neurotransmission. J Neurosci *19*, 8377-8388.

Housley, G. D., Morton-Jones, R., Vlajkovic, S. M., Telang, R. S., Paramananthasivam, V., Tadros, S. F., Wong, A. C., Froud, K. E., Cederholm, J. M., Sivakumaran, Y., *et al.* (2013). ATP-gated ion channels mediate adaptation to elevated sound levels. Proc Natl Acad Sci U S A *110*, 7494-7499.

Housley, G. D., Raybould, N. P., and Thorne, P. R. (1998). Fluorescence imaging of Na+ influx via P2X receptors in cochlear hair cells. Hear Res *119*, 1-13.

Housley, G. D., and Ryan, A. F. (1997). Cholinergic and purinergic neurohumoral signalling in the inner ear: a molecular physiological analysis. Audiol Neurootol *2*, 92-110.

Hu, B. H., Henderson, D., and Nicotera, T. M. (2006). Extremely rapid induction of outer hair cell apoptosis in the chinchilla cochlea following exposure to impulse noise. Hear Res *211*, 16-25.

Hu, B. H., and Zheng, G. L. (2008). Membrane disruption: an early event of hair cell apoptosis induced by exposure to intense noise. Brain Res *1239*, 107-118.

Huang, L. C., Barclay, M., Lee, K., Peter, S., Housley, G. D., Thorne, P. R., and Montgomery, J. M. (2012). Synaptic profiles during neurite extension, refinement and retraction in the developing cochlea. Neural Dev *7*, 38.

Huang, L. C., Greenwood, D., Thorne, P. R., and Housley, G. D. (2005). Developmental regulation of neuron-specific P2X3 receptor expression in the rat cochlea. J Comp Neurol *484*, 133-143.

Huang, L. C., Thorne, P. R., Housley, G. D., and Montgomery, J. M. (2007a). Spatiotemporal definition of neurite outgrowth, refinement and retraction in the developing mouse cochlea. Development.

Huang, L. C., Thorne, P. R., Housley, G. D., and Montgomery, J. M. (2007b). Spatiotemporal definition of neurite outgrowth, refinement and retraction in the developing mouse cochlea. Development *134*, 2925-2933.

Huang, L. C., Thorne, P. R., Vlajkovic, S. M., and Housley, G. D. (2010). Differential expression of P2Y receptors in the rat cochlea during development. Purinergic Signal *6*, 231-248.

Hurd, L. B., Hutson, K. A., and Morest, D. K. (1999). Cochlear nerve projections to the small cell shell of the cochlear nucleus: the neuroanatomy of extremely thin sensory axons. Synapse *33*, 83-117.

Ince, L. P., Greene, R. Y., Alba, A., and Zaretsky, H. H. (1987). A matching-to-sample feedback technique for training self-control of tinnitus. Health Psychol *6*, 173-182.

Ippolito, D. L., Xu, M., Bruchas, M. R., Wickman, K., and Chavkin, C. (2005). Tyrosine phosphorylation of K(ir)3.1 in spinal cord is induced by acute inflammation, chronic neuropathic pain, and behavioral stress. J Biol Chem *280*, 41683-41693.

Ito, K., and Dulon, D. (2002). Nonselective cation conductance activated by muscarinic and purinergic receptors in rat spiral ganglion neurons. Am J Physiol Cell Physiol *282*, C1121-1135.

Ives, J. H., Fung, S., Tiwari, P., Payne, H. L., and Thompson, C. L. (2004). Microtubule-associated protein light chain 2 is a stargazin-AMPA receptor complex-interacting protein in vivo. J Biol Chem *279*, 31002-31009.

Jarlebark, L. E., Housley, G. D., and Thorne, P. R. (2000). Immunohistochemical localization of adenosine 5'-triphosphate-gated ion channel P2X(2) receptor subunits in adult and developing rat cochlea. J Comp Neurol *421*, 289-301.

Jin, Z., Liang, G. H., Cooper, E. C., and Jarlebark, L. (2009). Expression and localization of K channels KCNQ2 and KCNQ3 in the mammalian cochlea. Audiol Neurootol *14*, 98-105.

Johnson, S. L., Beurg, M., Marcotti, W., and Fettiplace, R. (2011). Prestin-driven cochlear amplification is not limited by the outer hair cell membrane time constant. Neuron *70*, 1143-1154.

Junger, W. G. (2011). Immune cell regulation by autocrine purinergic signalling. Nat Rev Immunol *11*, 201-212.

Kalappa, B. I., Soh, H., Duignan, K. M., Furuya, T., Edwards, S., Tzingounis, A. V., and Tzounopoulos, T. (2015). Potent KCNQ2/3-Specific Channel Activator Suppresses In Vivo Epileptic Activity and Prevents the Development of Tinnitus. J Neurosci *35*, 8829-8842.

Kawate, T., Michel, J. C., Birdsong, W. T., and Gouaux, E. (2009). Crystal structure of the ATP-gated P2X(4) ion channel in the closed state. Nature *460*, 592-598.

Kerchner, G. A., and Nicoll, R. A. (2008). Silent synapses and the emergence of a postsynaptic mechanism for LTP. Nat Rev Neurosci *9*, 813-825.

Kerr, A. G., and Byrne, J. E. (1975). Surgery of violence. IV. Blast injuries of the ear. Br Med J *1*, 559-561.

Kew, J. N., and Kemp, J. A. (2005). Ionotropic and metabotropic glutamate receptor structure and pharmacology. Psychopharmacology (Berl) *179*, 4-29.

Khakh, B. S., Zhou, X., Sydes, J., Galligan, J. J., and Lester, H. A. (2000). State-dependent cross-inhibition between transmitter-gated cation channels. Nature *406*, 405-410.

Kharkovets, T., Hardelin, J. P., Safieddine, S., Schweizer, M., El-Amraoui, A., Petit, C., and Jentsch, T. J. (2000). KCNQ4, a K+ channel mutated in a form of dominant deafness, is expressed in the inner ear and the central auditory pathway. Proc Natl Acad Sci U S A *97*, 4333-4338.

Khimich, D., Nouvian, R., Pujol, R., Tom Dieck, S., Egner, A., Gundelfinger, E. D., and Moser, T. (2005). Hair cell synaptic ribbons are essential for synchronous auditory signalling. Nature *434*, 889-894.

Kiang, N. Y., Rho, J. M., Northrop, C. C., Liberman, M. C., and Ryugo, D. K. (1982). Hair-cell innervation by spiral ganglion cells in adult cats. Science *217*, 175-177.

Knipper, M., Kopschall, I., Rohbock, K., Kopke, A. K., Bonk, I., Zimmermann, U., and Zenner, H. (1997a). Transient expression of NMDA receptors during rearrangement of AMPA- receptor-expressing fibers in the developing inner ear. Cell Tissue Res *287*, 23-41.

Knipper, M., Kopschall, I., Rohbock, K., Kopke, A. K., Bonk, I., Zimmermann, U., and Zenner, H. (1997b). Transient expression of NMDA receptors during rearrangement of AMPA-receptor-expressing fibers in the developing inner ear. Cell Tissue Res *287*, 23-41.

149

Knirsch, M., Brandt, N., Braig, C., Kuhn, S., Hirt, B., Munkner, S., Knipper, M., and Engel, J. (2007). Persistence of Ca(v)1.3 Ca2+ channels in mature outer hair cells supports outer hair cell afferent signaling. J Neurosci *27*, 6442-6451.

Kobayashi, K., Fukuoka, T., Yamanaka, H., Dai, Y., Obata, K., Tokunaga, A., and Noguchi, K. (2006). Neurons and glial cells differentially express P2Y receptor mRNAs in the rat dorsal root ganglion and spinal cord. J Comp Neurol *498*, 443-454.

Kong, Q., Wang, M., Liao, Z., Camden, J. M., Yu, S., Simonyi, A., Sun, G. Y., Gonzalez, F. A., Erb, L., Seye, C. I., and Weisman, G. A. (2005). P2X(7) nucleotide receptors mediate caspase-8/9/3-dependent apoptosis in rat primary cortical neurons. Purinergic Signal *1*, 337-347.

Koundakjian, E. J., Appler, J. L., and Goodrich, L. V. (2007). Auditory neurons make stereotyped wiring decisions before maturation of their targets. J Neurosci *27*, 14078-14088.

Kreuzer, P. M., Landgrebe, M., Schecklmann, M., Staudinger, S., and Langguth, B. (2012). Trauma-associated tinnitus: audiological, demographic and clinical characteristics. PLoS One *7*, e45599.

Kubisch, C., Schroeder, B. C., Friedrich, T., Lutjohann, B., El-Amraoui, A., Marlin, S., Petit, C., and Jentsch, T. J. (1999). KCNQ4, a novel potassium channel expressed in sensory outer hair cells, is mutated in dominant deafness. Cell *96*, 437-446.

Kujawa, S. G., and Liberman, M. C. (2009). Adding insult to injury: cochlear nerve degeneration after "temporary" noise-induced hearing loss. J Neurosci *29*, 14077-14085.

Lahne, M., and Gale, J. E. (2008). Damage-induced activation of ERK1/2 in cochlear supporting cells is a hair cell death-promoting signal that depends on extracellular ATP and calcium. J Neurosci *28*, 4918-4928.

Lahne, M., and Gale, J. E. (2010). Damage-induced cell-cell communication in different cochlear cell types via two distinct ATP-dependent Ca waves. Purinergic Signal *6*, 189-200.

Lang, P. M., Fleckenstein, J., Passmore, G. M., Brown, D. A., and Grafe, P. (2008). Retigabine reduces the excitability of unmyelinated peripheral human axons. Neuropharmacology *54*, 1271-1278.

Lariviere, R. C., Nguyen, M. D., Ribeiro-da-Silva, A., and Julien, J. P. (2002). Reduced number of unmyelinated sensory axons in peripherin null mice. J Neurochem *81*, 525-532.

Lazarowski, E. R. (2012). Vesicular and conductive mechanisms of nucleotide release. Purinergic Signal *8*, 359-373.

Lazzaro, J. T., Paternain, A. V., Lerma, J., Chenard, B. L., Ewing, F. E., Huang, J., Welch, W. M., Ganong, A. H., and Menniti, F. S. (2002). Functional characterization of CP-465,022, a selective, noncompetitive AMPA receptor antagonist. Neuropharmacology *42*, 143-153.

Lechner, S. G., and Boehm, S. (2004). Regulation of neuronal ion channels via P2Y receptors. Purinergic Signal *1*, 31-41.

Lenzi, D., and von Gersdorff, H. (2001). Structure suggests function: the case for synaptic ribbons as exocytotic nanomachines. Bioessays *23*, 831-840.

Lerma, J., and Marques, J. M. (2013). Kainate receptors in health and disease. Neuron *80*, 292-311.

Lewis, C., Neidhart, S., Holy, C., North, R. A., Buell, G., and Surprenant, A. (1995). Coexpression of P2X2 and P2X3 receptor subunits can account for ATP-gated currents in sensory neurons. Nature *377*, 432-435.

Li, S., Choi, V., and Tzounopoulos, T. (2013). Pathogenic plasticity of Kv7.2/3 channel activity is essential for the induction of tinnitus. Proc Natl Acad Sci U S A *110*, 9980-9985.

Liberman, L. D., Wang, H., and Liberman, M. C. (2011). Opposing gradients of ribbon size and AMPA receptor expression underlie sensitivity differences among cochlear-nerve/hair-cell synapses. J Neurosci *31*, 801-808.

Liberman, M. C. (1978). Auditory-nerve response from cats raised in a low-noise chamber. J Acoust Soc Am *63*, 442-455.

Liberman, M. C. (1982). The cochlear frequency map for the cat: labeling auditory-nerve fibers of known characteristic frequency. J Acoust Soc Am *72*, 1441-1449.

Liberman, M. C., and Brown, M. C. (1986). Physiology and anatomy of single olivocochlear neurons in the cat. Hear Res *24*, 17-36.

Liberman, M. C., Dodds, L. W., and Pierce, S. (1990). Afferent and efferent innervation of the cat cochlea: quantitative analysis with light and electron microscopy. J Comp Neurol *301*, 443-460.

Liberman, M. C., and Kiang, N. Y. (1978). Acoustic trauma in cats. Cochlear pathology and auditory-nerve activity. Acta Otolaryngol Suppl *358*, 1-63.

Luscher, C., and Slesinger, P. A. (2010). Emerging roles for G protein-gated inwardly rectifying potassium (GIRK) channels in health and disease. Nat Rev Neurosci *11*, 301-315.

Lutz, S., Freichel-Blomquist, A., Yang, Y., Rumenapp, U., Jakobs, K. H., Schmidt, M., and Wieland, T. (2005). The guanine nucleotide exchange factor p63RhoGEF, a specific link between Gq/11-coupled receptor signaling and RhoA. J Biol Chem *280*, 11134-11139.

Lv, P., Wei, D., and Yamoah, E. N. (2010). Kv7-type channel currents in spiral ganglion neurons: involvement in sensorineural hearing loss. J Biol Chem *285*, 34699-34707.

Malin, S. A., Davis, B. M., Koerber, H. R., Reynolds, I. J., Albers, K. M., and Molliver, D. C. (2008). Thermal nociception and TRPV1 function are attenuated in mice lacking the nucleotide receptor P2Y2. Pain *138*, 484-496.

Mammano, F., and Ashmore, J. F. (1996). Differential expression of outer hair cell potassium currents in the isolated cochlea of the guinea-pig. J Physiol *496 (Pt 3)*, 639-646.

Mammano, F., Frolenkov, G. I., Lagostena, L., Belyantseva, I. A., Kurc, M., Dodane, V., Colavita, A., and Kachar, B. (1999a). ATP-Induced Ca(2+) release in cochlear outer hair cells: localization of an inositol triphosphate-gated Ca(2+) store to the base of the sensory hair bundle. J Neurosci *19*, 6918-6929.

Mammano, F., Frolenkov, G. I., Lagostena, L., Belyantseva, I. A., Kurc, M., Dodane, V., Colavita, A., and Kachar, B. (1999b). ATP-Induced Ca(2+) release in

cochlear outer hair cells: localization of an inositol triphosphate-gated Ca(2+) store to the base of the sensory hair bundle. J Neurosci *19*, 6918-6929.

Marcotti, W., and Kros, C. J. (1999). Developmental expression of the potassium current IK,n contributes to maturation of mouse outer hair cells. J Physiol *520 Pt 3*, 653-660.

Matsubara, A., Laake, J. H., Davanger, S., Usami, S., and Ottersen, O. P. (1996a). Organization of AMPA receptor subunits at a glutamate synapse: A quantitative immunogold analysis of hair cell synapses in the rat organ of Corti. J Neurosci *16*, 4457-4467.

Matsubara, A., Laake, J. H., Davanger, S., Usami, S., and Ottersen, O. P. (1996b). Organization of AMPA receptor subunits at a glutamate synapse: a quantitative immunogold analysis of hair cell synapses in the rat organ of Corti. J Neurosci *16*, 4457-4467.

Matsubara, A., Takumi, Y., Nakagawa, T., Usami, S., Shinkawa, H., and Ottersen, O. P. (1999). Immunoelectron microscopy of AMPA receptor subunits reveals three types of putative glutamatergic synapse in the rat vestibular end organs. Brain Res *819*, 58-64.

McLean, W. J., Smith, K. A., Glowatzki, E., and Pyott, S. J. (2009). Distribution of the Na,K-ATPase alpha subunit in the rat spiral ganglion and organ of corti. J Assoc Res Otolaryngol *10*, 37-49.

Menniti, F. S., Chenard, B. L., Collins, M. B., Ducat, M. F., Elliott, M. L., Ewing, F. E., Huang, J. I., Kelly, K. A., Lazzaro, J. T., Pagnozzi, M. J.*, et al.* (2000). Characterization of the binding site for a novel class of noncompetitive alpha-amino-3-hydroxy-5-

methyl-4-isoxazolepropionic acid receptor antagonists. Mol Pharmacol *58*, 1310-1317.

Meyer, A. C., Frank, T., Khimich, D., Hoch, G., Riedel, D., Chapochnikov, N. M., Yarin, Y. M., Harke, B., Hell, S. W., Egner, A., and Moser, T. (2009). Tuning of synapse number, structure and function in the cochlea. Nat Neurosci *12*, 444-453.

Meyers, J. R., MacDonald, R. B., Duggan, A., Lenzi, D., Standaert, D. G., Corwin, J. T., and Corey, D. P. (2003). Lighting up the senses: FM1-43 loading of sensory cells through nonselective ion channels. J Neurosci *23*, 4054-4065.

Michna, M., Knirsch, M., Hoda, J. C., Muenkner, S., Langer, P., Platzer, J., Striessnig, J., and Engel, J. (2003). Cav1.3 (alpha1D) Ca2+ currents in neonatal outer hair cells of mice. J Physiol *553*, 747-758.

Mishina, M., Sakimura, K., Mori, H., Kushiya, E., Harabayashi, M., Uchino, S., and Nagahari, K. (1991). A single amino acid residue determines the Ca2+ permeability of AMPA-selective glutamate receptor channels. Biochem Biophys Res Commun *180*, 813-821.

Mockett, B. G., Housley, G. D., and Thorne, P. R. (1994). Fluorescence imaging of extracellular purinergic receptor sites and putative ecto-ATPase sites on isolated cochlear hair cells. J Neurosci *14*, 6992-7007.

Moriyama, T., Iida, T., Kobayashi, K., Higashi, T., Fukuoka, T., Tsumura, H., Leon, C., Suzuki, N., Inoue, K., Gachet, C.*, et al.* (2003). Possible involvement of P2Y2 metabotropic receptors in ATP-induced transient receptor potential vanilloid receptor 1-mediated thermal hypersensitivity. J Neurosci *23*, 6058-6062.

Moser, T., Brandt, A., and Lysakowski, A. (2006). Hair cell ribbon synapses. Cell Tissue Res *326*, 347-359.

Muller, M. (1991a). Developmental changes of frequency representation in the rat cochlea. Hear Res *56*, 1-7.

Muller, M. (1991b). Frequency representation in the rat cochlea. Hear Res *51*, 247-254.

Munoz, D. J., Kendrick, I. S., Rassam, M., and Thorne, P. R. (2001). Vesicular storage of adenosine triphosphate in the guinea-pig cochlear lateral wall and concentrations of ATP in the endolymph during sound exposure and hypoxia. Acta Otolaryngol *121*, 10-15.

Munoz, D. J., Thorne, P. R., Housley, G. D., and Billett, T. E. (1995). Adenosine 5'-triphosphate (ATP) concentrations in the endolymph and perilymph of the guinea-pig cochlea. Hear Res *90*, 119-125.

Nadol, J. B., Jr. (1981). Reciprocal synapses at the base of outer hair cells in the organ of corti of man. Ann Otol Rhinol Laryngol *90*, 12-17.

Nadol, J. B., Jr. (1983). Serial section reconstruction of the neural poles of hair cells in the human organ of Corti. II. outer hair cells. Laryngoscope *93*, 780-791.

Nadol, J. B., Jr. (1988). Comparative anatomy of the cochlea and auditory nerve in mammals. Hear Res *34*, 253-266.

Naisbitt, S., Kim, E., Weinberg, R. J., Rao, A., Yang, F. C., Craig, A. M., and Sheng, M. (1997). Characterization of guanylate kinase-associated protein, a postsynaptic density protein at excitatory synapses that interacts directly with postsynaptic density-95/synapse-associated protein 90. J Neurosci *17*, 5687-5696.

Nakagawa, T., Akaike, N., Kimitsuki, T., Komune, S., and Arima, T. (1990). ATP-induced current in isolated outer hair cells of guinea pig cochlea. J Neurophysiol *63*, 1068-1074.

Nayagam, B. A., Muniak, M. A., and Ryugo, D. K. (2011). The spiral ganglion: connecting the peripheral and central auditory systems. Hear Res *278*, 2-20.

Neef, A., Khimich, D., Pirih, P., Riedel, D., Wolf, F., and Moser, T. (2007). Probing the mechanism of exocytosis at the hair cell ribbon synapse. J Neurosci *27*, 12933-12944.

Nicke, A., Baumert, H. G., Rettinger, J., Eichele, A., Lambrecht, G., Mutschler, E., and Schmalzing, G. (1998). P2X1 and P2X3 receptors form stable trimers: a novel structural motif of ligand-gated ion channels. Embo j *17*, 3016-3028.

Nikolic, P., Housley, G. D., and Thorne, P. R. (2003). Expression of the P2X7 receptor subunit of the adenosine 5'-triphosphate-gated ion channel in the developing and adult rat cochlea. Audiol Neurootol *8*, 28-37.

Nishikawa, S., and Sasaki, F. (1996). Internalization of styryl dye FM1-43 in the hair cells of lateral line organs in Xenopus larvae. J Histochem Cytochem *44*, 733-741.

Nockemann, D., Rouault, M., Labuz, D., Hublitz, P., McKnelly, K., Reis, F. C., Stein, C., and Heppenstall, P. A. (2013). The K(+) channel GIRK2 is both necessary and sufficient for peripheral opioid-mediated analgesia. EMBO Mol Med *5*, 1263-1277.

North, R. A. (2002). Molecular physiology of P2X receptors. Physiol Rev *82*, 1013-1067.

Ocana, M., Cendan, C. M., Cobos, E. J., Entrena, J. M., and Baeyens, J. M. (2004). Potassium channels and pain: present realities and future opportunities. Eur J Pharmacol *500*, 203-219.

Oliver, D., Knipper, M., Derst, C., and Fakler, B. (2003). Resting potential and submembrane calcium concentration of inner hair cells in the isolated mouse cochlea are set by KCNQ-type potassium channels. J Neurosci *23*, 2141-2149.

Paloff, A. M., and Usunoff, K. G. (1992). Projections to the inferior colliculus from the dorsal column nuclei. An experimental electron microscopic study in the cat. J Hirnforsch *33*, 597-610.

Pankratov, Y., Lalo, U., Krishtal, O. A., and Verkhratsky, A. (2009). P2X receptors and synaptic plasticity. Neuroscience *158*, 137-148.

Pankratov, Y., Lalo, U., Verkhratsky, A., and North, R. A. (2006). Vesicular release of ATP at central synapses. Pflugers Arch *452*, 589-597.

Pankratov, Y., Lalo, U., Verkhratsky, A., and North, R. A. (2007). Quantal release of ATP in mouse cortex. J Gen Physiol *129*, 257-265.

Pankratov, Y. V., Lalo, U. V., and Krishtal, O. A. (2002). Role for P2X receptors in long-term potentiation. J Neurosci *22*, 8363-8369.

Passmore, G. M., Selyanko, A. A., Mistry, M., Al-Qatari, M., Marsh, S. J., Matthews, E. A., Dickenson, A. H., Brown, T. A., Burbidge, S. A., Main, M., and Brown, D. A. (2003). KCNQ/M currents in sensory neurons: significance for pain therapy. J Neurosci *23*, 7227-7236.

Paternain, A. V., Morales, M., and Lerma, J. (1995). Selective antagonism of AMPA receptors unmasks kainate receptor-mediated responses in hippocampal neurons. Neuron *14*, 185-189.

Paukert, M., Agarwal, A., Cha, J., Doze, V. A., Kang, J. U., and Bergles, D. E. (2014). Norepinephrine controls astroglial responsiveness to local circuit activity. Neuron *82*, 1263-1270.

Perkins, R. E., and Morest, D. K. (1975). A study of cochlear innervation patterns in cats and rats with the Golgi method and Nomarkski Optics. J Comp Neurol *163*, 129-158.

Piazza, V., Ciubotaru, C. D., Gale, J. E., and Mammano, F. (2007). Purinergic signalling and intercellular Ca2+ wave propagation in the organ of Corti. Cell Calcium *41*, 77-86.

Pillsbury, H. C., 3rd (1996). Lorente de No's "Anatomy of the eighth nerve. I. The central projection of the nerve endings of the internal ear; III. General plan of structure of the primary cochlear nuclei." (Laryngoscope. 1933;43:1-38 & 327-350). Laryngoscope *106*, 533-534.

Rae, M. G., Rowan, E. G., and Kennedy, C. (1998). Pharmacological properties of P2X3-receptors present in neurones of the rat dorsal root ganglia. Br J Pharmacol *124*, 176-180.

Rivera-Arconada, I., and Lopez-Garcia, J. A. (2006). Retigabine-induced population primary afferent hyperpolarisation in vitro. Neuropharmacology *51*, 756-763.

Robbins, J., Marsh, S. J., and Brown, D. A. (2006). Probing the regulation of M (Kv7) potassium channels in intact neurons with membrane-targeted peptides. J Neurosci *26*, 7950-7961.

Roberts, J. A., Vial, C., Digby, H. R., Agboh, K. C., Wen, H., Atterbury-Thomas, A., and Evans, R. J. (2006). Molecular properties of P2X receptors. Pflugers Arch *452*, 486-500.

Robertson, D. (1984). Horseradish peroxidase injection of physiologically characterized afferent and efferent neurones in the guinea pig spiral ganglion. Hear Res *15*, 113-121.

Robertson, D., Sellick, P. M., and Patuzzi, R. (1999). The continuing search for outer hair cell afferents in the guinea pig spiral ganglion. Hear Res *136*, 151-158.

Romand, M. R., and Romand, R. (1987). The ultrastructure of spiral ganglion cells in the mouse. Acta Otolaryngol *104*, 29-39.

Romand, R., and Romand, M. R. (1984). The ontogenesis of pseudomonopolar cells in spiral ganglion of cat and rat. Acta Otolaryngol *97*, 239-249.

Rouiller, E. M., Cronin-Schreiber, R., Fekete, D. M., and Ryugo, D. K. (1986). The central projections of intracellularly labeled auditory nerve fibers in cats: an analysis of terminal morphology. J Comp Neurol *249*, 261-278.

Ruan, H. Z., and Burnstock, G. (2003). Localisation of P2Y1 and P2Y4 receptors in dorsal root, nodose and trigeminal ganglia of the rat. Histochem Cell Biol *120*, 415-426.

Ruel, J., Bobbin, R. P., Vidal, D., Pujol, R., and Puel, J. L. (2000). The selective AMPA receptor antagonist GYKI 53784 blocks action potential generation and excitotoxicity in the guinea pig cochlea. Neuropharmacology *39*, 1959-1973.

Ryan, A. F., Woolf, N. K., and Bone, R. C. (1980). Ultrastructural correlates of selective outer hair cell destruction following kanamycin intoxication in the chinchilla. Hear Res *3*, 335-351.

Ryugo, D. K., and Sento, S. (1991). Synaptic connections of the auditory nerve in cats: relationship between endbulbs of held and spherical bushy cells. J Comp Neurol *305*, 35-48.

Saito, K. (1990). Freeze-fracture organization of hair cell synapses in the sensory epithelium of guinea pig organ of Corti. J Electron Microsc Tech *15*, 173-186.

Salih, S. G., Housley, G. D., Burton, L. D., and Greenwood, D. (1998). P2X2 receptor subunit expression in a subpopulation of cochlear type I spiral ganglion neurones. Neuroreport *9*, 279-282.

Sanada, M., Yasuda, H., Omatsu-Kanbe, M., Sango, K., Isono, T., Matsuura, H., and Kikkawa, R. (2002). Increase in intracellular Ca(2+) and calcitonin gene-related peptide release through metabotropic P2Y receptors in rat dorsal root ganglion neurons. Neuroscience *111*, 413-422.

Sandkuhler, J. (2009). Models and mechanisms of hyperalgesia and allodynia. Physiol Rev *89*, 707-758.

Seal, R. P., Akil, O., Yi, E., Weber, C. M., Grant, L., Yoo, J., Clause, A., Kandler, K., Noebels, J. L., Glowatzki, E.*, et al.* (2008). Sensorineural deafness and seizures in mice lacking vesicular glutamate transporter 3. Neuron *57*, 263-275.

Sheng, M. (1997). Excitatory synapses. Glutamate receptors put in their place. Nature *386*, 221, 223.

Shore, S. E., and Zhou, J. (2006). Somatosensory influence on the cochlear nucleus and beyond. Hear Res *216-217*, 90-99.

Siegel, J. H., and Brownell, W. E. (1981). Presynaptic bodies in outer hair cells of the chinchilla organ of Corti. Brain Res *220*, 188-193.

Sim, J. A., Chaumont, S., Jo, J., Ulmann, L., Young, M. T., Cho, K., Buell, G., North, R. A., and Rassendren, F. (2006). Altered hippocampal synaptic potentiation in P2X4 knock-out mice. J Neurosci *26*, 9006-9009.

Simmons, D. D., and Liberman, M. C. (1988a). Afferent innervation of outer hair cells in adult cats: I. Light microscopic analysis of fibers labeled with horseradish peroxidase. J Comp Neurol *270*, 132-144.

Simmons, D. D., and Liberman, M. C. (1988b). Afferent innervation of outer hair cells in adult cats: II. Electron microscopic analysis of fibers labeled with horseradish peroxidase. J Comp Neurol *270*, 145-154.

Smith, C., and Sjostrand, F. (1961). A synaptic structure in the hair cells of the guinea pig cochlea. J Ultrastruct Res *5*, 184-192.

Sobkowicz, H. M., Slapnick, S. M., and August, B. K. (1993). Presynaptic fibres of spiral neurons and reciprocal synapses in the organ of Corti in culture. J Neurocytol *22*, 979-993.

Sperlagh, B., Heinrich, A., and Csolle, C. (2007). P2 receptor-mediated modulation of neurotransmitter release-an update. Purinergic Signal *3*, 269-284.

Spoendlin, H. (1969). Innervation patterns in the organ of corti of the cat. Acta Otolaryngol *67*, 239-254.

Spoendlin, H. (1971a). Degeneration behaviour of the cochlear nerve. Arch Klin Exp Ohren Nasen Kehlkopfheilkd *200*, 275-291.

Spoendlin, H. (1971b). Primary structural changes in the organ of Corti after acoustic overstimulation. Acta Otolaryngol *71*, 166-176.

Straub, C., Hunt, D. L., Yamasaki, M., Kim, K. S., Watanabe, M., Castillo, P. E., and Tomita, S. (2011). Distinct functions of kainate receptors in the brain are determined by the auxiliary subunit Neto1. Nat Neurosci *14*, 866-873.

Sugasawa, M., Erostegui, C., Blanchet, C., and Dulon, D. (1996). ATP activates non-selective cation channels and calcium release in inner hair cells of the guinea-pig cochlea. J Physiol *491 (Pt 3)*, 707-718.

Suh, B. C., and Hille, B. (2002). Recovery from muscarinic modulation of M current channels requires phosphatidylinositol 4,5-bisphosphate synthesis. Neuron *35*, 507-520.

Suh, B. C., Horowitz, L. F., Hirdes, W., Mackie, K., and Hille, B. (2004). Regulation of KCNQ2/KCNQ3 current by G protein cycling: the kinetics of receptor-mediated signaling by Gq. J Gen Physiol *123*, 663-683.

Suh, B. C., Inoue, T., Meyer, T., and Hille, B. (2006). Rapid chemically induced changes of PtdIns(4,5)P2 gate KCNQ ion channels. Science *314*, 1454-1457.

Szucs, A., Szappanos, H., Toth, A., Farkas, Z., Panyi, G., Csernoch, L., and Sziklai, I. (2004). Differential expression of purinergic receptor subtypes in the outer hair cells of the guinea pig. Hear Res *196*, 2-7.

Thiers, F. A., Burgess, B. J., and Nadol, J. B., Jr. (2002). Axodendritic and dendrodendritic synapses within outer spiral bundles in a human. Hear Res *164*, 97-104.

Thiers, F. A., Nadol, J. B., Jr., and Liberman, M. C. (2008). Reciprocal synapses between outer hair cells and their afferent terminals: evidence for a local neural network in the mammalian cochlea. J Assoc Res Otolaryngol *9*, 477-489.

Treede, R. D., Meyer, R. A., Raja, S. N., and Campbell, J. N. (1992). Peripheral and central mechanisms of cutaneous hyperalgesia. Prog Neurobiol *38*, 397-421.

Tritsch, N. X., Rodriguez-Contreras, A., Crins, T. T., Wang, H. C., Borst, J. G., and Bergles, D. E. (2010). Calcium action potentials in hair cells pattern auditory neuron activity before hearing onset. Nat Neurosci *13*, 1050-1052.

Tritsch, N. X., Yi, E., Gale, J. E., Glowatzki, E., and Bergles, D. E. (2007). The origin of spontaneous activity in the developing auditory system. Nature *450*, 50-55.

Tsantoulas, C., and McMahon, S. B. (2014). Opening paths to novel analgesics: the role of potassium channels in chronic pain. Trends Neurosci *37*, 146-158.

Vignes, M., Clarke, V. R., Parry, M. J., Bleakman, D., Lodge, D., Ornstein, P. L., and Collingridge, G. L. (1998). The GluR5 subtype of kainate receptor regulates excitatory synaptic transmission in areas CA1 and CA3 of the rat hippocampus. Neuropharmacology *37*, 1269-1277.

Vlajkovic, S. M., Housley, G. D., Munoz, D. J., Robson, S. C., Sevigny, J., Wang, C. J., and Thorne, P. R. (2004). Noise exposure induces up-regulation of ecto-nucleoside triphosphate diphosphohydrolases 1 and 2 in rat cochlea. Neuroscience *126*, 763-773.

Vlajkovic, S. M., Thorne, P. R., Munoz, D. J., and Housley, G. D. (1996). Ectonucleotidase activity in the perilymphatic compartment of the guinea pig cochlea. Hear Res *99*, 31-37.

Vlajkovic, S. M., Vinayagamoorthy, A., Thorne, P. R., Robson, S. C., Wang, C. J., and Housley, G. D. (2006). Noise-induced up-regulation of NTPDase3 expression in the rat cochlea: Implications for auditory transmission and cochlear protection. Brain Res *1104*, 55-63.

von Kugelgen, I., and Harden, T. K. (2011). Molecular pharmacology, physiology, and structure of the P2Y receptors. Adv Pharmacol *61*, 373-415.

Wagner, H. J. (1997). Presynaptic bodies ("ribbons"): from ultrastructural observations to molecular perspectives. Cell Tissue Res *287*, 435-446.

Waguespack, J., Salles, F. T., Kachar, B., and Ricci, A. J. (2007). Stepwise morphological and functional maturation of mechanotransduction in rat outer hair cells. J Neurosci *27*, 13890-13902.

Wall, M. J., and Dale, N. (2007). Auto-inhibition of rat parallel fibre-Purkinje cell synapses by activity-dependent adenosine release. J Physiol *581*, 553-565.

Wang, H. C., Lin, C. C., Cheung, R., Zhang-Hooks, Y., Agarwal, A., Ellis-Davies, G., Rock, J., and Bergles, D. E. (2015). Spontaneous Activity of Cochlear Hair Cells Triggered by Fluid Secretion Mechanism in Adjacent Support Cells. Cell *163*, 1348-1359.

Wang, J. C., Raybould, N. P., Luo, L., Ryan, A. F., Cannell, M. B., Thorne, P. R., and Housley, G. D. (2003). Noise induces up-regulation of P2X2 receptor subunit of ATP-gated ion channels in the rat cochlea. Neuroreport *14*, 817-823.

Wang, Q., and Green, S. H. (2011). Functional role of neurotrophin-3 in synapse regeneration by spiral ganglion neurons on inner hair cells after excitotoxic trauma in vitro. J Neurosci *31*, 7938-7949.

Wang, Y., Haughey, N. J., Mattson, M. P., and Furukawa, K. (2004). Dual effects of ATP on rat hippocampal synaptic plasticity. Neuroreport *15*, 633-636.

Wang, Y., Hirose, K., and Liberman, M. C. (2002). Dynamics of noise-induced cellular injury and repair in the mouse cochlea. J Assoc Res Otolaryngol *3*, 248-268.

Wangemann, P. (2006). Supporting sensory transduction: cochlear fluid homeostasis and the endocochlear potential. J Physiol *576*, 11-21.

Weisz, C., Glowatzki, E., and Fuchs, P. (2009). The postsynaptic function of type II cochlear afferents. Nature *461*, 1126-1129.

Weisz, C. J., Glowatzki, E., and Fuchs, P. A. (2014). Excitability of type II cochlear afferents. J Neurosci *34*, 2365-2373.

Weisz, C. J., Lehar, M., Hiel, H., Glowatzki, E., and Fuchs, P. A. (2012). Synaptic transfer from outer hair cells to type II afferent fibers in the rat cochlea. J Neurosci *32*, 9528-9536.

White, P. N., Thorne, P. R., Housley, G. D., Mockett, B., Billett, T. E., and Burnstock, G. (1995). Quinacrine staining of marginal cells in the stria vascularis of the guinea-pig cochlea: a possible source of extracellular ATP? Hear Res *90*, 97-105.

Winks, J. S., Hughes, S., Filippov, A. K., Tatulian, L., Abogadie, F. C., Brown, D. A., and Marsh, S. J. (2005). Relationship between membrane phosphatidylinositol-4,5-bisphosphate and receptor-mediated inhibition of native neuronal M channels. J Neurosci *25*, 3400-3413.

Wittig, J. H., Jr., and Parsons, T. D. (2008). Synaptic ribbon enables temporal precision of hair cell afferent synapse by increasing the number of readily releasable vesicles: a modeling study. J Neurophysiol *100*, 1724-1739.

Wong, A. C., and Ryan, A. F. (2015). Mechanisms of sensorineural cell damage, death and survival in the cochlea. Front Aging Neurosci *7*, 58.

Wright, D. D., and Ryugo, D. K. (1996). Mossy fiber projections from the cuneate nucleus to the cochlear nucleus in the rat. J Comp Neurol *365*, 159-172.

Yamazaki, Y., Kaneko, K., Fujii, S., Kato, H., and Ito, K. (2003). Long-term potentiation and long-term depression induced by local application of ATP to hippocampal CA1 neurons of the guinea pig. Hippocampus *13*, 81-92.

Yan, D., Zhu, Y., Walsh, T., Xie, D., Yuan, H., Sirmaci, A., Fujikawa, T., Wong, A. C., Loh, T. L., Du, L*., et al.* (2013). Mutation of the ATP-gated P2X(2) receptor leads to progressive hearing loss and increased susceptibility to noise. Proc Natl Acad Sci U S A *110*, 2228-2233.

Yang, W. P., Henderson, D., Hu, B. H., and Nicotera, T. M. (2004). Quantitative analysis of apoptotic and necrotic outer hair cells after exposure to different levels of continuous noise. Hear Res *196*, 69-76.

Yegutkin, G. G. (2008). Nucleotide- and nucleoside-converting ectoenzymes: Important modulators of purinergic signalling cascade. Biochim Biophys Acta *1783*, 673-694.

Zhan, X., and Ryugo, D. K. (2007). Projections of the lateral reticular nucleus to the cochlear nucleus in rats. J Comp Neurol *504*, 583-598.

Zhang-Hooks, Y., Agarwal, A., Mishina, M., and Bergles, D. E. (2016). NMDA
Receptors Enhance Spontaneous Activity and Promote Neuronal Survival in the
Developing Cochlea. Neuron *89*, 337-350.

Zhang, H., Craciun, L. C., Mirshahi, T., Rohacs, T., Lopes, C. M., Jin, T., and
Logothetis, D. E. (2003). PIP(2) activates KCNQ channels, and its hydrolysis
underlies receptor-mediated inhibition of M currents. Neuron *37*, 963-975.

Zhang, Y., Deng, P., Li, Y., and Xu, Z. C. (2006). Enhancement of excitatory
synaptic transmission in spiny neurons after transient forebrain ischemia. J
Neurophysiol *95*, 1537-1544.

Zhang, Y. H., Chen, Y., and Zhao, Z. Q. (2001). Alteration of spontaneous firing
rate of primary myelinated afferents by ATP in adjuvant-induced inflamed rats.
Brain Res Bull *54*, 141-144.

Zhao, H. B., Yu, N., and Fleming, C. R. (2005). Gap junctional hemichannel-
mediated ATP release and hearing controls in the inner ear. Proc Natl Acad Sci U S A
102, 18724-18729.

Zhong, Y., Dunn, P. M., Bardini, M., Ford, A. P., Cockayne, D. A., and Burnstock,
G. (2001). Changes in P2X receptor responses of sensory neurons from P2X3-
deficient mice. Eur J Neurosci *14*, 1784-1792.

Curriculum Vitae

Name: Chang Liu

Date of Birth: Jan 20, 1986

Place of Birth: Yantai, Shandong, China

Email: cc8601@gmail.com

Education

2008-present   Ph.D. candidate in Neuroscience, Johns Hopkins University School of Medicine *(PhD expected: Spring 2016)*

2004-2008   B.S. in Biological Sciences, Peking University School of Life Sciences, China

Research Experience

Sep 2011 – present   PhD student, Johns Hopkins University, Baltimore, USA
Advisors: Paul Albert Fuchs and Elisabeth Glowatzki

Jan 2009 – Aug 2011   PhD student, Johns Hopkins University, Baltimore, USA
Advisor: King-Wai Yau

Aug 2008 – Dec 2008   Rotation student, Johns Hopkins University, Baltimore, USA
Advisor: Craig Montell

Aug 2006 – May 2008   Undergraduate student, Peking University, Beijing, China
Advisors: Jianzhong Xi and Zhuan Zhou

Publications

• **Liu, C.**, Glowatzki, E. and Fuchs, P.A. Unmyelinated type II afferent neurons report cochlear damage. *Proc Natl Acad Sci U S A*. 2015 ; published ahead of print November 9, 2015, doi:10.1073/pnas.1515228112

• Martinez Monedero, R.*, **Liu, C.***, Weisz, C.J., Vyas, P., Fuchs, P.A. and Glowatzki, E. GluA2-containing AMPA receptors distinguish active from silent afferent contacts on rat cochlear hair cell. Submitted * **co-first author**.

• Copley, C.O., Duncan, J.S., **Liu, C.**, Cheng, H. and Deans, M.R. Postnatal refinement of auditory hair cell planar polarity deficits occurs in the absence of vangl2. *J Neurosci* 2013; 33, 14001-14016.

• Lou, C., Liu, X., Ni, M., Huang, Y., Huang, Q., Huang, L., Jiang, L., Lu, D., Wang, M., **Liu, C.**, et al. Synthesizing a novel genetic sequential logic circuit: a push-on push-off switch. *Mol Syst Biol*; 6, 350.

Research Presentations

<u>Podium Presentations</u>

• **Liu, C.**, Glowatzki, E. and Fuchs, P.A. Purinergic modulation of type II cochlear afferents: sensing trauma in the ear? Association for Research in Otolaryngology 37th Annual Midwinter Meeting. San Diego, CA. Feb 24, 2014.

• **Liu, C.,** Glowatzki, E. and Fuchs, P.A. Purinergic modulation of type II cochlear afferents. 12th Annual Eastern Auditory Retreat. Boston, MA. June 28, 2013.

• **Liu, C.,** Glowatzki, E. and Fuchs, P.A. Purinergic modulation of type II cochlear afferents. Johns Hopkins Neuroscience Department Lab Lunch. Baltimore, MD. November 6, 2012.

• **Liu, C**. Transduction channel of drosophila olfaction. Johns Hopkins Neuroscience Department Journal Club Research Presentation. Baltimore, MD. April 18, 2011.

<u>Poster Presentations</u>

• **Liu, C.,** Glowatzki, E. and Fuchs P.A. Cochlear Hair Cell Damage Activates Type II afferent Neurons. Association for Research in Otolaryngology 38th Annual Midwinter Meeting. Baltimore, MD. Feb 21, 2015.

• **Liu, C.,** Glowatzki, E. and Fuchs P.A. Cochlear Hair Cell Damage Activates Type II afferent Neurons. The Society of General Physiologists 68th Annual Meeting and Symposium. Woods Hole, MA. September 3, 2014.

• **Liu, C.,** Glowatzki, E. and Fuchs P.A. Purinergic modulation of type II cochlear afferents: sensing trauma in the ear. Johns Hopkins Annual Neuroscience Retreat. St Michaels, MD. September 6, 2013.

• **Liu, C.,** Glowatzki, E. and Fuchs P.A. Purinergic modulation of type II cochlear afferents: sensing trauma in the ear. The Society of Neuroscience Annual Meeting. San Diego, CA. November 10, 2013.

• Lou, C., Yang,Y., Liu, X., **Liu, C.,** et al. Towards bacterial assembly line. Team poster presentation, International Genetically Engineered Machine Competition. Boston, MA. November 3, 2007.

Professional Services

Ad-hoc Reviewer for *Journal of Ophthalmic Science*.

Student and postdoc representative in the Program Committee, Association for Research in Otolaryngology Annual Meeting. Feb 2014 and Feb 2015

Associated Faculty Member, Faculty of 1000. Dec 2012 - present

Practitioner in Preparing Future Faculty teaching academy. Johns Hopkins University. Aug 2013 – Oct 2014

Teaching assistant, Nervous System & Special Senses course for Johns Hopkins medical students. Johns Hopkins University School of Medicine. Apr - Jun 2012.

Honors and Awards

68th Annual Meeting Symposium Award. The Society of General Physiologists. Sep 2014

ARO Travel Awards. The Association for Research in Otolaryngology. Feb 2014

GSA Travel Awards. Johns Hopkins University School of Medicine. Sep 2013

Outstanding Graduate. Peking University. July 2008
Gold Medalist, International Genetically Engineered Machine Competition (iGEM). Nov 2007
Presidential Award from Peking University. Nov 2007
Kwang-Hua Scholarship. in two consecutive years. Peking University. Nov 2006 and Nov 2005